Geneeskundige Stichting Koningin Elisabeth
Fondation Médicale Reine Elisabeth
Königin-Elisabeth-Stiftung für Medizin
Queen Elisabeth Medical Foundation

Verslag – Rapport – Bericht – Report

2020

G.S.K.E. – F.M.R.E. – K.E.S.M. – Q.E.M.F.

www.fmre-gske.be
www.fmre-gske.eu
www.fmre-gske.com

Geneeskundige Stichting Koningin Elisabeth
2020
Inleiding verslag activiteiten van de GSKE – FMRE

In 2020 heeft de virale pandemie ook de activiteiten van de Stichting fel beïnvloed.
De jaarlijkse academische zitting van de Stichting waarin de onderzoekskredieten worden uitgereikt kon niet plaatsvinden zoals gepland op 30 april 2020.
De sessie die ons de gelegenheid geeft om elkaar te ontmoeten, de winnaars te feliciteren en nieuwe perspectieven in de neurowetenschappen te ontdekken, is uitgesteld tot 2021, wellicht 21 oktober 2021
Het bezoek van H.K.H. Prinses Astrid, vergezeld door de Baron en Barones Delruelle en verantwoordelijken van de Stichting, gepland op 03 december 2020 aan het laboratorium van Prof. Benoit Vanhollebeke (ULB Site Gosselies), werd eveneens uitgesteld naar 2021.

Eind 2019 selecteerde het wetenschappelijk comité, bestaande uit Belgische en buitenlandse experten, verschillende projecten die gedurende drie jaar (2020-2022) door de Stichting zullen worden ondersteund. Onder de projecten zijn er:
- Interuniversitaire projecten
  Prof. Jean-Noël Octave (UCLouvain met UMONS en UGent), Prof. Sebastiaan Engelborghs (VUB en UGent), Prof. Vincent Van Rompaey (UAntwerpen en KU Leuven), Prof. An Goris (KU Leuven en UAntwerpen), Prof. Pascal Kienlen-Campard (UCLouvain, Uliège en UGent)
- Universitaire projecten
  Prof. Sarah Weckhuysen (UAntwerpen), Prof. Pierre Vanderhaeghen (KU Leuven), Prof. Lieve Moons (KU Leuven), Priof. Thomas Voets (KU Leuven) en Prof. Simon De Meyer (KULAK)
- Projecten van jonge onderzoekers
  Dr Lars Emil Larsen (UGent), Dr. Evelien Carrette (UGent), PhD Valerie Uytterhoeven (KU Leuven), PhD Aya Takeoka (KU Leuven-IMEC), PhD Eline Wauters (UAntwerpen), Prof. Bernard Hanseeuw (UCLouvain), PhD Emanuel Vandenbroeke (UCLouvain) en Prof. Riem El Tahry (UC Louvain)

Het ondersteuningsproject voor "Jonge onderzoekers" is een nieuw initiatief dat tot doel heeft hen aan te moedigen om hun werk voort te zetten en zich geleidelijk te integreren in een academische of klinische loopbaan binnen de universiteiten van het land.

Hetzelfde wetenschappelijk comité kende ook volgende wetenschappelijke prijzen toe:
- Prijs Burggravin Valine de Spoelberch aan Prof. dr. Peter Vangheluwe (KU Leuven)
- De UCB-award aan Prof. dr. Bart De Strooper (KU Leuven)
- De Ernest Solvay prijs aan Prof. dr. Benoit Vanhollebeke (ULB)
- De Janine en Jacques Delruelle prijs aan Prof. dr. Vincent Timmerman (UAntwerpen)

Deze onderscheidingen onderstrepen de zeer hoge kwaliteit van het werk dat in België wordt verricht in het domein van de neurowetenschappen.
Voor 2021 zijn de toekenningsregels gewijzigd om meer toegang te geven aan onderzoekers die niet door de Stichting worden gesteund. Deze regeling voorziet bijzondere aandacht voor onderzoeksthema's die de voorkeur genieten van een prijsgever.

Wij danken H.K.H Prinses Astrid, onze Erevoorzitster, de leden van de Raad van Bestuur en van het Wetenschappelijk Comité van harte voor het werk dat ze doen ten voordele van de neurowetenschappelijke onderzoekers in ons land die dankzij die dankzij de prijsgevers de ontwikkeling van Neurowetenschappen kunnen voortzetten.

Prof. dr. Jean-Marie Maloteaux,
wetenschappelijk directeur
Brussel, 30 december 2020

Fondation Médicale Reine Elisabeth
2020
Introduction rapport d'activités de la FMRE – GSKE

Cette année 2020 fut profondément perturbée par la pandémie virale, les activités de la Fondation s'en sont également ressenties.
La séance académique annuelle de la Fondation au cours de laquelle sont remis les Prix et les financements de recherche n'a pas pu avoir lieu le 30 avril 2020 comme prévu.
La séance qui nous donne l'occasion de nous réunir, de féliciter les lauréats et de découvrir de nouvelles perspectives en neurosciences a été reportée à 2021, probablement le 21 octobre 2021.
La visite de S.A.R. la Princesse Astrid en compagnie du Baron et de la Baronne Delruelle et de responsables de la Fondation a également été reportée, elle était prévue le 3 décembre 2020 au laboratoire du Professeur B. Vanhollebeke (ULB- site Gosselies), mais de nouveau reportée pour 2021

Fin 2019, le comité scientifique constitué des experts belges et étrangers a retenu plusieurs projets qui seront soutenus par la Fondation pendant trois ans 2020-2022. Parmi ces projets, il y a :
- des projets interuniversitaires:
  Prof. Jean-Noël Octave (UC Louvain avec l'UMONS et l'UGent), Prof. Sebastiaan Engelborghs (VUB et l'UGent), Prof. Vincent Van Rompaey (UA et le KU Leuven), Prof An Goris (KU Leuven et l'UA) et Prof. Pascal Kielen-Campard (UCLouvain, l'ULiège et l'UGent),
- des projets universitaires:
  Prof. Sarah Weckhuysen (Uantwerpen), Prof. Pierre Vanderhaeghen (KU Leuven), Prof. Lieve Moons (KU Leuven), Prof. Thomas Voets (KU Leuven), Prof. Simon De Meyer (KULAK) et
- les projets de jeunes chercheurs:
  Dr Lars Emil Larsen (UGent), Dr. Evelien Carrette (UGent), PhD. Valerie Uytterhoeven (KU Leuven), PhD Aya Takeoka (KU Leuven-IMEC), Eline Wauters (UAntwerpen), Prof. Bernard Hanseeuw (UCLouvain), PhD Emanuel Vandenbroeke (UCLouvain), Prof. Riëm El Tahry (UCLouvain).

Le projet de soutien aux "jeunes chercheurs" est une initiative nouvelle qui a pour objectif de les encourager à poursuivre leurs travaux tout en s'intégrant progressivement dans une carrière académique ou clinique au sein des universités du pays.

En 2020, ce même jury a attribué les Prix de la Fondation:
- Prix Vicomtesse Valine de Spoelberch au Prof. Peter Vangheluwe (KU Leuven)
- Prix UCB au Prof. Bart De Strooper (KU Leuven)
- Prix Ernest Solvay au Prof. Benoit Van Hollebeke (ULB)
- Prix Janine et Jacques Delruelle au Prof. Vincent Timmerman (UAntwerpen)

Ces prix soulignent la très haute qualité des travaux réalisés en Belgique dans le domaine des neurosciences. Pour 2021, le règlement d'attribution des Prix a été modifié pour y donner un accès plus large y compris à des chercheurs dont les travaux n'ont pas été subventionnés par la Fondation. Ce règlement prévoit une attention particulière à des thèmes de recherche éventuellement privilégiés par un mécène.

Nous remercions vivement S.A.R. la Princesse Astrid, notre Présidente d'Honneur, les membres du Conseil d'Administration et du Comité Scientifique pour le travail qu'ils accomplissent au bénéfice des chercheurs en neurosciences de notre pays qui grâce aux mécènes peuvent poursuivre le développement des Neurosciences.

Prof. dr. Jean-Marie Maloteaux,
directeur scientifique
Bruxelles, 30 décembre 2020

Progress reports of the research projects of young researchers, supported by the Queen Elisabeth Medical Fondation in collaboration with the following professors and doctors (2020)

1. Interuniversity research projects

2. University research projects

3. Research projects of young researchers

Geneeskundige Stichting Koningin Elisabeth
Fondation Médicale Reine Elisabeth
Königin-Elisabeth-Stiftung für Medizin
Queen Elisabeth Medical Foundation

Interuniversitaire onderzoeksprojecten 2020-2022 gefinancierd door de G.S.K.E.

Projets de recherche interuniversitaire 2020-2022 subventionnés par la F.M.R.E.

Interuniversity research projects 2020-2022 funded by the Q.E.M.F.

Universiteiten met onderzoeksprogramma's die gesteund worden door de G.S.K.E.

Universités ayant des programmes de recherche subventionnés par la F.M.R.E.

Universities having research programs supported by the Q.E.M.F.

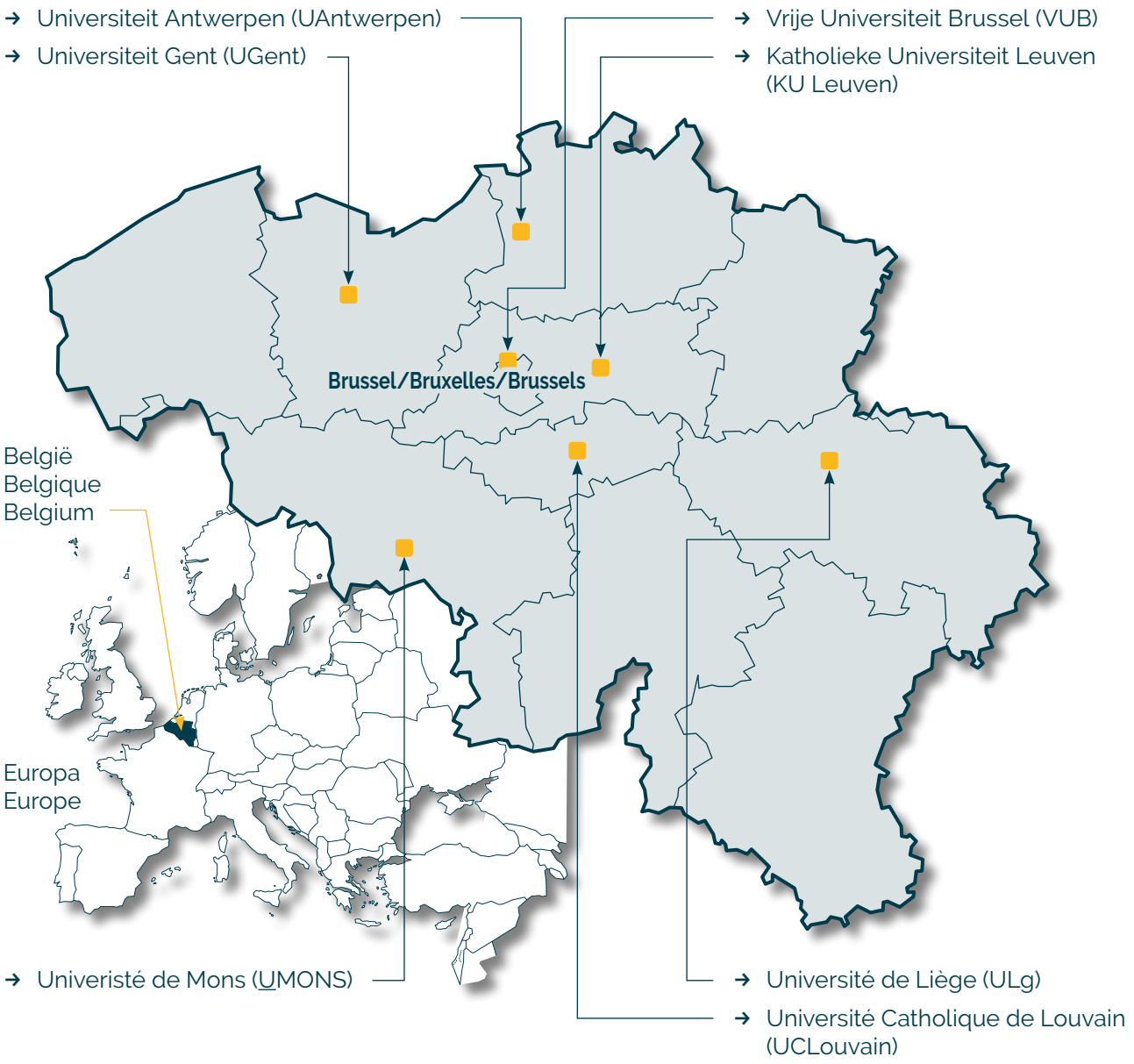

Interuniversitaire onderzoeksprojecten 2020-2022 gefinancierd door de G.S.K.E.

Projets de recherche interuniversitaire 2020-2022 subventionnés par la F.M.R.E.

Interuniversity research projects 2020-2022 funded by the Q.E.M.F.

Prof. dr. Jean-Noël Octave (UCLouvain)
Prof. dr. Philippe Gailly (UCLouvain)
Prof. dr. Nathalie Pierrot (UCLouvain)
Prof. dr. Laurence Ris (UMONS)
Prof. dr. Paul Boon (UGent)
Involvement of PPAR activation in the control of synaptic function by APP

Prof. dr. Sebastiaan Engelborghs (VUB)
Prof. dr. Chris Baeken (UGent)
Unraveling the link between depression and dementia to improve diagnostic and treatment options

Prof. dr. Vincent Van Rompaey (UAntwerpen)
Prof. dr. Peter Ponsaerts (UAntwerpen)
Prof. dr. Guy Van Camp (UAntwerpen)
Prof. Rik Gijsbers (KU Leuven)
Development of allele-specific CRISPR-nuclease gene therapy for late-onset sensorineural hearing impairment in a new humanized DFNA9 mouse model

Prof. dr. An Goris (KU Leuven)
Prof. Nathalie Cools (UAntwerpen)
Deep sequencing of myelin-reactive T-cells to elucidate new disease mechanisms and identify correlates for treatment responsiveness

Prof. dr. Pascal Kienlen-Campard (UCLouvain)
Prof. dr. Loïc Quinton (ULg)
Prof. dr. Jan Gettemans (UGent)
New analytical tools to identify and target pathogenic hexameric Aβ assemblies in Alzheimer's disease

Geneeskundige Stichting Koningin Elisabeth
Fondation Médicale Reine Elisabeth
Königin-Elisabeth-Stiftung für Medizin
Queen Elisabeth Medical Foundation

Progress report of the interuniversity research project of

Prof. dr. Jean-Noël Octave (UCLouvain)
Prof. dr. Philippe Gailly (UCLouvain)
Prof. dr. Nathalie Pierrot (UCLouvain)
Prof. dr. Laurence Ris (UMONS)
Prof. dr. Paul Boon (UGent)

Prof. dr. Jean-Noël Octave (UCLouvain)
Faculty of Pharmacy and Biomedical Sciences
Institute of neuroscience (IONS)
CEMO
Avenue Hippocrate 54/B1.54.10
1200 Woluwe-Saint-Lambert
jean-noel.octave@uclouvain.be

Prof. dr. Philippe Gailly (UCLouvain)
Institute of Neuroscience (IoNS)
Laboratory of Cell Physiology (FYCL)
Avenue Mounier, 53 - B1.53.17
1200 Brussels
philippe.gailly@uclouvain.be
Tel. + 32 (0)2 764 55 42

Prof. dr. Nathalie Pierrot (UCLouvain)
Institute of Neuroscience (IONS)
CEMO
Avenue Mounier 53/B1.53.03
1200 Woluwe-Saint-Lambert
nathalie.pierrot@uclouvain.be

Prof dr. Laurence Ris (UMONS)
Lecturer, head of the department of Neuroscience
Faculty of Medicine and Pharmacy
6A, avenue du Champ de Mars 7000 Mons
laurence.ris@umons.ac.be

Prof. dr. Paul Boon (UGent)
Professor and chairman Department of Neurology
Chairman Division of Head, Movement and Senses
Ghent University Hospital - Ghent University
10 Corneel Heymanslaan
9000 Gent
Paul.boon@ugent.be

Involvement of PPARα activation in the control of synaptic function by APP

1. The context

With a prevalence doubling every 5 years beyond 65, Alzheimer's disease (AD) is a devastating neurodegenerative disorder, which is the most common cause of dementia in the elderly. Together with a progressive loss of cognitive functions, AD is characterized by the existence of extracellular senile plaques containing the amyloid-β (Aβ) peptide generated from the sequential proteolytic processing of its precursor, the amyloid precursor protein (APP).

Although amyloid deposition occurring in the hippocampus and the cerebral cortex of AD patients potentially explains deficits in memory and cognitive function observed [1], it remains difficult to influence the course of AD by removing amyloid deposits. Indeed, even if immunotherapy efficiently removes senile plaques from AD brains, clinical trials indicate that cognition is not improved in AD patients. Therefore, a better knowledge of the underlying physiopathological mechanisms involved early in the neurodegenerative process is required. In particular, a considerable bulk of evidence supports that synaptic function is affected at the earliest stages of AD. Indeed, synaptic dysfunction leading to atypical neural synchrony and oscillations observed in AD brain might play an early role in the establishment of pathogenic cascades leading to AD and could contribute to cognitive deficits [2,3].

Synaptic deficits occur very early in AD patients [4]. Moreover, it was reported that people at risk for AD (*e.g.* ApoE4 carriers, see below) display increased neuronal excitability without dementia [5] and that cognitive and synaptic dysfunctions arise before the formation of plaques in transgenic mouse models of AD [6]. Using different methodological approaches, including electroencephalography (EEG) [7,8], a lack of functional connectivity between brain areas has been highlighted in AD [9,10].

We previously reported that increase or decrease in APP expression modulates both excitatory and inhibitory neuronal activity in primary rat cortical networks [11,12] [13]. These data suggest an **essential role of APP in the control of both excitatory and inhibitory neurotransmissions, which have to be perfectly balanced to regulate cognitive function.**

In the vast majority of late-onset sporadic AD cases (about 99 %), the source of Aβ accumulation in the brain is still unknown. Nevertheless, it is well established that the epsilon 4 allele of the *apolipoprotein E* (*ApoE*) gene, encoding the main transporter of cholesterol in the brain, is a genetic risk factor for AD[14]. Therefore, a **relationship between AD and lipid metabolism has been established.** We have previously demonstrated that the expression of the neuronal human APP (hAPP) isoform in cortical networks controls cholesterol turnover, needed for neuronal activity [15], by interacting with the sterol regulatory element binding protein 1 (SREBP1), a transcription factor that regulates expression of sterol- and lipogenic genes [16,17]. We reported that **hAPP expression inhibits biosynthesis of both cholesterol and fatty acids (FAs) in cortical cells in culture** [15].

FAs are the major constituents of brain lipids [18] and play a critical role in brain development and functioning [19]. Among them, essential brain polyunsaturated FAs (PUFAs) play a critical role in neurogenesis, synaptic function, inflammation, glucose homeostasis, mood and cognition [20]. PUFAs are ligands for retinoid X and peroxisome proliferator-activated receptors (RXRs and PPARs, respectively) [21], two nuclear receptors forming permissive heterodimers that belong

to the superfamily of ligand-dependent transcription factors [22]. PPARs act principally as lipid sensors [23] and due to their anti-inflammatory effects, PPARs activation with specific agonists emerged as promising approaches for treating brain pathologies in several mouse models of Parkinson, Huntington and Alzheimer diseases [24,25]. Recent *in vitro* and *in vivo* evidence point to PPAR as a promising therapeutic target in AD that we have recently reviewed[26]. Indeed, it was shown that PPAR agonists improved amyloid and tau pathologies, decreased neuroinflammation, ameliorated glucose and lipid dyshomeostasis and improved behavior in mouse models of AD [27].

We recently reported that **PPARα expression also plays a crucial role in synaptic function. Activation of PPAR with a specific agonist improves synaptic plasticity in a transgenic mouse model of AD** [28]. However, the cellular and molecular mechanisms underlying such effects are poorly understood.

2. The project and preliminary results

By combining *in vitro*, *ex vivo* and *in vivo* approaches, **the aim of the present project is to investigate whether APP is able to affect the activation of PPAR and thereby synaptic function**. APP expression has been therefore modulated in primary cortical cultures. PPAR activation and synaptic function have been measured in this model. Moreover PPAR activation or inhibition with specific agonists or antagonist has been tested as well.

In order to analyse the influence of APP expression on PPARα activation, primary culture of rat cortical cells (E17-18) were transduced with a recombinant adenovirus expressing the neuronal isoform of human APP (hAPP). Conversely, the knockdown of endogenous APP with APP shRNA lentiviruses has been investigated.

Activation of PPAR has been measured by quantification of the expression of PPARα target genes involved in FAs oxidation (*Cpt1*, *Acox1*) and glucose metabolism (*Pdk4*) using quantitative real time PCR analysis. While the expression of Cpt1 Acox1 and Pdk4 are decreased in hAPP expressing cells, we observe an opposite effect after down regulating the expression of rat endogenous APP compared to control cells expressing GFP protein in cortical cells (Figure 1A-C and 2A-C). These results indicate therefore that PPARα activation is reduced in hAPP cells but increased in APP shRNA cells.

In order to reverse the effects observed, hAPP and APPshRNA cells have been treated with a PPARα synthetic agonist (10 µM WY14643) or antagonist (5 µM GW6471), respectively. Under these conditions, we observed that PPARα activation is normalized in both conditions (Figure 1C and 2C). These results suggest that the pharmacological modulation of PPARα with specific agonist and antagonist is able to restore APP dependent modification in PPARα activation in cortical cells in culture.

As we previously reported an essential role of APP in the control of excitatory neurotransmission[11,12,15] and that PPARα expression plays a crucial role in synaptic function[28], we hypothesize that treatment with PPARα synthetic agonist or antagonist, would normalize decrease and increase in neuronal activity previously observed in hAPP and APP shRNA cells, respectively. By whole-cell patch-clamp analysis, our preliminary results indicate that activation of PPARα with agonist WY14643 (10µM) partly rescues synaptic activity impaired in hAPP cortical cells (Figure 1E and F). Moreover, resting membrane potential are less negative in treated hAPP expressing cells (Figure 1D). Opposite results were observed in shAPP cells treated with the GW6471 PPARα

antagonist (1 µM), (Figure 2D, E and F). All together these results indicate that **APP expression is able to affect the activation of PPAR and thereby synaptic function.**

The relevance of the results obtained *in vitro* has been tested in 3-4, 6-8 and 11-12 months old transgenic mouse model that overexpresses the neuronal wild type hAPP isoform (*hAppwt*) (Figure 3A and 3B).
Before analyzing how hAPP expression affects PPARα activation *in vivo*, we have first characterized this transgenic mouse model by using biochemical, morphological and electrophysiological approaches. Although these mice overexpress hAPP and accumulate soluble APPα and β, two APP metabolites produced from the shedding of hAPP, they did not present brain amyloid plaques[29]. We report that learning abilities and working memory were impaired in 6 and 12 months of hAPP mice (Figure 4). Moreover, we observed a decrease in neurogenesis at 3 months of age and a progressive caspase-3-related neuronal death at 12 months (Figure 5). Brain activity was also evaluated in these mice by intracranial EEG recording. Results obtained show abnormal epileptiform spikes in 6 and 12 months old hAPP mice (Figure 6, see also [30]). These epileptiform spikes were reduced by treating mice with baclofen, a -aminobutyric acid (GABA) analogue that acts as an agonist at central GABAB receptors. Based on previous results, we hypothesized that this hyperexcitability could be related to an APP-induced reduction of the expression of KCC2, a K^+-Cl^- transporter responsible for the extrusion of Cl^- in mature neurons. However, at 3 and 6 months, we did not observe any change in the expression of KCC2 and NKCC1 (the Na^+, K^+, Cl^- transporter responsible for the influx of Cl^- in neurons), suggesting that the excitatory / inhibitory imbalance was not due to the accumulation of chloride in neurons. Moreover, the expression of glutamate and GABA receptors was not modified, suggesting also that the epileptiform spikes were not due to a disequilibrium in the expression of glutamate/GABA receptors. However, we observed that GABA concentration was largely decreased in the hippocampus from hAPP mice (at 3, 6 and 12 months) while glutamate concentration was unchanged. Altogether, these results suggest that the hyperexcitable state might be explained by a reduced GABA synaptic release.
Furthermore, we observed that long term potentiation induced by a theta burst (TBS: 4 bursts at 5 Hz of 5 stimuli at 100Hz) was increased on hippocampal slices (Figure 7A). Interestingly, when we compared the response to the second burst compared with the first one, a large increase in hAPP mice was observed (Figure 7B). This could be related to a **presynaptic inhibition of GABA release that seemed to be more pronounced in hAPP, possibly due to the binding of soluble APP to the presynaptic GABAB receptor** [31]. Indeed, this effect was lost after treatment with 500 µM CGP36216 (which at this concentration, inhibits the presynaptic but not the postsynaptic GABAB receptor). Similarly, the responses to a train of 5 stimuli at 20Hz were higher in hAPP slices, but the difference between hAPP and Wt was lost after treatment with CGP36216 (Figure 7C).

After having thoroughly characterized this transgenic mouse model, our preliminary results indicate that *Acox1, Cpt1* and *Pdk4* (PPARα target genes) mRNA levels decrease in brain lysates from old *hAppwt* male mice compared to age-matched, non-transgenic littermates used as controls. (Figure 3 C-D). These results corroborate results previously obtained *in vitro* and sustain a potential involvement of hAPP expression in synaptic function mediated by the activation of PPARα.

3. Perspectives

In order to confirm the involvement of PPARα activation in the control of synaptic function by APP, we will first investigate the influence of APP expression on synaptic activity in cultured cortical cells from PPARα deficient (*Ppara*$^{-/-}$) transgenic mice.

Moreover, we will further investigate neuronal network activity, excitability and plasticity *ex vivo* on brain slices and *in vivo*. *In vivo*, mice will be stereotactically and bilaterally implanted with recording electrodes in parietal cortex and hippocampal CA1 and dentate gyrus. Spontaneous EEG will be recorded and compared between hAPP mice and age-matched non-transgenic littermates upon PPARα activation with the WY14643 agonist (40-80mg/kg).

Furthermore, *ex vivo* basal synaptic transmission, and paired-pulse facilitation (PPF) will be investigated by extracellular recordings on acute brain slices. The causal effect of PPAR activity on the observed deficits will be evaluated by treating hAPP mice with the WY14643 PPARα agonist and mouse deficient for APP (*App*$^{-/-}$) with the GW6471 PPARα antagonist. Acute slices will be treated with the PPARα agonist/antagonist on one out of two set-ups for 2 h. Basal synaptic transmission and PPF will be recorded before and after picrotoxin application on two slices in CA1 region in each set-ups. Results obtained from Wt and *App*$^{-/-}$ mice with and without GW6471 PPARα antagonist will be compared (5 µM, dose used in organotypic slices[32]). Moreover, basal excitability and epileptic activity induced by picrotoxin will be also compared in the different groups analyzed. In parallel, basal synaptic transmission and PPF will be recorded before and after picrotoxin application on acute slices from Wt and hAPP mice treated with the WY14643 PPARα agonist (1 µM/2h).

4. References

1. Pearson, R.C., Esiri, M.M., Hiorns, R.W., Wilcock, G.K. & Powell, T.P. Anatomical correlates of the distribution of the pathological changes in the neocortex in Alzheimer disease. *Proc. Natl. Acad. Sci. U. S. A* **82**, 4531-4534 (1985).
2. Uhlhaas, P.J. & Singer, W. Neural synchrony in brain disorders: relevance for cognitive dysfunctions and pathophysiology. *Neuron* **52**, 155-68 (2006).
3. Delbeuck, X., Van der Linden, M. & Collette, F. Alzheimer's disease as a disconnection syndrome? *Neuropsychol Rev* **13**, 79-92 (2003).
4. Martin, L.J., Pardo, C.A., Cork, L.C. & Price, D.L. Synaptic pathology and glial responses to neuronal injury precede the formation of senile plaques and amyloid deposits in the aging cerebral cortex. *Am. J. Pathol* **145**, 1358-1381 (1994).
5. Ponomareva, N.V., Korovaitseva, G.I. & Rogaev, E.I. EEG alterations in non-demented individuals related to apolipoprotein E genotype and to risk of Alzheimer disease. *Neurobiol. Aging* **29**, 819-827 (2008).
6. Sasaguri, H. *et al.* APP mouse models for Alzheimer's disease preclinical studies. *EMBO J* **36**, 2473-2487 (2017).
7. Lustig, C. *et al.* Functional deactivations: change with age and dementia of the Alzheimer type. *Proc. Natl. Acad. Sci. U. S. A* **100**, 14504-14509 (2003).
8. Sperling, R.A. *et al.* Amyloid deposition is associated with impaired default network function in older persons without dementia. *Neuron* **63**, 178-188 (2009).
9. Babiloni, C. *et al.* Brain neural synchronization and functional coupling in Alzheimer's disease as revealed by resting state EEG rhythms. *Int J Psychophysiol* **103**, 88-102 (2016).
10. Bokde, A.L., Ewers, M. & Hampel, H. Assessing neuronal networks: understanding Alzheimer's disease. *Prog Neurobiol* **89**, 125-33 (2009).
11. Santos, S.F. *et al.* Expression of human amyloid precursor protein in rat cortical neurons inhibits calcium oscillations. *J Neurosci* **29**, 4708-18 (2009).
12. Octave, J.N., Pierrot, N., Ferao, S.S., Nalivaeva, N.N. & Turner, A.J. From synaptic spines to nuclear signaling: nuclear and synaptic actions of the amyloid precursor protein. *J. Neurochem* **126**, 183-190 (2013).

13. Doshina, A. *et al.* Cortical cells reveal APP as a new player in the regulation of GABAergic neurotransmission. *Sci Rep* **7**, 370 (2017).
14. Di Battista, A.M., Heinsinger, N.M. & Rebeck, G.W. Alzheimer's Disease Genetic Risk Factor APOE-epsilon4 Also Affects Normal Brain Function. *Curr Alzheimer Res* **13**, 1200-1207 (2016).
15. Pierrot, N. *et al.* Amyloid precursor protein controls cholesterol turnover needed for neuronal activity. *EMBO Mol. Med* **5**, 608-625 (2013).
16. Shimano, H. *et al.* Isoform 1c of sterol regulatory element binding protein is less active than isoform 1a in livers of transgenic mice and in cultured cells. *J. Clin. Invest* **99**, 846-854 (1997).
17. Horton, J.D., Goldstein, J.L. & Brown, M.S. SREBPs: activators of the complete program of cholesterol and fatty acid synthesis in the liver. *J Clin Invest* **109**, 1125-31 (2002).
18. Chang, C.Y., Ke, D.S. & Chen, J.Y. Essential fatty acids and human brain. *Acta Neurol Taiwan* **18**, 231-41 (2009).
19. Luchtman, D.W. & Song, C. Cognitive enhancement by omega-3 fatty acids from child-hood to old age: findings from animal and clinical studies. *Neuropharmacology* **64**, 550-65 (2013).
20. Bazinet, R.P. & Laye, S. Polyunsaturated fatty acids and their metabolites in brain function and disease. *Nat. Rev. Neurosci* **15**, 771-785 (2014).
21. Desvergne, B. RXR: from partnership to leadership in metabolic regulations. *Vitam Horm* **75**, 1-32 (2007).
22. Evans, R.M. & Mangelsdorf, D.J. Nuclear Receptors, RXR, and the Big Bang. *Cell* **157**, 255-266 (2014).
23. Michalik, L. *et al.* International Union of Pharmacology. LXI. Peroxisome proliferator-activated receptors. *Pharmacol. Rev* **58**, 726-741 (2006).
24. Zolezzi, J.M. *et al.* PPARs in the central nervous system: roles in neurodegeneration and neuroinflammation. *Biol. Rev. Camb. Philos. Soc* **92**, 2046-2069 (2017).
25. Moutinho, M. & Landreth, G.E. Therapeutic potential of nuclear receptor agonists in Alzheimer's disease. *J. Lipid Res* **58**, 1937-1949 (2017).
26. Saez-Orellana, F., Octave, J.N. & Pierrot, N. Alzheimer's Disease, a Lipid Story: Involvement of Peroxisome Proliferator-Activated Receptor alpha. *Cells* **9**(2020).
27. D'Orio, B., Fracassi, A., Ceru, M.P. & Moreno, S. Targeting PPARalpha in Alzheimer's Disease. *Curr Alzheimer Res* **15**, 345-354 (2018).
28. Pierrot, N. *et al.* Sex-regulated gene dosage effect of PPARalpha on synaptic plasticity. *Life Sci Alliance* **2**(2019).
29. Mucke, L. *et al.* High-level neuronal expression of abeta 1-42 in wild-type human amyloid protein precursor transgenic mice: synaptotoxicity without plaque formation. *J. Neurosci* **20**, 4050-4058 (2000).
30. Johnson, E.C.B. *et al.* Behavioral and neural network abnormalities in human APP transgenic mice resemble those of App knock-in mice and are modulated by familial Alzheimer's disease mutations but not by inhibition of BACE1. *Mol Neurodegener* **15**, 53 (2020).
31. Rice, H.C. *et al.* Secreted amyloid-beta precursor protein functions as a GABABR1a ligand to modulate synaptic transmission. *Science* **363**(2019).
32. Koch, M. *et al.* Palmitoylethanolamide protects dentate gyrus granule cells via peroxisome proliferator-activated receptor-alpha. *Neurotox Res* **19**, 330-40 (2011).

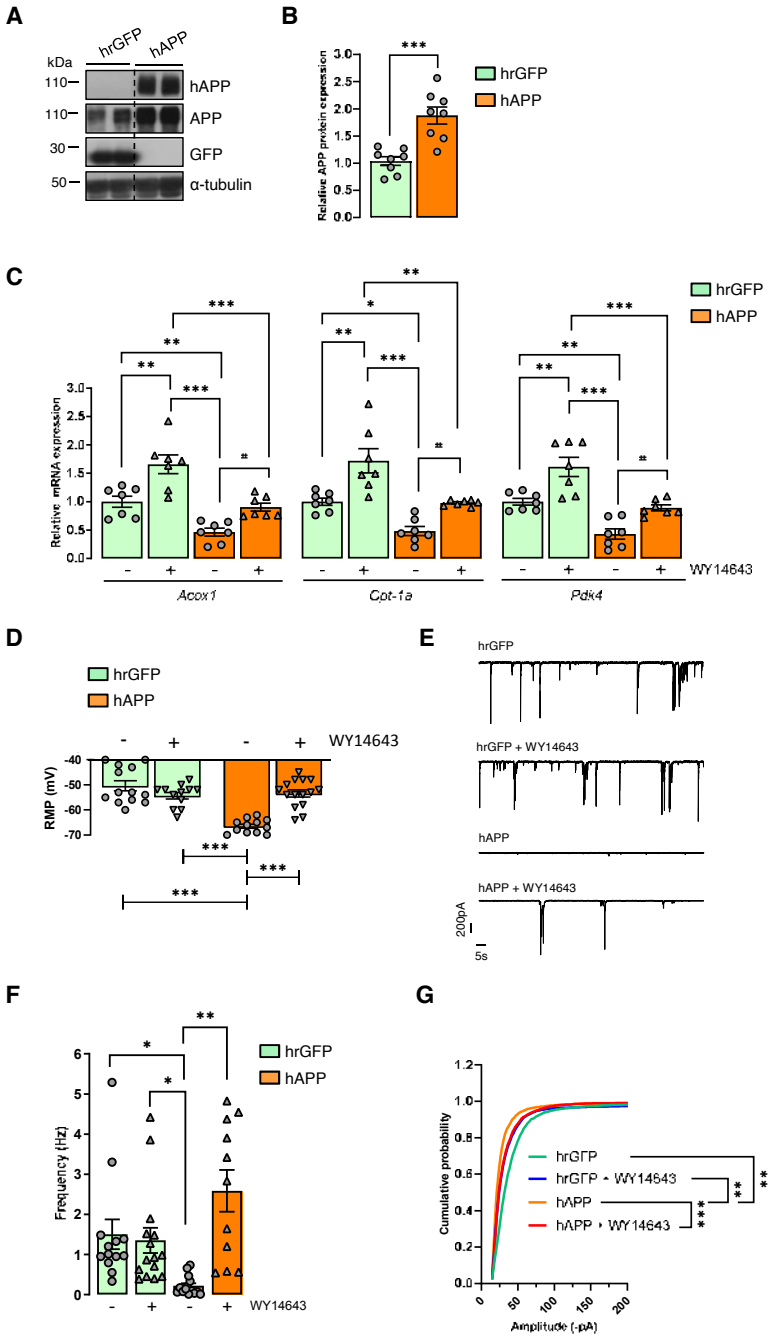

Figure 1. The PPARα agonist WY14643 inhibits human APP-induced decreases in PPARα activation and synaptic activity in cortical cultures. Primary cultures of rat cortical cells were infected with adenoviruses encoding human recombinant GFP (hrGFP) or APP (hAPP) proteins and treated (+) or not (–) with 10µM PPARα agonist WY14643 for 24h at 13-14 days *in vitro* (DIV). (**A**) Representative immunoblot of cell lysates from hrGFP control and hAPP expressing cells. The expression of hAPP was monitored with the specific WO2 antibody recognizing hAPP and anti-APP C-terminal antibody recognizing both hAPP and endogenous APP (APP). Immunoblots were further probed using anti-GFP and - tubulin antibodies. (**B**) Quantification of APP expression / tubulin ratios (n = 8 of each analysed in 4 independent experiments) were normalized compared to hrGFP control cells (mean ± SEM). A Student's t-test (APP protein, $P = 0.0608$) was used to assess significance of the mean. (**C**) Comparative quantitative real time PCR analyses for *Acox1*, *Cpt-1α* and *Pdk4* mRNA levels (n = 7 of each analysed in 4 independent experiments). Results were normalized to *Rpl32* mRNA and compared to respective untreated (–) hrGFP control cells. Results are shown as mean ± SEM and one-way ANOVA followed by Tukey's multiple comparisons test was used to assess significance of the mean ((–) hAPP vs (–) hrGFP: *Acox1* mRNA, $P = 0.009$, *Cpt-1α* mRNA, $P = 0.026$; *Pdk4* mRNA, $P = 0.003$; (+) hAPP vs (–) hAPP: *Acox1* mRNA, $P = 0.039$, *Cpt-1α* mRNA, $P = 0.035$; *Pdk4* mRNA, $P = 0.022$). (**D**) Resting membrane potential (RMP) was measured in hAPP and control hrGFP neurons between 13 and 17 DIV (n = 13-15 cells per group). (**E - G**) Representative traces of miniature excitatory postsynaptic currents (mEPSC) (**E**); mean values of mEPSCs frequencies (**F**, n = 15-24 cells per group cells analysed in 6 independent experiments) and cumulative probability plot of the amplitude distribution (**G,** n = 12) were measured in hrGFP and hAPP expressing neurons at 13-17 DIV in presence or not of WY14643. (**D** - **G**) Brown-Forsythe and Welch ANOVA tests followed by Dunnett's T3 multiple comparisons test. $^{*}P < 0.05$, $^{**}P < 0.01$, $^{***}P < 0.001$, $^{\#}P < 0.05$.

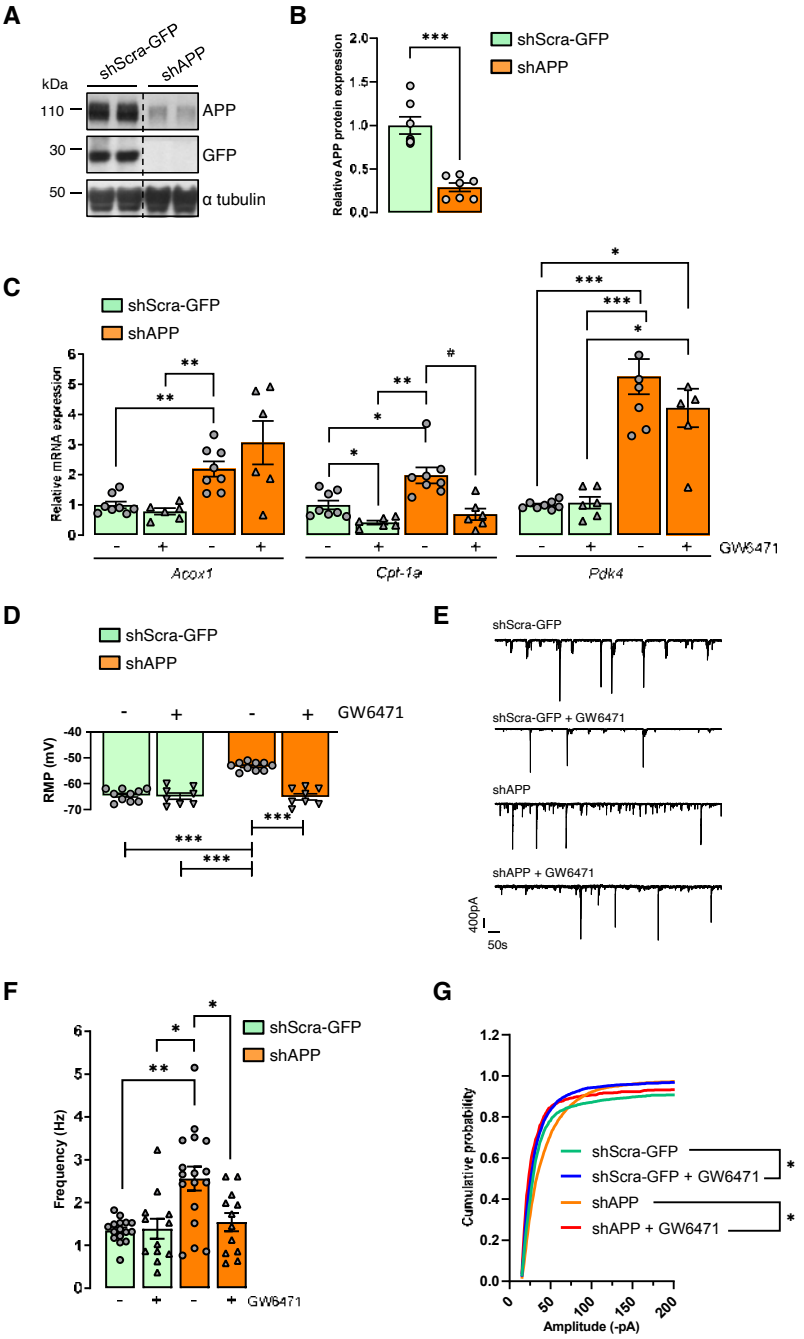

Figure 2. The PPARα antagonist GW6471 inhibits APP knockdown-induced increases in PPARα activation and synaptic activity in cortical cultures. Primary cultures of rat cortical cells were infected with lentiviruses encoding a shRNA construct designed to target endogenous APP (shAPP) or a scrambled shRNA encoding GFP (shScra-GFP). At 13-14 DIV, cells were treated (+) or not (–) with PPARα antagonist GW6471 for 24h. (**A**) Representative immunoblot of cell lysates from shScra-GFP control and shAPP infected cells. The expression of endogenous rat APP was monitored with an anti-APP C-terminal antibody. Immunoblots were further probed using anti-GFP and - tubulin antibodies. (**B**) Quantification of APP expression / tubulin ratios (n = 7 of each analysed in 4 independent experiments) were normalized compared to shScra-GFP control cells (mean ± SEM). A Student's t-test (APP protein, $P < 0.001$) was used to assess significance of the mean. (**C**) Cells were treated or not with 5µM GW6471 and comparative quantitative real time PCR analyses for *Acox1*, *Cpt-1a* and *Pdk4* mRNA levels (n = 6-8 for each condition analysed in 6 independent experiments) were carried out. Results were normalized to *Rpl32* mRNA and compared to respective untreated (–) shScra-GFP control cells. Results are shown as mean ± SEM and Brown-Forsythe and Welch ANOVA tests followed by Dunnett's T3 multiple comparisons test were used to assess significance of the mean ((–) shAPP vs (–) shScra-GFP: *Acox1* mRNA, $P = 0.008$, *Cpt-1a* mRNA, $P = 0.043$; *Pdk4* mRNA, $P = 0.0009$; (+) shScra-GFP vs (–) shScra-GFP: *Cpt-1a* mRNA, $P = 0.026$; (+) shAPP vs (–) shAPP: *Cpt-1a* mRNA, $P = 0.010$). (**D** - **G**) Cells were treated or not with 1µM GW6471 and resting membrane potential (RMP) (**D**) was measured in shAPP and control shScra-GFP neurons between 13 and 17 DIV (n = 8-10 cells per group analysed). (**E**) Representative traces of miniature excitatory postsynaptic currents (mEPSC). (**F**) Mean values of mEPSCs frequencies (n = 12-17 cells per group cells analysed in 6 independent experiments) and (**G**) cumulative probability plot of the amplitude distribution (n = 12 cells per group cells) were measured in shAPP and control shScra-GFP neurons at 13-17 DIV in presence or not of GW6471. (**D** - **G**) Brown-Forsythe and Welch ANOVA tests followed by Dunnett's T3 multiple comparisons test. $^{*}P < 0.05$, $^{**}P < 0.01$, $^{***}P < 0.001$, $^{\#}P < 0.05$.

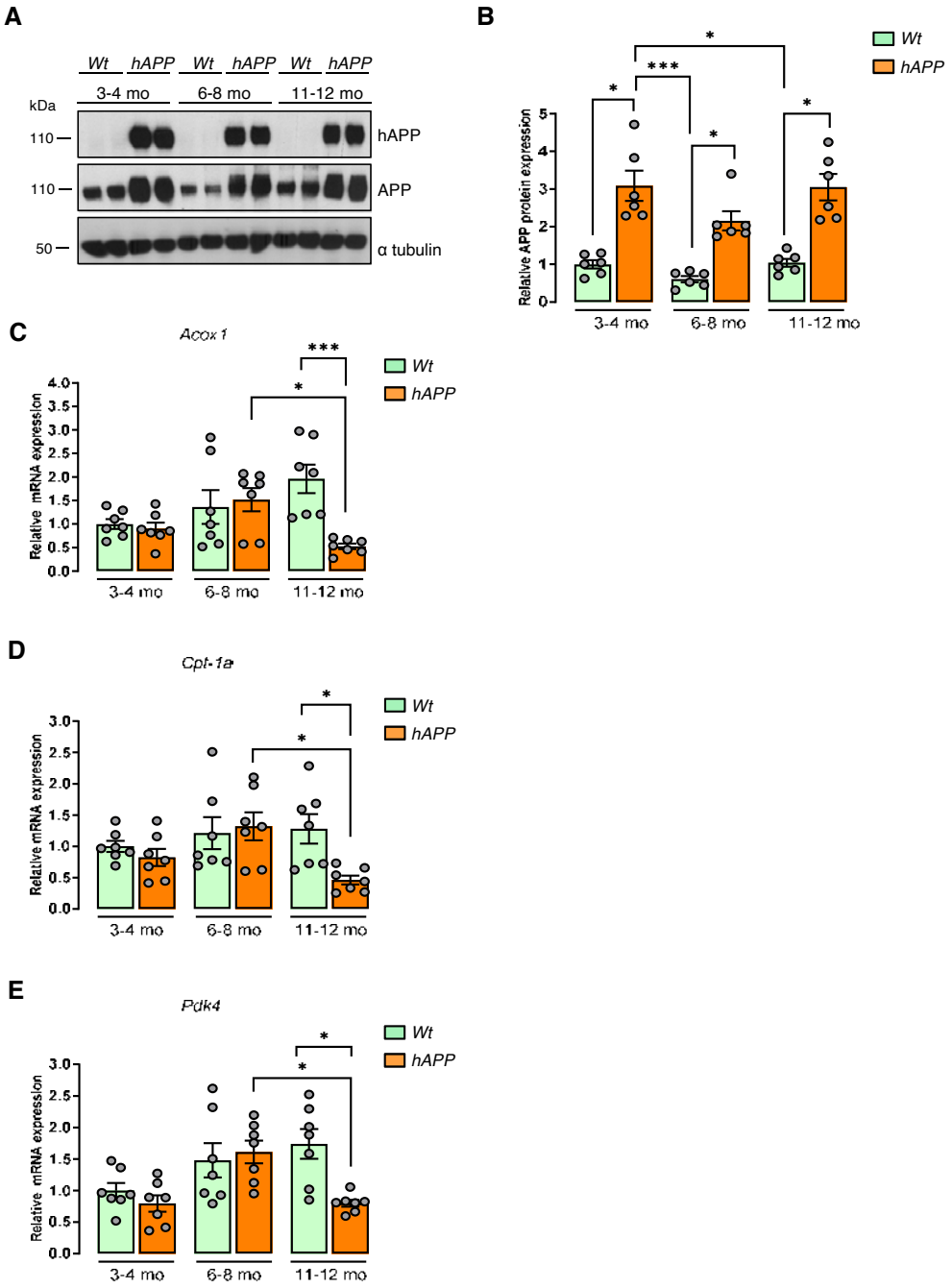

Figure 3. Human APP expression decreases PPARα activation in old mice. Brain frontal cortex tissues from transgenic mice overexpressing non-mutated human APP (*hAPP*) and wild type (Wt) littermates were analyzed at 3-4, 6-8 and 11-12 months old (mo). (**A**) The expression of hAPP was investigated in mice brain lysates (n = 6 of each) by immunoblot analysis with the specific WO2 antibody recognizing hAPP and anti-APP C-terminal antibody recognizing both hAPP and endogenous APP (APP). Blots were further probed using anti- tubulin antibody. (**B**) Relative density of APP expression was compared with α-tubulin. Results were normalized compared to 3-4 mo *Wt* and are shown as mean ± SEM. A Kruskal-Wallis test followed by Dunn's multiple comparisons post-test was used to assess significance of the mean (APP protein expression at 3-4, 6-8 and 11-12 mo, $P < 0.05$). (**C-E**) Quantitative real time PCR analyses for *Acox1*, *Cpt-1α* and *Pdk4* mRNA levels. Results were normalized to *Rpl32* mRNA, compared to 3-4 mo *Wt* and shown as mean ± SEM. A Kruskal-Wallis test followed by Dunn's multiple comparisons post-test was used to assess significance of the mean (11-12 mo hAPP mice: *Acox1* mRNA, $P = 0.0008$, *Cpt-1α* mRNA, $P = 0.031$; *Pdk4* mRNA, $P = 0.022$), $^{*}P < 0.05$, $^{***}P < 0.001$.

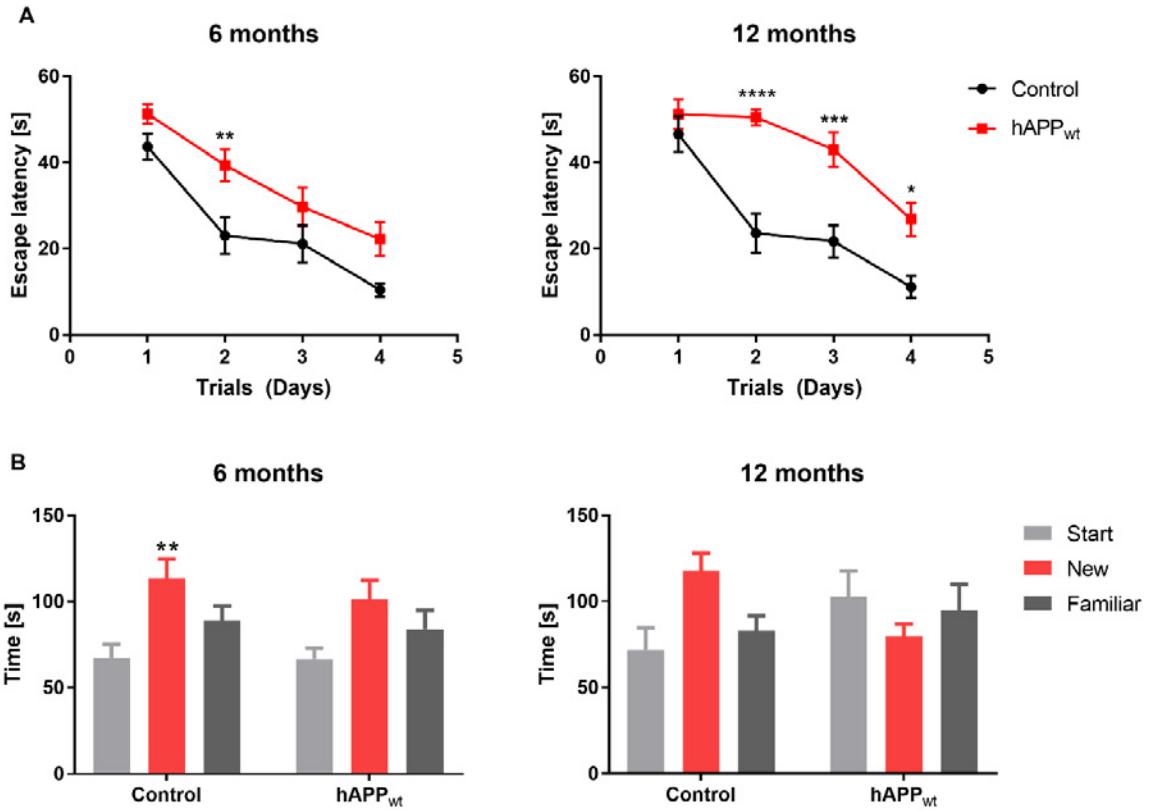

Figure 4. Performance of hAPP$_{wt}$ mice vs. wild type littermates (6 and 12 months) in Morris water maze and modified Y-maze. (**A**) Escape latency in invisible platform trials. Significant difference between hAPP$_{wt}$ (n=16) and WT (n=12) at 6 months on second trial day. (**B**) Significantly impaired spatial memory in hAPP$_{wt}$ (n=8) vs WT (n=12) at 12 months. (**C**) Impaired spatial learning and memory in hAPPwt (n=16) vs. WT (n=12) at 6 months following exploration of new vs familiar arms of the modified Y-maze. D) No significant difference between hAPPwt (n=8) and WT (n=12) in modified Y-maze at 12 months. Values are means ±SEM ; * P≤0.05, ** P≤0,01, *** P≤0,001, **** P≤0,0001, 2-way ANOVA.

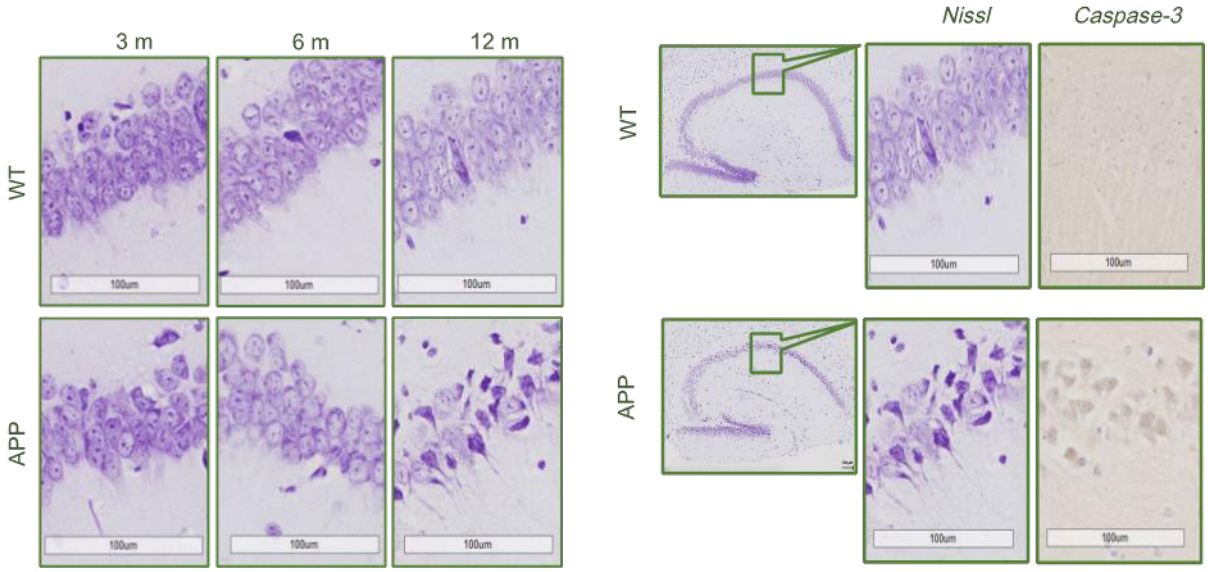

Figure 5. Morphology of CA1 region in hAPPwt 3, 6 and 12 months. Left panels show a pronounced neuronal death in hAPP hippocampi at 12 months. Right panels present caspase-3 immunostaining.

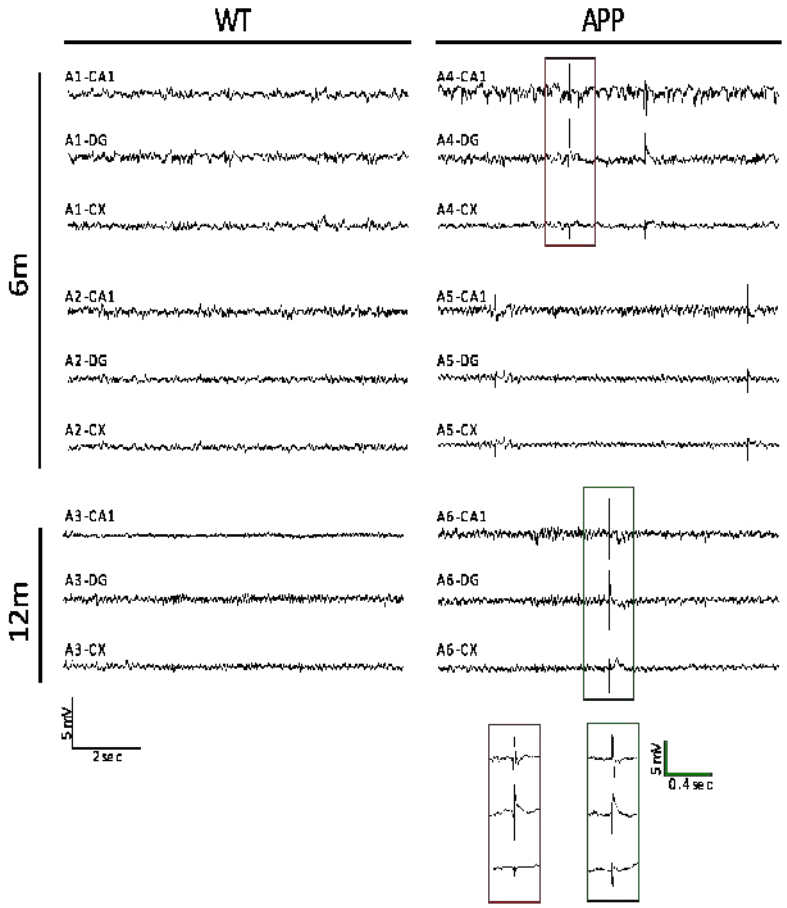

Figure 6. Intracerebral EEG (CA1, DG and cortex) in WT and hAPP mice. Note the abnormal epileptiform spikes.

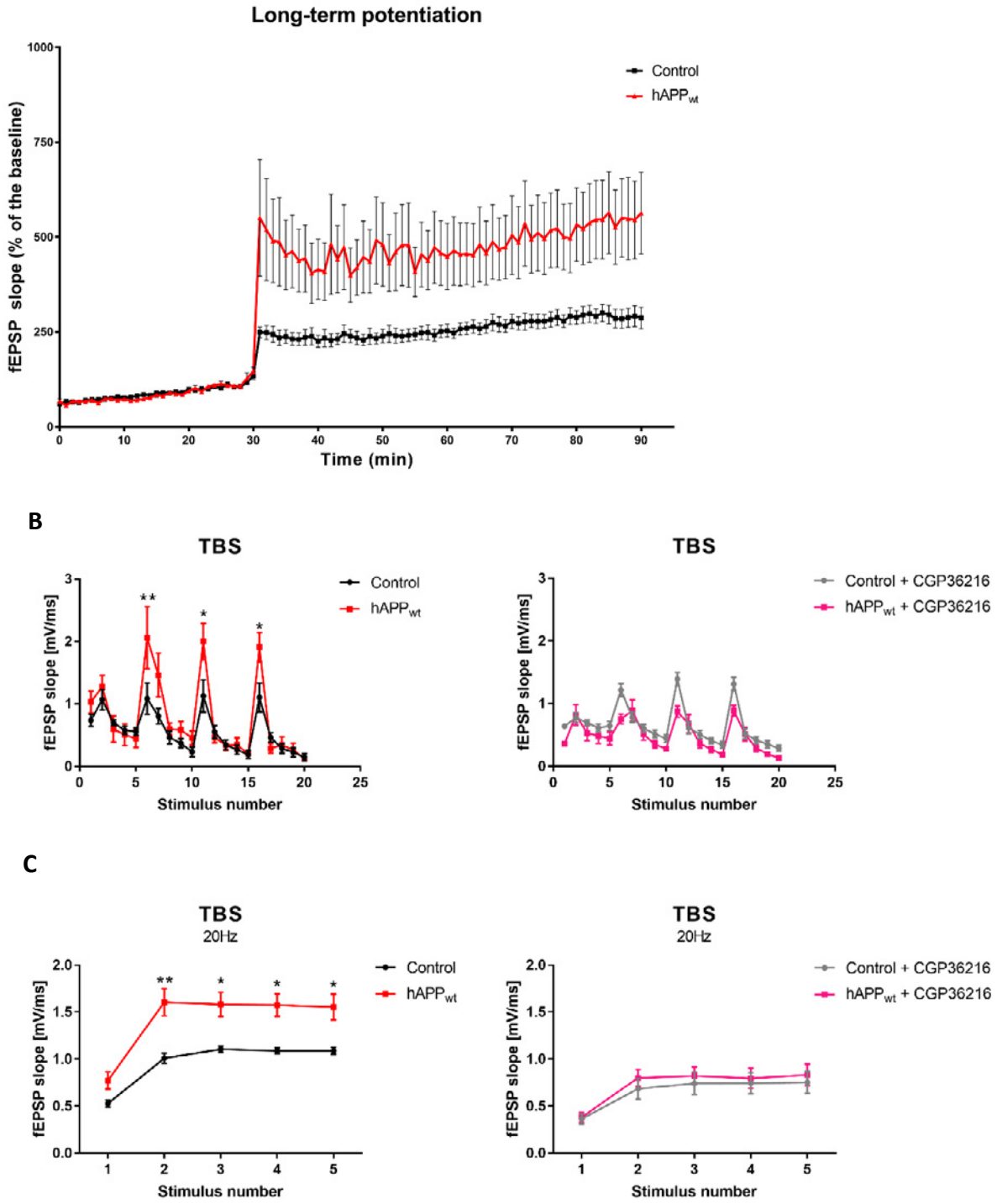

Figure 7. Electrophysiological characterization. (**A**) LTP induced by a theta burst. (**B**) TBS response and (**C**) response to 20 Hz stimulation in the absence or in the presence of CGP36216, an inhibitor of presynaptic $GABA_B$ receptors.

Geneeskundige Stichting Koningin Elisabeth
Fondation Médicale Reine Elisabeth
Königin-Elisabeth-Stiftung für Medizin
Queen Elisabeth Medical Foundation

Progress report of the interuniversity research project of

Prof. dr. Sebastiaan Engelborghs (VUB)
Prof. dr. Chris Baeken (UGent)

Prof. dr. Sebastiaan Engelborghs
Vrije Universiteit Brussel (VUB)
Center for Neurosciences (C4N)
Laarbeeklaan 103, 1090 Brussel

Prof. dr. Chris Baeken
Universiteit Gent
Department of Psychiatry & Neuropsychology
C. Heymanslaan 10, 9000 Gent

Unraveling the link between depression and dementia to improve diagnostic and treatment options

1. Systematic literature review on the relationship between late-life depression and incident dementia.

Publication: *Wiels W, Baeken C, Engelborghs S. Depressive Symptoms in the Elderly-An Early Symptom of Dementia? A Systematic Review. Front Pharmacol. 2020;11:34. Published 2020 Feb 7. doi:10.3389/fphar.2020.00034*

1.1. Abstract

Background: Depression and dementia are common incapacitating diseases in old age. The exact nature of the relationship between these conditions remains unclear, and multiple explanations have been suggested: depressive symptoms may be a risk factor for, a prodromal symptom of, or a coincidental finding in dementia. They may even be unrelated or only connected through common risk factors. Multiple studies so far have provided conflicting results.

Objectives: To determine whether a systematic literature review can clarify the nature of the relation between depressive symptoms and dementia.

Methods: Using the Patient/Problem/Population, Intervention, Comparator, Outcome or PICO paradigm, a known framework for framing healthcare and evidence questions, we formulated the question "whether depressive symptoms in cognitively intact older adults are associated with a diagnosis of dementia later in life." We performed a systematic literature review of MEDLINE and PsycINFO in November 2018, looking for prospective cohort studies examining the aforementioned question.

Results: We critically analysed and listed 31 relevant papers out of 1,656 and grouped them according to the main hypothesis they support: depressive symptoms as a risk factor, not a risk factor, a prodromal symptom, both, or some specific other hypothesis. All but three studies used clinical diagnostic criteria for dementia alone (i.e., no biomarkers or autopsy confirmation). Several studies contain solid arguments for the hypotheses they support, yet they do not formally contradict other findings or suggested explanations and are heterogeneous.

Conclusions: The exact nature of the relationship between depressive symptoms and dementia in the elderly remains inconclusive, with multiple studies supporting both the risk factor and prodromal hypotheses. Some provide arguments for common risk factors. It seems unlikely that there is no connection at all. We conclude that at least in a significant part of the patients, depressive symptoms and dementia are related. This may be due to common risk factors and/or depressive symptoms being a prodromal symptom of dementia and/or depression being a risk factor for dementia. These causal associations possibly overlap in some patients. Further research is warranted to develop predictive biomarkers and to develop interventions that may attenuate the risk of "conversion" from depressive symptoms to dementia in the elderly.

2. Research stay (February – April) at the University of Maastricht. (WP1)

Research stay abroad by PhD student Wietse Wiels. Data collection and cleaning in the broader multicenter Amyloid Biomarker Project (>10.000 subjects) of the Limburg Alzheimer Centre (information in Dutch: www.alzheimercentrumlimburg.nl/2016-amyloid-biomarker). Local contacts: Dr. Willemijn Jansen, Prof. Dr. Frans Verhey.

This is a major epidemiological data collection project, including individuals with known amyloid status (either by CSV analysis, amyloid-PET, or both), that are recruited by contacting centers using these biomarkers in their publications. Subjects included are healthy volunteers or suffer from SCD, MCI, or dementia. Various amounts of medical comorbidities and other epidemiological data are available for these subjects. This initiative produces multiple high-impact publications: e.g. doi:10.1001/jamapsychiatry.2017.3391, doi:10.1001/jama.2015.4668).

We screened the available data for availability of information on depressive symptoms/a history of depression, and contacted collaborating centers on missing information, in order to obtain as large a sample as possible. We also collaborated on a similar project examining the role of vascular risk factors.

We planned future analyses, to be started upon completion of data collection and linking.

The research stay ended prematurely due to the covid-19 pandemic. Due to restrictions in data access from a distance and frequent prohibitions on crossing the Belgium-Netherlands border and physically working at the university, several aspects of this project experienced delays.

3. Evaluation of parameters of depression in an existing *Behavioral and Psychological Symptoms of Dementia (BPSD)* database

We evaluated the relationship between cognitive status, amyloid positivity, and depressive symptoms in an existing database of MCI patients from Antwerp. This resulted in an abstract that was accepted as a poster presentation at the (online) Alzheimer's Association International Congress (AAIC) in July 2020 – *Wiels W, Nous A, Wittens M, Engelborghs S. Cerebrospinal fluid amyloid status and affective symptoms in Mild Cognitive Impairment.*

3.1. Abstract:

Background: Affective and cognitive symptoms are common in old age, and frequently overlap in clinical practice. Mild cognitive impairment (MCI), for example, is a risk state for later dementia where neuropsychiatric symptoms such as depression and anxiety are common. The exact nature of this overlap remains unclear - affective symptoms may be both causative of cognitive issues, they may be related to an underlying neurodegenerative disease, or may stem from common risk factors. Biomarkers of brain diseases such as Alzheimer's can help determine the etiology of MCI and aid in predicting the risk of progression to dementia. Aims: To determine whether CSF-based amyloid positive and amyloid negative individuals with MCI differ in the nature and prevalence of affective symptoms.

Method: An existing database of 476 individuals with MCI will be used. All subjects underwent extensive cognitive and behavioral assessment at baseline and follow-up (up to 7 years). Behavior was assessed covering a period of 2 weeks prior to inclusion and at each follow-up visit

using a battery of behavioral assessment scales: Middelheim Frontality Score (MFS), Behave-AD, Cohen-Mansfield Agitation Inventory, Cornell Scale for Depression in Dementia and Geriatric Depression Scale (30 items). In a significant subgroup of these patients (N=97), the standard AD CSF biomarkers (A, T-tau, P-tau181) have been analyzed. We will evaluate whether subgroups with differing amyloid status (i.e. normal vs. abnormal CSF biomarkers) are significantly different in the nature and prevalence of affective symptoms as determined by several scales (Behave-AD, Geriatric Depression Scale, Cornell Scale for Depression in Dementia).

Results: Amyloid Positive and Negative groups differed significantly in Tau and Phospho-Tau values, and slightly in MMSE value. We found no clear difference in various behavioral scales between groups. Conclusion: In a historic cohort of MCI patients, we found no clear difference in the nature and prevalence of affective symptoms when comparing (CSF-based) amyloid positive and negative groups. Since full data was available for only 72 individuals, this evaluation was possibly underpowered. It should be reproduced on larger datasets.

4. 'Depressive Symptoms and Risk of Dementia (DSDR)' study (WP2)

The protocol for this study was drafted, reviewed, and finished. It aims to examine the prognostic relevance of depressive symptoms and amyloid status in the elderly, through a prospective evaluation of healthy controls, depressed patients, and the cognitively impaired (all groups >65 years of age). All groups will receive serial clinical, imaging, neuropsychological as well as affective/behavioural, and neurochemical assessment. Furthermore, the added value of plasma-based amyloid tests will be evaluated. Due to the covid-19 pandemic and its consequences on healthcare and research, both the final approval by the ethical committee and the possibility of recruiting participants were delayed. We expect this study to start recruiting during Q1 2021.

5. 'Neuromodulation in the elderly depressed: a brain imaging approach' study (WP3)

The protocol for this study was drafted, reviewed, and finished. It will evaluate neurostimulatory techniques on the elderly depressed, and the impact of this treatment on imaging parameters. FAGG agreement (since it includes medical devices) was obtained. Ethical committee review is ongoing. As in the above study, the covid-19 pandemic delayed several aspects of this study. Recruitment is expected to start during Q1 2021.

6. Recruitment of a research nurse: budget implications

As budgeted, we recruited a research nurse to be appointed on this project. Miss Sifra Müller will spend half of her time at UGent, and half at the VUB. As the recruitment of subjects was not able to start before Q1 2021 due to the covid-19 pandemic, the contract was made effective on January 1st 2021. **We thus did not use any money of the budget till this date, and would like to ask GSKE if we could obtain a budget-neutral prolongation of our project with one year.**

Geneeskundige Stichting Koningin Elisabeth
Fondation Médicale Reine Elisabeth
Königin-Elisabeth-Stiftung für Medizin
Queen Elisabeth Medical Foundation

Progress report of the interuniversity research project of

Prof. dr. Vincent Van Rompaey (UAntwerpen)
Prof. dr. Peter Ponsaerts (UAntwerpen)
Prof. dr. Guy Van Camp (UAntwerpen)
Prof. Rik Gijsbers (KU Leuven)

Prof. dr. Vincent Van Rompaey (UAntwerpen)
Experimental laboratory of Translational Neurosciences Dept. of Translational Neurosciences
University of Antwerp
Universiteitsplein 1
2610 Antwerp, Belgium
vincent.vanrompaey@uantwerpen.be

Prof. dr. Peter Ponsaerts (UAntwerpen)
Laboratory of Experimental Hematology Vaccine and Infectious Disease Institute University of Antwerp
Universiteitsplein 1
2610 Antwerp, Belgium
Peter.Ponsaerts@uantwerpen.be

Prof. dr. Guy Van Camp (UAntwerpen)
Human Molecular Genetics laboratory
Center of Medical Genetics, University of Antwerp
Universiteitsplein 1
2610 Antwerp, Belgium
guy.vancamp@uantwerpen.be

Prof. Rik Gijsbers (KU Leuven)
Laboratory of Viral Vector Technology and Gene Therapy Department of Pharmaceutical and Pharmacological Sciences Faculty of Medicine, KU Leuven
RK-Herestraat 49, box 1023
3000 Leuven, Belgium
Rik.Gijsbers@kuleuven.be

Dr. Erwin Van Wijk
Department of Otorhinolaryngology
Radboud University Nijmegen Medical Center Geert Grooteplein 10
6525 GA Nijmegen, The Netherlands
Erwin.vanWyk@radboudumc.nl

Dr. Erik De Vrieze
Departments of Otorhinolaryngology and Human Genetics Radboud University Medical Centre
Geert Grooteplein Zuid 10
P.O. box 9101, 6500 HB
Nijmegen, The Netherlands

Development of allele-specific CRISPR-nuclease gene therapy for late-onset sensorineural hearing impairment in a new humanized DFNA9 mouse model

Work-package 1: The new DFNA9$^{hP51S/hWT}$ mouse model is in the last stage of generation at Genoway (expected to be ready in February 2021). The development had some delay due to the Covid pandemic. In February we will start with the backcrossing of the DFNA9$^{hP51S/hWT}$ mice with the C57BL/6 (Cdh23$^{753A>G}$) mice to correct the mutation that leads to early deafness in the BL6 background. The C57BL/6 (Cdh23$^{753A>G}$) mice were purchased from the MRC Maxwell institute in October 2019 and have been bred in the animal facility of the University of Antwerp for over a year to obtain a population of 300 mice (150 for the injection experiments (WP2) and the others for backcrossing with the DFNA9$^{hP51S/hWT}$ mice). In addition, we sequenced the Cdh23 gene of this mice to confirm that the Cdh23$^{753A>G}$ mutation was corrected and the mice were tested at the age of 1 year to assess vestibular and hearing function. Results showed that their vestibular function and hearing thresholds were indeed not affected at the age of 1 year. The patient organisation supported the purchase of a device to measure the Vestibular Ocular Reflex (VOR) (device arrived in October 2020) which is an objective tool to assess vestibular function in mice. We will use this technique to follow up the vestibular function of our new DFNA9$^{hP51S/hWT}$ mouse model.

Work-package 2: This experiment had some delay due to the Covid pandemic but in January 2021 we will start with rAAV injection in the inner ear of C57BL/6 (Cdh23$^{753A>G}$) mice. We already obtained 8 rAAV2 serotypes from the Viral Vector Core of the KU Leuven expressing eGFP and luciferase to follow-up transduction efficiency. We will inject these rAAV2 serotypes in the inner ear of C57BL/6 (Cdh23$^{753A>G}$) mice by using the posterior semi- circular canal approach. Eight different groups (n=10) will be injected with rAAV as well as a control group that will be injected with PBS and a control group that will not be injected. Mice will be tested for vestibular and hearing function at baseline (before injection) and one and two weeks after injection to assess safety of viral virus injection in the inner ear of mice. After one- and two-weeks mice will undergo bioluminescence to follow up transduction efficiency and finally after two weeks mice will be euthanized and we will look at eGFP expression in the fibrocytes of the spiral ligament to assess transduction efficiency. The two best performing viral vectors will be used to assess long-term safety. In this experiment (expect to start in May 2021) we will inject 4 groups of mice with rAAV (two doses of each AAV will be used) and one control group (n=10). All mice will be assessed longitudinally at the age of 3, 6, 9, 12, 15, 18 and 21 months by BLI as well as for hearing and vestibular function.

Work-package 4: injections with the chosen rAAV (WP2) encoding the chosen CRISPR nuclease and suitable gRNA sequences (WP3) will be performed at our new DFNA9$^{hP51S/hWT}$ mouse model. We expect that backcrossing of the DFNA9$^{hP51S/hWT}$ mice with the C57BL/6 (Cdh23$^{753A>G}$) mice and breeding of these mice to obtain a bigger population will take over a year. This experiment is expected to start in May 2022 where we will look at the genome editing efficiency of the different gRNA's in DFNA9$^{hP51S/hWT}$ mice.

Work-package 5: when WP4 is completed we can finally evaluate if the CRISPR nuclease can prevent hearing and vestibular loss in our new DFNA9$^{hP51S/hWT}$ mouse model. We expected to inject our DFNA9$^{hP51S/hWT}$ mouse model with the established CRISPR based gene therapy in October 2022.

1. Use of GSKE budget:

The GSKE budget was used for the maintenance and breeding of the C57BL/6 (Cdh23$^{753A>G}$) mice in the animalarium of the University of Antwerp. Furthermore, in the last year, different protocols for histological analyses that are needed to complete the work-packages were tested and optimized.

- Whole mount dissection of the Organ of Corti to stain hair cells, neurons and synapses.
- Cryosectioning of the inner ear in order to visualize coch expression and inflammation in the spiral ligament.

The GSKE budget was used to purchase material and antibodies for the optimization of these IHC stainings.

Geneeskundige Stichting Koningin Elisabeth
Fondation Médicale Reine Elisabeth
Königin-Elisabeth-Stiftung für Medizin
Queen Elisabeth Medical Foundation

Progress report of the interuniversity research project of

Prof. dr. An Goris (KU Leuven)
Prof. Nathalie Cools (UAntwerpen)

Prof. dr. An Goris (KU Leuven)
Department of Neurosciences
Laboratory for Neuroimmunology
T +32 16 33 07 72
an.goris@kuleuven.be

Prof. Nathalie Cools (UAntwerpen)
Laboratory for Experimental Hematology
University of Antwerp
nathalie.cools@uza.be

Table of contents

Deep sequencing of myelin-reactive T-cells to elucidate new disease mechanisms and identify correlates for treatment responsiveness in multiple sclerosis

1. Summary and current status of research program

Multiple sclerosis (MS) is one of the most common neurological disorders in young adults, affecting around 10,000 people in Belgium and 2.5 million worldwide. The disease can lead to important physical as well as cognitive disability at a time that is crucial in the personal and professional development of patients. MS is characterized by three hallmarks: inflammation, demyelination and neuronal loss[1]. The exact cause of MS still remains to be elucidated but the past few years have seen exciting progress in the field. Over the last decade, we have – in an international collaborative context as part of the International Multiple Sclerosis Genetics Consortium (IMSGC) – identified >230 genetic risk factors for MS. These include several risk as well as protective variants in the Human Leukocyte Antigen (HLA) region[2], which in combination with the T- and B-cell receptor likely determine the target of the autoimmune reaction[3], and 200 variants throughout the genome, enriched for immunological function and implicating the interplay between B-cells, T-cells, and innate immune cells[4-8]. Hence, the complex interactions between the identified genetic and environmental factors affect the predominantly immune-mediated underlying mechanisms of the disease.

With previous GSKE support (A. Goris, 2017-2019 and Prize Viscountess Valine de Spoelberch), we focused on the role of B-cells and demonstrated an imbalance between pathogenic and immunoregulatory B-cells in MS that is amenable to treatment[9-11] (Smets et al., *Brain Commun*, revision submitted). Besides, it is currently generally accepted that autoimmunity against antigens expressed in the central nervous system (CNS) is mediated by T-cells. Indeed, $CD4^+$ T-cells, in particular Th1 and Th17 cells, directed towards various myelin-derived antigens, including myelin basic protein (MBP), proteolipid protein (PLP), myelin oligodendrocyte glycoprotein (MOG) and B-crystallin have been identified in patients with MS[12-15], and are shown to migrate between blood and CNS[16,17]. Nonetheless, these autoreactive T-cells that are thought to be the culprit in MS form a very small subset in the peripheral blood which has hampered their investigation.

Thanks to the previous and current support of GSKE, we were able to implement state-of-the-art genetic methods allow to analyze DNA and RNA at the level of single B- or T-cells (single-cell sequencing) (Van Horebeek et al., manuscript in preparation). This makes it now timely to turn our attention to a detailed understanding of their characteristics that make them pathogenic in MS. The combined expertise of our interuniversity team in immunology and characterization of autoreactive T-cells (N. Cools, U Antwerp) on the one hand and in genetics and single-cell sequencing (A. Goris, KU Leuven) on the other makes it now feasible, timely and innovative to investigate the pathogenic characteristics of autoreactive T-cells in MS. For this, the following three aims have been set forth:

1. What is the TCR repertoire of autoreactive T-cells in MS?
2. What are the transcriptional characteristics of autoreactive T-cells?
3. Can the autoreactive T-cell clonotype repertoire be used as a correlate for therapy responsiveness?

2. Achievements

2.1. Achievement 1. TCR repertoire of autoreactive T-cells in MS

1. Summary

T-cells recognize complexes of specific antigenic peptides and autologous HLA molecules through their TCR. In fact, the TCR sequence functions as a unique fingerprint for each T-cell. Hence, analysis of T-cell clonal expansion can allow the identification of T-cells that are assumed to be involved in the disease process. Since autoreactive T-cells may occur naturally in less than 1 in 300 T-cells[18], clonal expansion by activation and proliferation of antigen-specific T-cells can be provoked by *ex vivo* recognition of antigen.

2. Current status

N. Cools has established a unique protocol for enrichment of autoreactive T-cells using a broad antigen panel, and this protocol has been transferred to the lab of A. Goris so that both sites apply the same methodology according to shared protocols for this project. PBMCs will be stimulated *in vitro* in the presence of a selected panel of myelin oligodendrocyte glycoprotein (MOG)-, myelin basic protein (MBP)-, and proteolipid protein (PLP)-derived synthetic peptides that has previously been demonstrated as immunodominant[12-15] and acting in part independently of HLA-DR[13,19,20]. Myelin-reactive T-cells are observed using flow cytometric detection of the CD154 (for $CD4^+$) or CD137 (for $CD8^+$) T-cell activation marker following one-week stimulation of T-cells with a pool of myelin-derived peptides (Figure 1). Using this methodology results in an average of 0.35% of $CD4^+$ and 0.71% of $CD8^+$ T cells in MS patients being characterized as autoreactive.

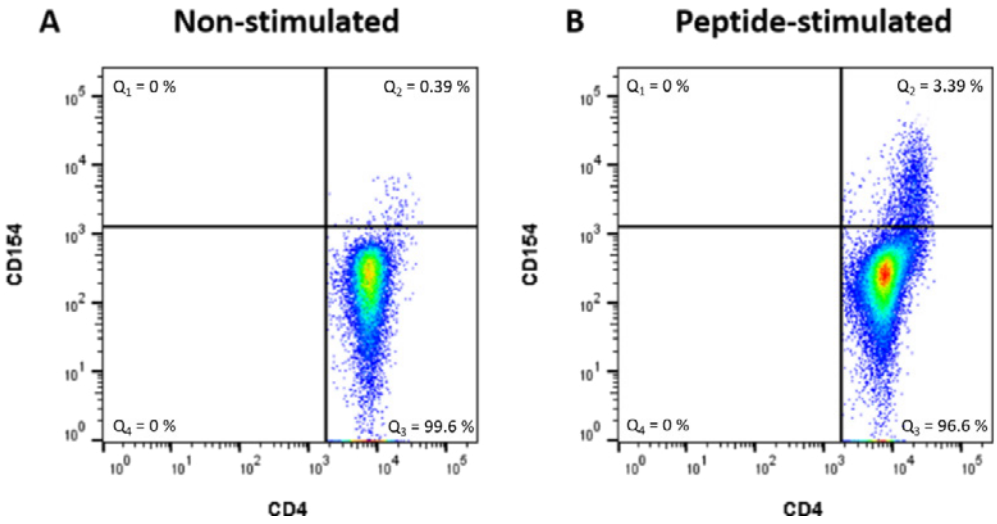

Figure 1. Representative dotplot of myelin-reactive CD154-positive T-cells in a MS patient. (A) indicates the activated $CD4^+$ T-cells from unstimulated cells in quadrant Q2, while (B) depicts the activated $CD4^+$ T-cells after myelin-derived peptide stimulation in quadrant Q2.

We will use these sorted autoreactive $CD4^+$ and/or $CD8^+$ T-cells as input for the Chromium Single Cell V(D)J Solution on the 10x Genomics[21] platform available at our institution. We will obtain full-length V(D)J sequences and pair and sequences to establish TCR repertoires of autoreactive T-cells on a cell-by-cell basis. For that purpose, we have now implemented the Chromium Single Cell V(D)J Solution on the 10x Genomics[21] platform available at KU Leuven and the bio-informatics pipelines necessary to identify clonal expansions based on identical or highly identical immune cell receptors (Van Horebeek et al., manuscript in preparation).

Similarly, patient-derived myelin-specific CD4+ T cells are single-cell sorted using FACS, followed by an RT-PCR using 76 TCR-primers, by the Antwerp team. The products are used in a second and third PCR reaction, incorporating individual barcodes into each well. Libraries are purified and sequenced using the Illumina MiSeq platform, after which the resulting paired-end raw sequencing reads are assembled and deconvoluted using barcode identifiers at both ends of each sequence. The resulting sequences are then analyzed using the program MiXCR and the CDR3 nucleotide sequences are extracted and translated. First sequencing results were translated into the full functional sequence of a patient-derived MBP_{85-99}-specific and MOG_{97-109}-specific TCR and the development of their TCR-encoding constructs. Their expression was tested in two TCR-deficient T cell lines (2D3 and SKW-3) by means of TCR-encoding mRNA electroporation. Our preliminary data show a transgene MBP85-99-TCR expression as high as 90% over the course of 4 days (Figure 2).

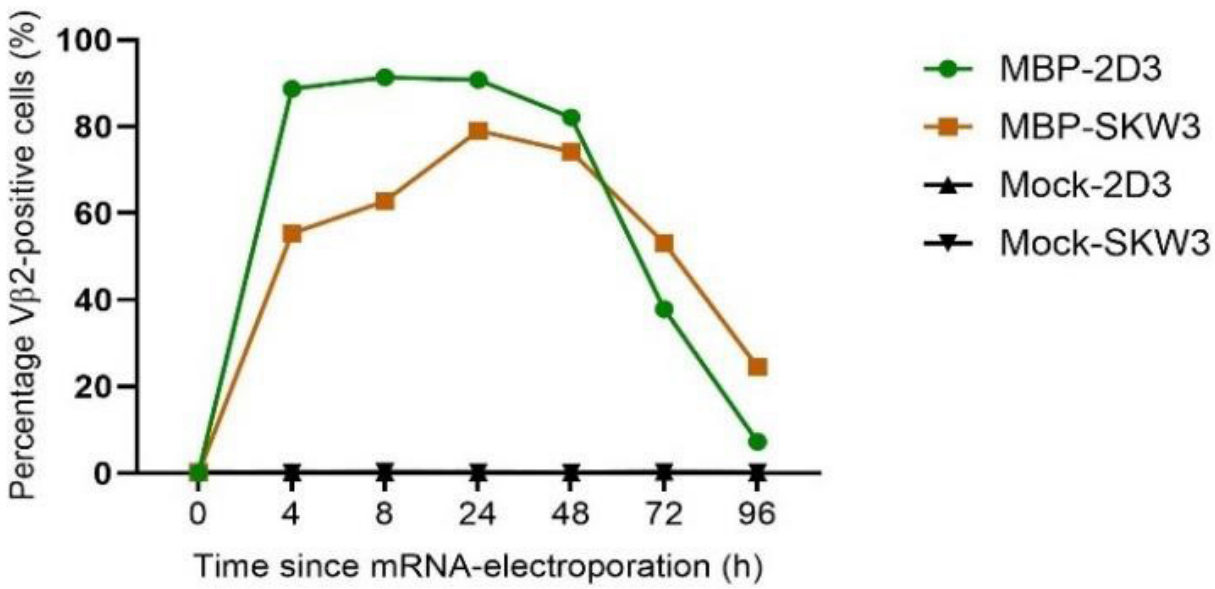

Figure 2: MBP85-99-TCR-encoding mRNA electroporation of TCR-deficient T cell lines. Transgene MBP85-99-TCRexpression is visualized using flow cytometry and a fluorochrome-labeled antibody to V2, binding the variable domain of the newly introduced TCR. As a negative control, a MOCK condition is used, to which no mRNA is added.

3. Future plans

We will perform further validation of the protocol for autoreactive T-cell selection, including demonstrating the repeatability. We will also confirm the relevance of this selection of myelin peptides in MS pathogenesis in our setting. This was previously demonstrated by others for a similar protocol through a positive T-cell proliferative response to this peptide mix in 74% of RR-MS patients as compared to 30% of healthy controls[22]. Subsequently, we will extend the single-cell sequencing pipelines from B-cell receptor to T-cell receptor repertoire. Moreover, we envisage to be able to test different myelin-specific TCRs with different affinities and avidities[23].

Finally, we will investigate using this methodology peripheral blood mononuclear cells (PBMCs) from newly diagnosed and untreated patients diagnosed with MS according to the revised McDonald criteria[24] (N=15). Access to patient samples is possible by already existing collaborations of both PIs with University Hospitals Leuven (Prof. B. Dubois) and Antwerp (Dr. B. Willekens), respectively.

2.2. Achievement 2. Transcriptional characteristics of autoreactive T-cells.

1. Summary

Autoreactive cells in WP1 undergo proliferation and activation as part of the enrichment, which may influence their transcriptome but not TCR. We can, however, use the TCR "fingerprint" of autoreactive T-cells established in WP1 to identify these autoreactive cells amongst *ex vivo* T-cells in WP2. As TCR is a critical determinant of T-cell fate, we will establish whether autoreactive T-cells have related transcriptional programs as previously demonstrated in mice[25].

2. Current status

From PBMCs as collected above, we have sorted ($CD4^+$/$CD8^+$) T-cells using negative selection magnetic beads (EasySep) as input for the 10x Genomics Chromium Single Cell Solution. We established the required bio-informatics pipelines. Data are processed using CellRanger v3.0.2 and further analyzed with Seurat v3.0.0. Bio-informatics. Differentially expressed genes for each cluster are identified and clusters are annotated. A representative example for all T-cells is given in Figure 3.

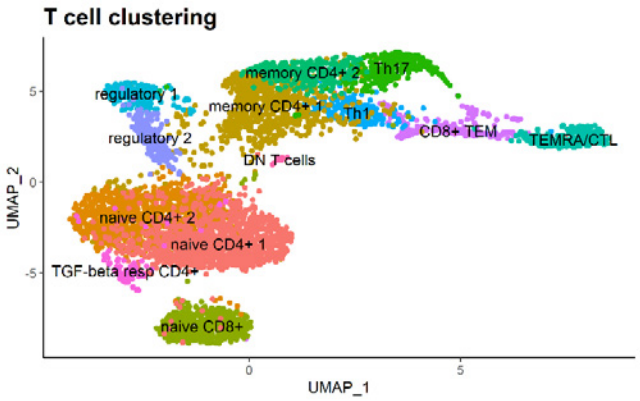

Figure 3. Representative clustering and annotation of single-cell transcriptomics from a T cell sample.

3. Future plans

Based on the single-cell transcriptome and immune cell receptor repertoire data of WP1 and WP2, we will overlay autoreactive T-cells as determined by their TCR fingerprint. This will indicate whether autoreactive T-cells have related transcriptomes within and across patients, and to characterize differentially expressed genes.

2.3. Achievement 3. The autoreactive T-cell clonotype repertoire as a correlate for therapy responsiveness.

1. Summary

Whereas careful patient monitoring is essential in the development path of novel therapies for MS, conventional outcome measures do not correlate well with long-term disability. Alternatively, immunological assays may provide a valuable alternative as measures of the effect of this and other immunotherapies. In this perspective, the sequences of myelinreactive T-cells from blood could be used to track T-cells from the same clone over time.

2. Current status

First, we assessed the kinetics of myelin-specific autoreactive T-cell responses in MS patients. For this, we conducted a prospective cohort study in the MS clinic of the Antwerp University Hospital. PBMC were isolated from 14 MS patients treated with natalizumab at different time points. The mean age of the patients was 41.36 years (SD 10,20, range 24-59). The median EDSS score was 2.0 (range 1-6). Disease duration since first symptoms ranged between 1 year and 20 years (median 8,13 years). Duration of treatment with natalizumab ranged between 6 months

and almost 10 years (median 2.25 years). PBMCs were stimulated *in vitro* in the presence of a selected panel of myelin oligodendrocyte glycoprotein (MOG)-, myelin basic protein (MBP)-, and proteolipid protein (PLP)-derived synthetic peptides, as described in WP1. Next, the frequency of myelin-specific autoreactive T cells was determined using IFN-gamma ELISPOT and analysis. We found that T-cell reactivity towards a mixture of myelin-peptides in natalizumab treated MS patients is highly variable. Whereas 80% of patients demonstrate myelin reactivity at baseline, only 30-40% of patients demonstrate myelin-specific autoreactive T cells at every time point that was assessed longitudinally (t=0, t= 8 weeks, t=12 weeks, t= 24 weeks). This underlines that the baseline presence of autoreactive T cells in the peripheral blood of MS patients may be a critical factor when investigating rare cell populations. The observed high intra-patient variability poses some challenges for current project and warrants further investigation.

3. Future plans
We will follow the T-cell repertoire fingerprint in MS patients receiving tolDC treatment, as previously described in MS patients treated with stem cell transplantation[26]. For this, paired PBMCs banked in the context of the clinical trial evaluating the feasibility and safety of the use of tolDC loaded with the selected pool of peptides for the treatment of MS (ClinicalTrials.gov Identifier: NCT02618902), before and after the cell therapy vaccination cycle (N=9x2), will be analyzed as in WP1.

3. Networking and collaborations

Building on expertise gained with GSKE support (A. Goris, 2017-2019 and Prize Viscountess Valine de Spoelberch), the current GSKE project (2020-2022) was set up in collaboration with Prof. Nathalie Cools (U Antwerpen) and was awarded.

Prof. An Goris recently became coordinator of the International Multiple Sclerosis Genetics Consortium (www.imsgc.org), and her research group is a member of the EU Horizon2020 Consortium MultipleMS (www.multiplems.eu).

Prof. Nathalie Cools is the coordinator of the EU H2020 Restore project https://cordis.europa.eu/project/rcn/213047_en.html, promotor of the EU-EFRO Anicells project (1108, https://www.vlaio.be/nl/andere-doelgroepen/europees-fonds-voor-regionale-ontwikkeling-efro/ontdek-efro-vlaanderen/overzicht) and consortium beneficiary of the EU H2020 Marie Curie Training network INsTRuCT, a network of European scientists from academia and industry focused on developing innovative myeloid regulatory cell (MRC)-based immunotherapies.

Over the project duration, members of our research groups attended the online European Conference on the Treatment and Research in Multiple Sclerosis (ECTRIMS) MSVirtual, the online MS Data Alliance Meeting and the online European Charcot Foundation Meeting.

4. Relevance and future perspectives

The relevance of clonal expansions in MS – as recognized in other autoimmune diseases such as rheumatoid arthritis – sprouts, with very recent single-cell sequencing studies demonstrating clonal expansions of both B- and T-cells in MS[27-29]. However, characterization of culprit and favorable clonal expansions is sparse, which is where our approach adds novelty. We anticipate that T-cell repertoire sequencing and transcriptomic profiling of autoreactive T cells will become a critical tool in both biomedical discovery and clinical management of patients.

Moreover, recent advances in TCR and chimeric antigen receptor (CAR) engineering may provide prospects for patient-specific treatment strategies with fewer side effects. Indeed, there is a significant and unmet need for safe and effective therapies for MS that are well-tolerated and target the cause of disease to reduce duration and frequency of therapy and to limit side-effects. A better alternative to systemic treatment of inflammation with generalized immunosuppressants would be specific therapies that target only the detrimental and aberrant immune response against the specific disease-associated antigen(s) involved. This approach is known as antigen-specific therapy. While the antigen-specific activation of pathogenic T-cells is considered essential in the initiation and maintenance of MS, leveraging the body's attempt to prevent autoimmunity, i.e. tolerization, focuses on the underlying cause of the disease and could be the key to solving neuro-inflammation.

Finally, the identification of expanded autoreactive TCRs may allow administration of TCR-specific inhibitors in both acute and chronic autoimmune disease, or eventually a new paradigm of targeted T-cell depletion for these disorders.

5. Financial report

As foreseen, GSKE project support has been assigned for consumable costs dedicated to this project. The support of the Prize Viscountess Valine de Spoelberch has been used to attract new staff, thereby ensuring continuity of the research group, and consumable costs. The UA and KU Leuven Financial Departments will provide a detailed report.

The Covid-19 pandemic has resulted in lab closure in March-April and reduced lab activity due to restrictions on the number of researchers that are allowed to work in the lab at the same time for the remainder of 2020. Hence, we have shifted some of the wet-lab work to later in the project and moved bio-informatics work to earlier in the project. As our universities provided the necessary structure to efficiently carry out bio-informatics work remotely (remote network access, high-throughput computing cluster, …), this has allowed us to make substantial progress during the first year of this project, albeit with an altered project time-planning. This also means that part of the budget of the GSKE support will be transferred to the upcoming years.

6. Publications under GSKE support 2020

* indicates shared first/senior authors and @ indicates corresponding author

- Van Horebeek L., Goris A.@ Transcript-specific regulation in T-cells in multiple sclerosis susceptibility. *European Journal of Human Genetics* (invited Comment), *28* (7), 849-850. IF 3.65
- Janssens I@, Cools N. (2020) Regulating the regulators: Is introduction of an antigen-specific approach in regulatory T cells the next step to treat autoimmunity? *Cell Immunol*; 358:104236. IF 4.078

7. Team publications 2020

* indicates shared first/senior authors and @ indicates corresponding author

- Smets, I.*, Goris, A.*, Vandebergh, M., Demeestere, J., Sunaert, S., Dupont, P., Dubois, B. (2021). Quantitative MRI phenotypes capture biological heterogeneity in multiple sclerosis patients. *Scientific Reports*, 11(1):1573. IF 3.998
- Vandebergh, M., Goris, A. @ (2020). Smoking and multiple sclerosis risk: a Mendelian randomization study. *Journal of Neurology*, 267, 3083–3091. IF 3.783
- Oldoni, E., Smets, I., Mallants, K., Vandebergh, M., Van Horebeek, L., Poesen, K., Dupont, P., Dubois, B.*, Goris, A.*@ (2020). CHIT1 at Diagnosis Reflects Long-Term Multiple Sclerosis Disease Activity. *Annals of Neurology*, 87 (4), 633-645. IF 9.037
- Van Horebeek L., Goris A.@ Transcript-specific regulation in T-cells in multiple sclerosis susceptibility. *European Journal of Human Genetics* (invited Comment), *28* (7), 849-850. IF 3.65
- Derdelinckx J@, Nkansah I, Ooms N, Van Bruggen L, Emonds MP, Daniëls L, Reynders T, Willekens B, Cras P, Berneman ZN, Cools N. (2020) HLA Class II Genotype Does Not Affect the Myelin Responsiveness of Multiple Sclerosis Patients. *Cells*; 9 (12): 2703. IF 4.829
- Janssens I@, Cools N. (2020) Regulating the regulators: Is introduction of an antigen-specific approach in regulatory T cells the next step to treat autoimmunity? *Cell Immunol*; 358:104236. IF 4.078
- Joossen C, Baán A, Moreno-Cinos C, Joossens J, Cools N, Lanckacker E, Moons L, Lemmens K, Lambeir AM, Fransen E, Delputte P, Caljon G, Van Der Veken P, Maes L, De Meester I, Kiekens F, Augustyns K, Cos P@. (2020) A novel serine protease inhibitor as potential treatment for dry eye syndrome and ocular inflammation. Sci Rep.; 10 (1): 17268. IF 3.998
- Maes E, Cools N, Willems H, Baggerman G@. (2020) FACS-Based Proteomics Enables Profiling of Proteins in Rare Cell Populations. Int J Mol Sci.; 21 (18): 6557. IF 4.556

8. References

1. Dendrou, C. A., Fugger, L. & Friese, M. A. Immunopathology of multiple sclerosis. *Nat Rev Immunol* **15**, 545-558 (2015).
2. Moutsianas, L. *et al.* Class II HLA interactions modulate genetic risk for multiple sclerosis. *Nat Genet* **47**, 1107-1113 (2015).
3. Goris, A. & Liston, A. The immunogenetic architecture of autoimmune disease. *Cold Spring Harb Perspect Biol* **4**, a007260 (2012).
4. The International Multiple Sclerosis Genetics Consortium & The Wellcome Trust Case Control Consortium 2. Genetic risk and a primary role for cell-mediated immune mechanisms in multiple sclerosis. *Nature* **476**, 214-219 (2011).
5. The International Multiple Sclerosis Genetics Consortium. Analysis of immune-related loci identifies 48 new susceptibility variants for multiple sclerosis. *Nat Genet* **45**, 1353-1360 (2013).
6. The International Multiple Sclerosis Genetics Consortium. Low-Frequency and Rare-Coding Variation Contributes to Multiple Sclerosis Risk. *Cell* **175**, 1679-1687 e1677 (2018).
7. The International Multiple Sclerosis Genetics Consortium. Multiple sclerosis genomic map implicates peripheral immune cells and microglia in susceptibility. *Science* **365** (2019).
8. The International Multiple Sclerosis Genetics, C., ,. A systems biology approach uncovers cell-specific gene regulatory effects of genetic associations in multiple sclerosis. *Nature communications* **10**, 2236 (2019).

9. Smets, I. *et al.* Multiple sclerosis risk variants alter expression of co-stimulatory genes in B cells. *Brain* **141**, 786-796 (2018).
10. Dooley, J. *et al.* Immunological profiles of multiple sclerosis treatments reveal shared early B cell alterations *Neurol Neuroimmunol Neuroinflamm* **3**, e240 (2016).
11. Lagou, V. *et al.* Genetic Architecture of Adaptive Immune System Identifies Key Immune Regulators. *Cell Rep* **25**, 798-810 e796 (2018).
12. Kerlero de Rosbo, N. *et al.* Predominance of the autoimmune response to myelin oligodendrocyte glycoprotein (MOG) in multiple sclerosis: reactivity to the extracellular domain of MOG is directed against three main regions. *Eur J Immunol* **27**, 3059-3069 (1997).
13. Hellings, N. *et al.* T-cell reactivity to multiple myelin antigens in multiple sclerosis patients and healthy controls. *J. Neurosci. Res.* **63**, 290-302 (2001).
14. Wallstrom, E. *et al.* Increased reactivity to myelin oligodendrocyte glycoprotein peptides and epitope mapping in HLA DR2(15)+ multiple sclerosis. *Eur J Immunol* **28**, 3329-3335 (1998).
15. Jingwu, Z. *et al.* Myelin basic protein-specific T lymphocytes in multiple sclerosis and controls: precursor frequency, fine specificity, and cytotoxicity. *Ann Neurol* **32**, 330-338 (1992).
16. Battistini, L. *et al.* CD8+ T cells from patients with acute multiple sclerosis display selective increase of adhesiveness in brain venules: a critical role for P-selectin glycoprotein ligand-1. *Blood* **101**, 4775-4782 (2003).
17. Ifergan, I. *et al.* Central nervous system recruitment of effector memory CD8+ T lymphocytes during neuroinflammation is dependent on alpha4 integrin. *Brain* **134**, 3560-3577 (2011).
18. Bieganowska, K. D. *et al.* Direct ex vivo analysis of activated, Fas-sensitive autoreactive T cells in human autoimmune disease. *J Exp Med* **185**, 1585-1594 (1997).
19. Van der Aa, A. *et al.* T cell vaccination in multiple sclerosis patients with autologous CSF-derived activated T cells: results from a pilot study. *Clin Exp Immunol* **131**, 155-168 (2003).
20. Bielekova, B. *et al.* Expansion and functional relevance of high-avidity myelin-specific CD4+ T cells in multiple sclerosis. *J Immunol* **172**, 3893-3904 (2004).
21. Zheng, G. X. *et al.* Massively parallel digital transcriptional profiling of single cells. *Nature communications* **8**, 14049 (2017).
22. Grau-Lopez, L. *et al.* Specific T-cell proliferation to myelin peptides in relapsing-remitting multiple sclerosis. *Eur J Neurol* **18**, 1101-1104 (2011).
23. Sprouse, M. L. *et al.* Cutting Edge: Low-Affinity TCRs Support Regulatory T Cell Function in Autoimmunity. *J Immunol* **200**, 909-914 (2018).
24. Thompson, A. J. *et al.* Diagnosis of multiple sclerosis: 2017 revisions of the McDonald criteria. *Lancet Neurol* **17**, 162-173 (2018).
25. Zemmour, D. *et al.* Single-cell gene expression reveals a landscape of regulatory T cell phenotypes shaped by the TCR. *Nat Immunol* **19**, 291-301 (2018).
26. Muraro, P. A. *et al.* T cell repertoire following autologous stem cell transplantation for multiple sclerosis. *J Clin Invest* **124**, 1168-1172 (2014).
27. Pappalardo, J. L. *et al.* Transcriptomic and clonal characterization of T cells in the human central nervous system. *Sci Immunol* **5** (2020).
28. Ramesh, A. *et al.* A pathogenic and clonally expanded B cell transcriptome in active multiple sclerosis. *Proc Natl Acad Sci U S A* **117**, 22932-22943 (2020).
29. Schafflick, D. *et al.* Integrated single cell analysis of blood and cerebrospinal fluid leukocytes in multiple sclerosis. *Nature communications* **11**, 247 (2020).

Geneeskundige Stichting Koningin Elisabeth
Fondation Médicale Reine Elisabeth
Königin-Elisabeth-Stiftung für Medizin
Queen Elisabeth Medical Foundation

Progress report of the interuniversity research project of

Prof. dr. Pascal Kienlen-Campard (UCLouvain)
Prof. dr. Loïc Quinton (ULg)
Prof. dr. Jan Gettemans (UGent)

Partners of the network

UCLouvain :
Prof. dr. Pascal Kienlen-Campard (PI, spokesperson) – partner 1 (P1)
Institute of Neuroscience
IONS-CEMO, Avenue Mounier 53 bte B1.53.02
B-1200 Brussels

Prof. Bernard Hanseeuw, PhD and **Adrian Ivanoiu** (collaborators) – partner 2 (P2)
Cliniques St Luc, UCLouvain
IoNS- NEUR

ULiège
Prof. dr. Loïc Quinton (PI) – partner 3 (P3)
MS-LAB, UR MolSys
Allée du six Aout 11 - Quartier Agora - Liège Université
B4000 -Liège 1

Ghent University
Prof. dr. Jan Gettemans – partner 4 (P4)
Department of Biomolecular Medicine
Faculty of Medicine & Health Sciences
Campus Rommelaere
A. Baertsoenkaai 3
B-9000 Ghent

New analytical tools to identify and target pathogenic hexameric Aβ assemblies in Alzheimer's disease

1. Context

With an estimated 47 million people affected worldwide, dementia is recognized as the 5th leading cause of death (www.who.int). This number is expected to double within the next 20 years as age is identified as being the biggest risk factor of disease. Alzheimer's disease (AD) is the most common form of dementia and accounts for over 60 per cent of diagnoses, with more than 150.000 cases in Belgium.

A major obstacle in developing a treatment for AD has been the lack of reliable diagnostic markers and straightforward target to block the disease onset and progression. It is therefore imperative to (i) develop a reliable and easy-to-use diagnostic (ii) identify efficient therapeutic targets to treat AD. Several clinical trials have focused on targeting either A production or its accumulation, an early event in AD pathogenesis. The high potential interest to target pathologic A forms has for instance been evaluated in passive immunotherapies trials. Unfortunately, they failed so far to improve cognitive function in subjects with mild or moderate AD (Salloway et al., 2014). Indeed, these negative results could stem from two reasons: (i) possibly irrelevant A targets; (ii) therapies targeting amyloid pathologies might be inefficient if administrated in the late phases of the disease.

Recent studies including ours indicate that A neurotoxicity is attributed to oligomers of A (Decock et al., 2016;Marshall et al., 2016). Oligomers are intermediary species formed on the self-assembly pathway of A from monomers to mature amyloid fibrils. With this in mind, we identify the following points as important research objectives:

1. A better identification of the pathologic A forms to be targeted. Our work hypothesis is that toxicity is highly attributed to hexameric assemblies of A found in cellular models.
2. Make available clinical samples to evaluate the relevance of A oligomers (likely hexamers) we identified in cells to the human AD pathology, possibly at very early stages.
3. The improvement and standardization of analytical approaches as reliable tools to measure A oligomers, both in biological models and patient samples.
4. The development of a novel approach to efficiently target A oligomers. We will develop an approach based on nanobodies, which appear much more promising than whole antibodies used so far. Their comparatively low molecular mass leads to a better permeability in tissues and allows them to bind to hidden epitopes that are not accessible to whole antibodies. In addition, they do not show complement system triggered cytotoxicity as they lack an Fc region.

2. Current progress in the different objectives

2.1. Identification of the pathogenic A oligomers

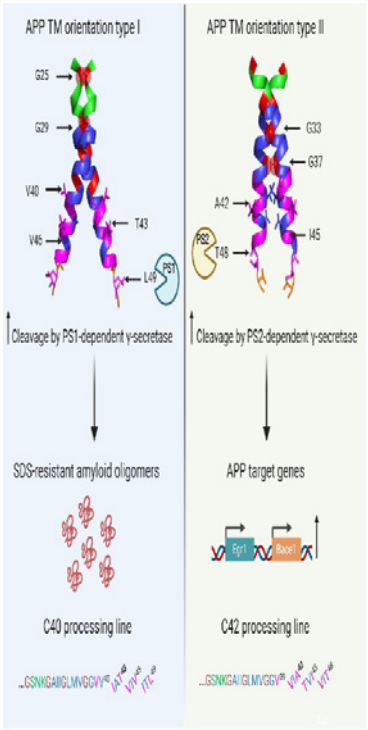

With the support of the FMRE, we finalized a first project aimed at identifying the molecular conformations of the Amyloid precursor protein (APP) triggering the production of pathological A assemblies. We demonstrated that dimeric orientations of amyloidogenic APP C-terminal fragments (C99) regulate the precise cleavage by -secretase that releases A. We found that one precise orientation of C99 favored processing to A43/40 forms, promoting formation of SDS oligomers, reminiscent of Aß peptide oligomers. (See Figure on the right, from Perrin et al., 2020). This work has been published in iScience, December 2020 (Perrin et al., 2020). The publication is joined to the progress report. **This work involved P1.**

We further investigated the nature and the properties of A assemblies that we identified in cellular models. The misfolding of A leads to subsequent amyloid fibril formation by nucleated polymerization. This requires an initial and critical nucleus for self-assembly. We identified and characterized the composition and self-assembly properties of cell-derived hexameric A42 and showed its assembly enhancing properties which are dependent on the A monomer availability. Identification of nucleating assemblies that contribute to self-assembly in this way may serve as therapeutic targets to prevent the formation of toxic oligomers. The results obtained are currently under revision for publication in Scientific reports. A preprint is available at www.biorxiv.org/content/10.1101/2020.12.15.422916v1 . **This work involved P1 and P3**. We isolated these hexameric A assemblies from a cellular model and assessed its effect on primary neuron viability *in vitro*, and its contribution to amyloid deposition in vivo. In 5xFAD mice, where human A species are pre-existing, the hippocampal injection of cell-derived A hexamers aggravated A deposition, in agreement with its previously described nucleation properties. Finally, by editing human cell lines, we investigated the respective contribution of Presenilin 1 (PS1) and 2 (PS2)-dependent -secretases, which are responsible for the release of monomeric A, to this process. We found experimental evidence suggesting a direct link between PS2-dependent activity and the release of hexameric A in extracellular vesicles. The results are submitted for publication in the Journal of Neuroscience and a preprint is available at www.biorxiv.org/content/10.1101/2020.12.23.424094v1 . **This work involved P1, P2 and P3**

2.2. Patient cohort and clinical samples workflow

2.3. Standardization of analytical approaches

The serum samples from the UCLouvain/St Luc Hospital cohort is currently formed by AD patients (N=10), age-matched controls (N=18), non-inflammatory neurological disease (NIND) with dementia (N=16) and non-demented NIND (N=16), and will be extended according to the requirement of the project. By recruiting additional SCI (n=5), MCI (n=15), AD (n=10) patients with cognitive, medical, or amyloid-PET data available, we will extend the cohort and incorporate CSF samples (**P2**). *This in currently in progress*. Standard AD biomarkers will be evaluated for each patient sample (A42:40 ratio, cognitive assays and amyloid PET imaging when possible). Our aim is to establish a to check whether A hexamers are present in CSF, in case to concentrate them for further analysis by mass spectrometry (**P3**) the A isoforms composing them. A correlation

with other amyloid biomarkers will be estimated (**P2**). A PhD student has been recruited (Emilien Boyer, MD. **P1** supervisor, **P2** co-supervisor). He is currently setting the procedures to measure A oligomers in blood samples and already evaluates the ability of some nanobodies (**P4**) to detect oligomeric A in biological models (cell lines). To note, funds have been awarded (FNRS equipment 2020, **P1** and **P2**) to acquire the Single Molecular Array equipment (SIMOA®, Quanterix) that offer an unprecedent sensitivity for the detection of blood biomarkers.

2.4. Development of nanobodies targeting Aβ hexamers

The team at Ghent university (**P4**) obtained single domain antibodies, or nanobodies as they are called, against serum amyloid P component or SAP from human or murine origin. Biochemical experiments indicate that these nanobodies are highly specific to their respective isoforms and do not cross-react. SAP is known to interact with amyloid fibrils and to strengthen them, making the degradation of fibrils even more difficult. Experiments in the group of **P1** showed that amyloid peptides migrate at "28 kDa", which is far above their expected molecular weight. It was hypothesized that these peptides could interact with SAP (25 kDa in monomeric form). To this end, a small amount of plasma obtained from different AD patients was incubated with HA-tagged anti human SAP nanobody, fractionated by SDS-PAGE and subsequently prepared for Western blotting using anti-amyloid beta antibody (provided by **P1**). We did not observe a signal indicating that at least for these patients no interaction could be demonstrated between peripherally circulating SAP and amyloid beta peptide. **P4** is keen to understand which proteins interact with SAP and for this anti-human SAP nanobodies that were coupled directly and covalently onto Tosyl beads were used. Nanobodies that do not contain lysine residues in their CDRs were chosen to prevent their potential inactivation when coupled to Tosyl. The experiment was prepared in with **P3** who will further conduct mass spectrometric analysis towards identification of proteins that potentially interact with SAP in a pathological context.

3. Dissemination

The restrictions related to the COVID pandemic have prevented the organization of research meeting/symposia on the topic in 2020 but the network organized remote meetings (Teams) to ensure the exchange of materials and the monitoring of information necessary for the progress of the project.

4. Reference List

- Decock M, Stanga S, Octave JN, Dewachter I, Smith SO, Constantinescu SN, Kienlen-Campard P (2016) Glycines from the APP GXXXG/GXXXA Transmembrane Motifs Promote Formation of Pathogenic Abeta Oligomers in Cells. Front Aging Neurosci 8:107.
- Marshall KE, Vadukul DM, Dahal L, Theisen A, Fowler MW, Al-Hilaly Y, Ford L, Kemenes G, Day IJ, Staras K, Serpell LC (2016) A critical role for the self-assembly of Amyloid-beta1-42 in neurodegeneration. Sci Rep 6:30182.
- Perrin F, Papadopoulos N, Suelves N, Opsomer R, Vadukul DM, Vrancx C, Smith SO, Vertommen D, Kienlen-Campard P, Constantinescu SN (2020) Dimeric Transmembrane Orientations of APP/C99 Regulate gamma-Secretase Processing Line Impacting Signaling and Oligomerization. iScience 23:101887.
- Salloway S, et al. (2014) Two phase 3 trials of bapineuzumab in mild-to-moderate Alzheimer's disease. N Engl J Med 370:322-333.

Geneeskundige Stichting Koningin Elisabeth
Fondation Médicale Reine Elisabeth
Königin-Elisabeth-Stiftung für Medizin
Queen Elisabeth Medical Foundation

Universitaire onderzoeksprojecten 2020-2022 gefinancierd door de G.S.K.E.

Projets de recherche universitaire 2020-2022 subventionnés par la F.M.R.E.

University research projects 2020-2022 funded by the Q.E.M.F.

Universiteiten met onderzoeksprogramma's die gesteund worden door de G.S.K.E.

Universités ayant des programmes de recherche subventionnés par la F.M.R.E.

Universities having research programs supported by the Q.E.M.F.

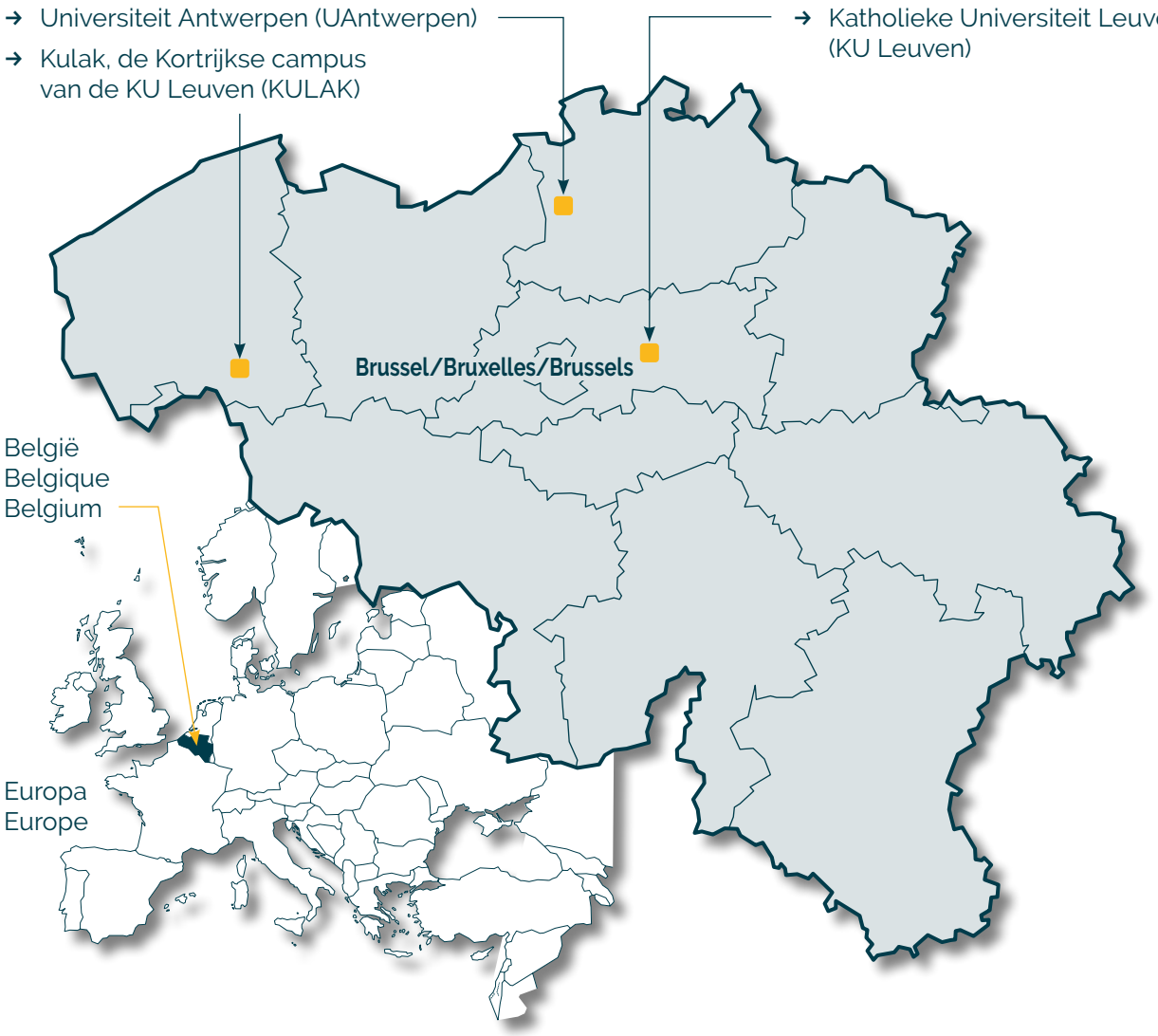

Universitaire onderzoeksprojecten 2020-2022 gefinancierd door de G.S.K.E.

Projets de recherche universitaire 2020-2022 subventionnés par la F.M.R.E.

University research projects 2020-2022 funded by the Q.E.M.F.

UAntwerpen

Prof. dr. Sarah Weckhuysen, MD, PhD
Study and targeted treatment development for epileptic encephalopathies using 2D and 3D human induced plupripotent stem cell-derived neuronal cultures

KU Leuven

Prof. Pierre Vanderhaeghen, MD, PhD (VIB)
Deciphering the mechanisms underlying intellectual deficiency and autism spectrum disorders by cellular modelling in human neurons in vivo

Prof. dr. Lieve Moons & dr. Lies De Groef
Oligodendrocytes in Wolfram syndrome: bystanders or partners in crime?

Prof. dr. Thomas Voets (VIB)
Unraveling the cellular and molecular basis of noxious cold sensing

KULAK

Prof. dr. ir. Simon De Meyer
Unravelling the thrombo-inflammatory role of von Willebrand factor in neurodegeneration after ischemic stroke

Geneeskundige Stichting Koningin Elisabeth
Fondation Médicale Reine Elisabeth
Königin-Elisabeth-Stiftung für Medizin
Queen Elisabeth Medical Foundation

Progress report of the university research project of

Prof. dr. ir. Simon De Meyer
Kulak, de Kortrijkse campus van de KU Leuven (KULAK)

Prof. dr. ir. Simon De Meyer
Professor, Dept. of Cardiovascular Sciences
Laboratory for Thrombosis Research
KU Leuven Campus Kulak Kortrijk
E. Sabbelaan 53
8500 Kortrijk
Belgium
Tel: +32 56 246232
simon.demeyer@kuleuven.be
www.kuleuven-kulak.be/irf/thrombosis

Table of contents

Unravelling the thrombo-inflammatory role of von Willebrand factor in neurodegeneration after ischemic stroke

1. Summary of the project

Ischemic stroke is one of the leading causes of death and sustained disability worldwide. Blockade of blood flow to the brain by an occlusive thrombus leads to irreversible damage of the associated brain tissue. The enormous clinical, economic and social burden of ischemic stroke is in strong contrast with the limited treatment options that are currently available. In acute ischemic stroke, the mainstay of acute treatment is rapid recanalization of the occluded blood vessel, either via pharmacological thrombolysis or via mechanical thrombectomy.

In recent years, it has become clear that rapid recanalization of the occluded blood vessel is not sufficient to fully salvage the threatened brain tissue. Novel insights show that cerebral ischemia and subsequent reperfusion elicit a thrombo-inflammatory cascade that promotes progressive brain damage in stroke patients.[1] This problem does not only occur after successful thrombolysis but also often complicates stroke outcome after successful mechanical thrombectomy.[2] This so-called ischemia/reperfusion injury (I/R injury) is a complex process that interrelates thrombosis with inflammation, leading to several pathophysiological effects in the neuro-vascular unit. The exact mechanisms of how cerebral I/R injury accelerates neurodegeneration are still poorly understood. Yet, such insights will be crucial to develop effective strategies to promote neuroprotection in stroke management. One of our major findings in the last decade is our discovery that von Willebrand factor (VWF) plays a crucial role in cerebral I/R injury. [1,3-6] VWF is a large multimeric plasma glycoprotein that recruits platelets at sites of vascular injury and that promotes both thrombosis and inflammation. Remarkably, we found that initial VWF-mediated platelet adhesion rather than subsequent platelet aggregation contributes to cerebral I/R injury with a prominent role for the interaction between the VWF A1 domain and platelet glycoprotein (GP)Ib.[4,6-8] At present we do not know exactly how VWF contributes to thrombo-inflammation in the (post-)ischemic brain. Our hypothesis is that VWF, after release by activated (hypoxic) endothelial cells recruits and activates both platelets and leukocytes, leading to obstruction of the microvasculature and local inflammation.

The general objective of this research project was to elucidate the mechanisms by which VWF mediates cerebral I/R injury in ischemic stroke. More specifically, we are aiming at (i) unravelling the inflammatory component of VWF-mediated I/R injury and (ii) at visualizing the molecular and cellular interactions of VWF-mediated thrombo-inflammation in the brain via advanced 3D microscopy.

2. Progress and next steps

In order to successfully complete this project, two delineated work packages (WP) were defined:

- WP1: Elucidating the inflammatory component of VWF in cerebral I/R injury
- WP2: Advanced 3D microscopy to map VWF-mediated thrombo-inflammation in the brain

In this section, the 1-year progress for each work package is detailed, as well as the planned next steps for the following years.

2.1. WP 1: Elucidating the inflammatory component of VWF in cerebral I/R injury

OBSERVATION 1: VWF-deficiency reduces immune cell recruitment to the brain after ischemic stroke

To examine the cerebral immune cell response mediated by VWF, we performed flow cytometric analysis of single cell suspensions prepared from brain tissue isolated from WT and VWF KO mice subjected to stroke. After stroke, mice were perfused, their brains harvested and subsequently divided into ipsilateral (affected by stroke) and contralateral (unaffected) hemispheres. Interestingly, we observed significantly reduced cerebral infarcts in VWF KO mice, compared to WT mice ($p < 0.01$, Figure 1A). Twenty-four hours after stroke, the ipsilateral hemisphere showed an increased amount of infiltrated white blood cells (WBCs) compared to the contralateral hemisphere in both the WT ($p < 0.005$) and VWF KO mice ($p < 0.05$). However, averaged recruitment of WBC in the ipsilateral hemisphere of VWF KO mice was two-fold lower than in WT mice (5596 ± 1644 vs. 12435 ± 2083, respectively; $p < 0.05$, Figure 1B). Both the amount of myeloid and lymphoid white blood cells was significantly reduced in the brains of VWF KO mice compared to WT mice ($p < 0.05$, Figure 1C-D).

OBSERVATION 2: VWF deficiency leads to reduced recruitment of inflammatory monocytes, neutrophils and T-cells

To better determine which inflammatory cells were potentially recruited by VWF to the affected brain tissue during stroke, we used two antibody cocktails that allowed discrimination and quantification of recruited inflammatory monocytes, neutrophils, T-cells and $CD3^{neg}$ lymphocytes (B cells and NK cells) (Table 1).

As shown in figure 1E-H, all four subsets of immune cells were significantly increased in the ipsilateral brain of WT mice 24 hours after stroke, compared to the unaffected contralateral hemisphere. However, despite the presence of an infarct core in the affected ipsilateral hemisphere of VWF KO mice, the numbers of neutrophils and T-cells did not increase and remained similar to the baseline values of the contralateral hemisphere (Figure 1E and 1F). Hence, the absolute numbers of recruited neutrophils and T- cells was significantly higher in the ischemic brain of WT mice compared to VWF KO mice (2017 ± 733 vs 512 ± 203, $p < 0.05$ and 974 ± 184 vs 244 ± 44, $p < 0.01$ respectively). These results suggest an important role for VWF in recruiting both neutrophils and T-cells to the affected brain tissue during ischemic stroke.

A similar, yet less outspoken, trend was observed for inflammatory monocytes (Figure 1G). In VWF KO mice, the ischemic hemisphere contained significantly more inflammatory monocytes than the unaffected hemisphere, but this was still significantly lower than the number of inflammatory monocytes that were recruited in the ischemic brain of WT mice (2466 ± 955 vs 6760 ± 1414; $p < 0.05$).

No differences regarding $CD3^{neg}$ lymphocytes were observed between WT and VWF KO mice as similar numbers were recruited in the ischemic hemisphere of both groups (1162 ± 245 vs 585 ± 188 respectively, $p > 0.05$, Figure 1H). Leukocyte blood counts and circulating platelet-leukocyte complexes were similar between VWF KO and VWF WT mice 24 hours after stroke (data not shown).

Table 1. Antibodies cocktails used to discriminate between different white blood cell subtypes.

	antigen	supplier
Antibody cocktail 1	CD45 APC-Cy7	Biolegend
	CD11b PE-Cy7	eBioscience
	Ly6G BV510	Biolegend
	Ly6C FITC	Biolegend
	CD16/CD32 (Fc-block)	eBioscience
	Live/Death Fixable Violet Dead Cell Stain Kit	ThermoFisher
Antibody cocktail 2	CD45-APC-Cy7	Biolegend
	CD11b PE-Cy7	eBioscience
	CD11c PerCp-Cy5	eBioscience
	CD3e FITC	eBioscience
	CD16/CD32 (Fc-block)	eBioscience
	Live/Death Fixable Violet Dead Cell Stain Kit	ThermoFisher

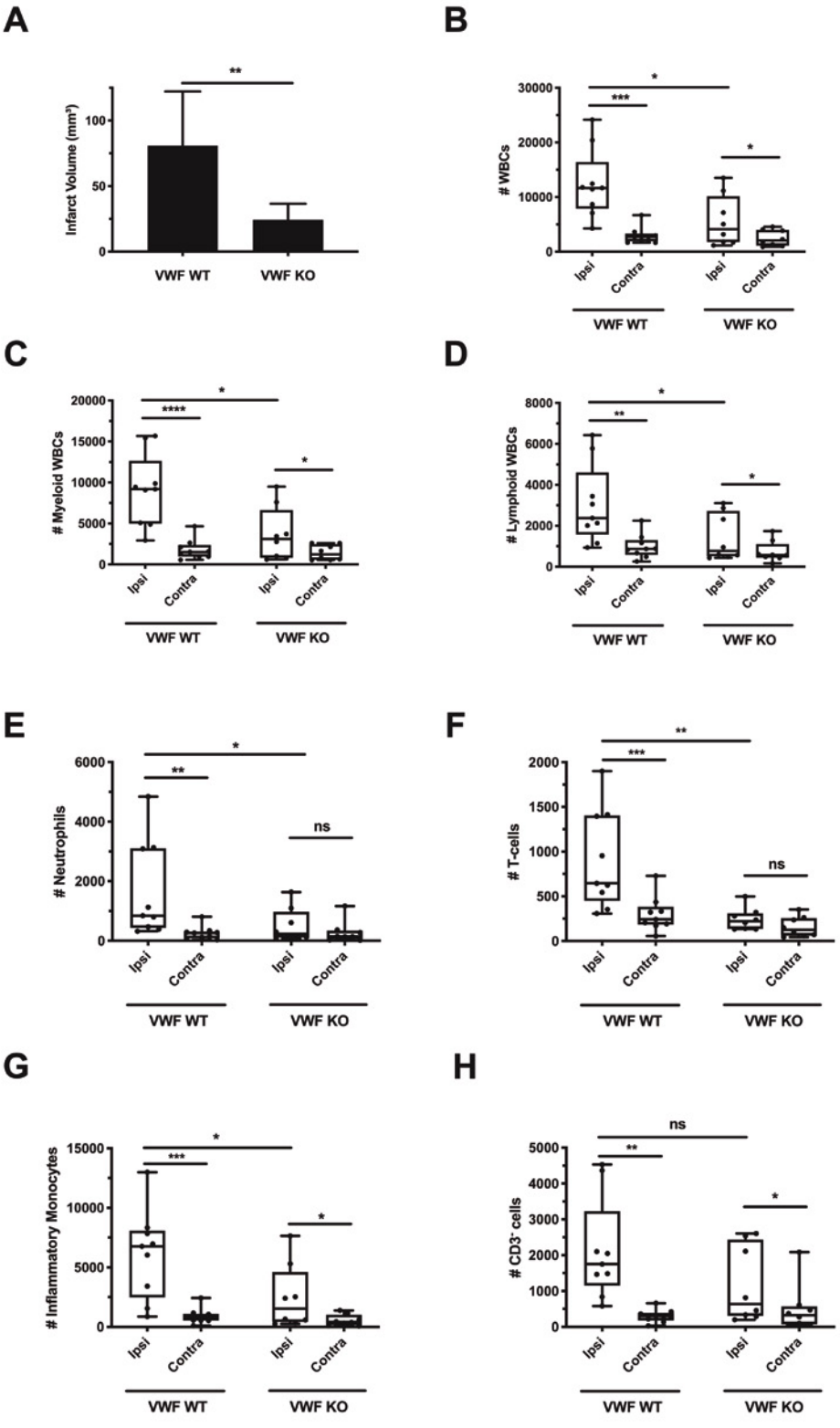

Figure 1: VWF deficiency leads to a reduction of the number of monocytes, neutrophils and T-cells to the brain after acute ischemic stroke. Transient focal cerebral ischemia was induced by 60 minutes occlusion of the right middle cerebral artery (tMCAO), followed by 23 hours of reperfusion in WT and VWF KO mice, after which edema-corrected brain infarct volumes were quantified by planimetric analysis **(A)** and WBC recruitment to each hemisphere was determined by flow cytometry. Total amount of white blood cells ($CD45^{high}$) was analyzed **(B)** as well as the myeloid ($CD45^{high}$; $CD11b^{+}$) **(C)** and lymphoid white blood cells ($CD45^{high}$; $CD11b^{-}$; $CD11c^{-}$) **(D)**. More specifically: Neutrophils ($CD45^{high}$; $CD11b^{+}$; $Ly6G^{+}$) **(E)**; T-cells ($CD45h^{igh}$; $CD11b^{-}$; $CD11c^{-}$; $CD3e^{+}$) **(F)**; Inflammatory Monocytes ($CD45^{high}$; $CD11b^{+}$; $Ly6C^{+}$; $Ly6G^{-}$) **(G)**; CD3neg lymphocytes ($CD45^{high}$; $CD11b^{-}$; $CD11c^{-}$; $CD3e^{-}$) **(H)** were quantified. Data are represented as box plots showing all data points and the median value, except for infarct size which is shown as mean ± standard deviation. * $p < 0.05$; **, $p<0.01$; ***: $p < 0.005$; ****, $p<0.001$. (n = 8-9)

OBSERVATION 3: VWF-mediated thromboinflammation in the ischemic stroke brain via fluorescence microscopy

For visualization of VWF-mediated thromboinflammation, immunofluorescent staining of platelets and leukocytes was performed on brains obtained from VWF WT and KO mice 24 hours after stroke (Figures 2 and 3). In VWF KO mice, very few platelet accumulations were found within the ipsilateral brain (Figure 2A). In contrast, platelet/VWF-rich microthrombi were found frequently throughout the ipsilateral brain of VWF WT mice, underscoring the importance of VWF-mediated platelet adhesion in the ischemic stroke brain (Figure 2B-D). Platelet/VWF-rich microthrombi were absent in the contralateral hemisphere of both WT and VWF KO mice (data not shown).

Next, we visualized immune cell recruitment in VWF WT and KO mice. Since previous studies found no major role for monocytes, but an important detrimental role for both T-cells[9] and neutrophils[10] in the acute phase of ischemic stroke, we focused on visualizing neutrophils and T-cells in the stroke brain. To stain the vasculature in both VWF WT and KO mice, a sensitive lectin staining of the endothelium was performed (Figure 3). Using a specific histological marker for neutrophils (Ly6G), we observed that neutrophils were more frequently present within the ipsilateral side of the brain of VWF WT mice compared to VWF KO mice (Figure 3A-B). Since the smaller infarct sizes observed in VWF KO mice might bias neutrophil quantification by flow cytometry, we also quantified neutrophil recruitment in the ischemic infarct core in both VWF KO and WT mice by histology. Importantly, analysis of fixed areas of 1 mm^2 in the infarct core corroborated our flow cytometric data, arguing against a nonspecific effect related to smaller infarct sizes. Quantification of neutrophil recruitment to the infarct core revealed a two-fold reduction of neutrophil density in VWF KO brains compared to WT mice (Figure 3C). Intriguingly, neutrophils were frequently observed within the microcirculation (Figure 3A-B). To investigate this further, intra – and extravascular neutrophils were counted in brain sections of VWF WT mice. On average, 66 ± 4% of neutrophils were found within the vasculature of the ischemic hemisphere, while the remaining neutrophils were already extravasated (Figure 3D). A comparable observation was made when we stained for T-cells, which were also occasionally found within the microvasculature of VWF WT mice (Figure 3E). Due to the low number of T-cells within the ischemic brain, quantification of T-cells was not feasible. Lastly, T-cells were virtually absent in the ipsilateral brain hemisphere of VWF KO mice (Figure 3F), confirming our flow cytometric data.

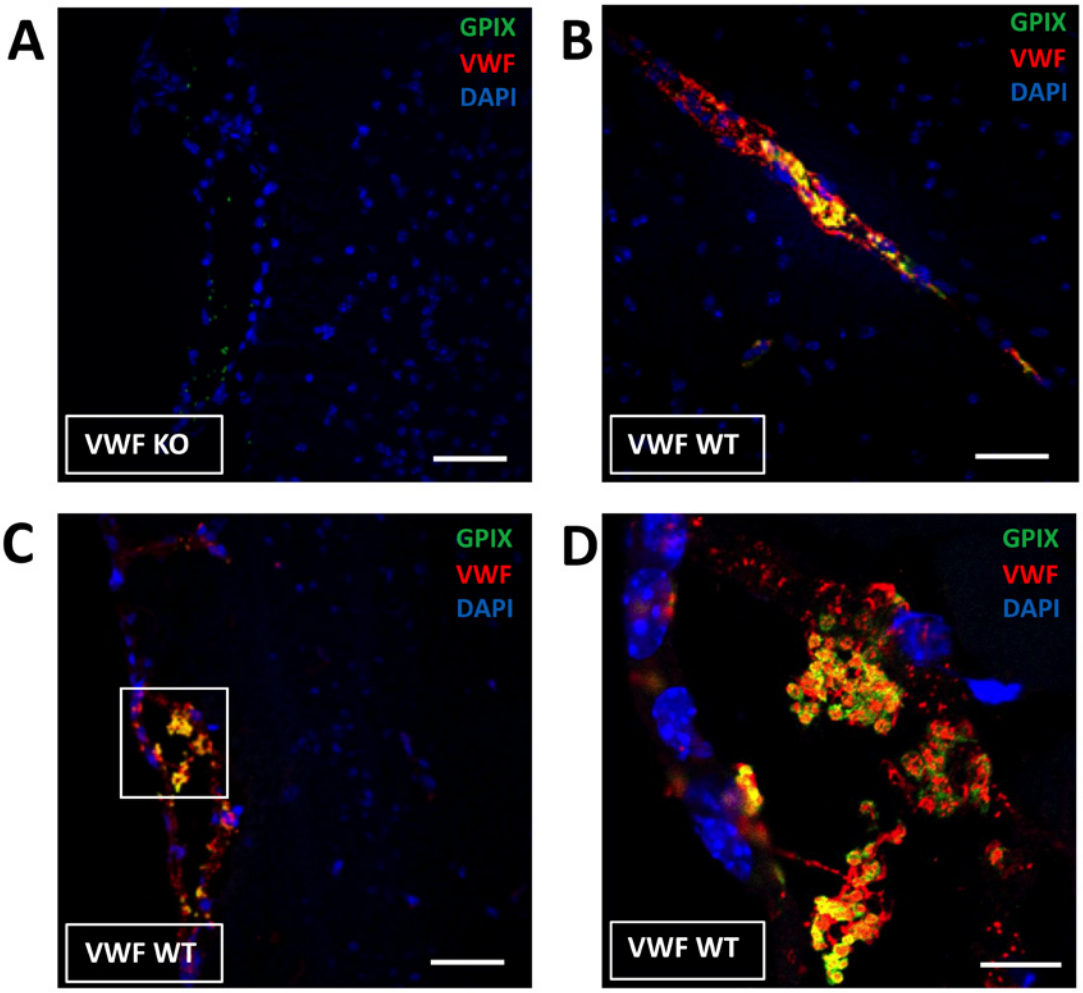

Figure 2: Immunofluorescent visualization of thromboinflammation in the ipsilateral hemisphere of mice 24 hours after ischemic stroke brain injury. Transient focal cerebral ischemia was induced by 60 minutes occlusion of the right middle cerebral artery (tMCAO), followed by 23 hours of reperfusion in VWF WT or KO mice, after which, brain-sections were stained for VWF (red), platelets (green) and nuclei (blue). **A.** Only a few platelets are found within the ischemic brain of VWF KO mice. **B-D.** Clumps of VWF together with platelets were frequently found attached to the vessel wall within the ipsilateral hemisphere. Panel D is a magnification of the white box in panel C. Scale bars are 50μm except for panel D where the scale bar is 25μm. Images are representative for n = 3 per genotype.

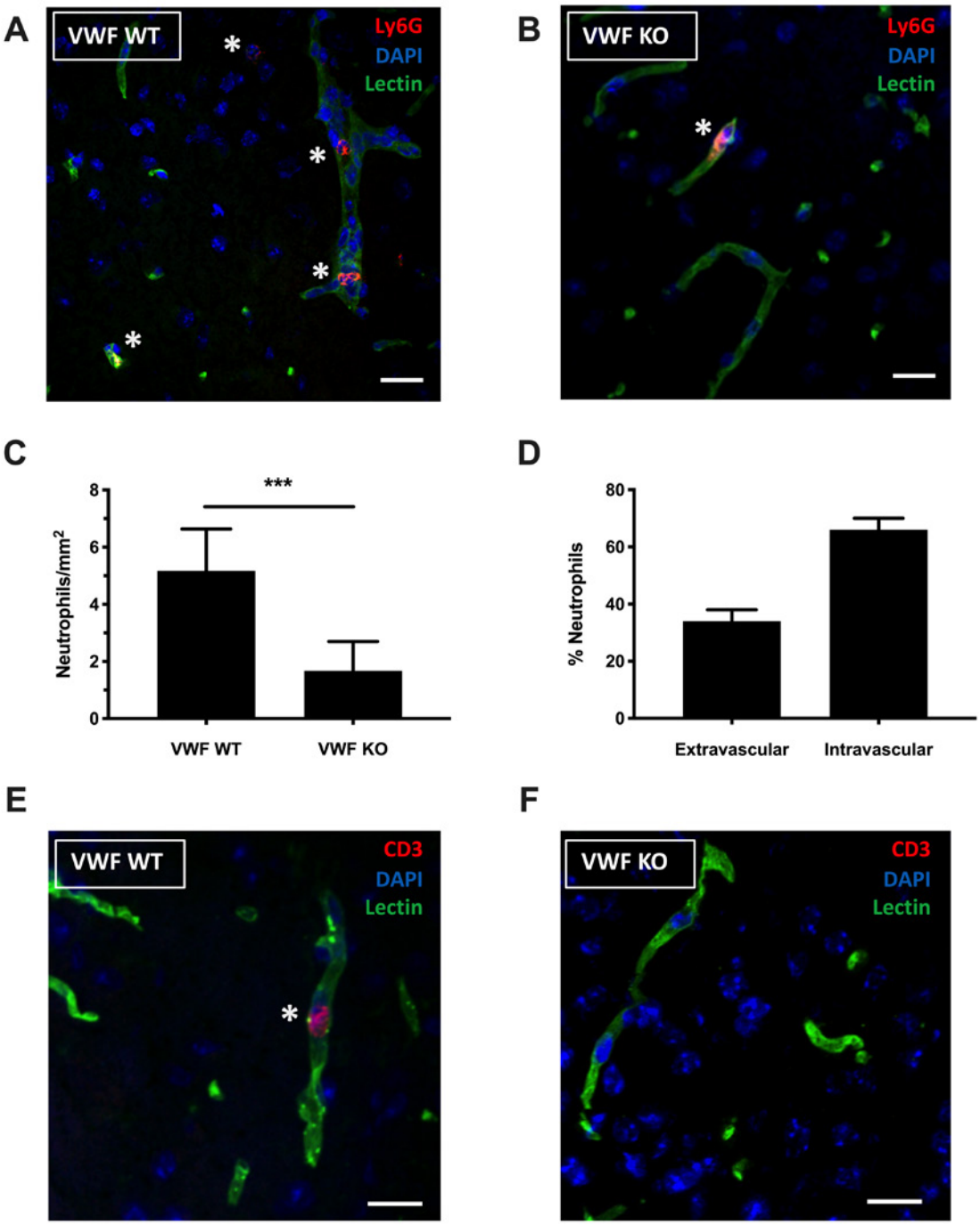

Figure 3: Immunofluorescent visualization of neutrophils and T-cells in the ipsilateral hemisphere of mice 24 hours after ischemic stroke brain injury. Transient focal cerebral ischemia was induced by 60 minutes occlusion of the right middle cerebral artery (tMCAO), followed by 23 hours of reperfusion in VWF WT and KO mice, after which, brain-sections were stained for blood vessels and neutrophils or T-cells. **A-B.** Neutrophils were stained with a marker for Ly6G (red) and blood vessels with a lectin staining (green). Neutrophils are marked with a *. **C.** Quantification of the number of neutrophils/mm² in the infarct core of WT and VWF KO mice. (n = 3) Data is represented as mean ± standard deviation. D. The number of neutrophils within and outside the vasculature (n = 3). Data is represented as mean ± standard deviation. **E and F.** T-cells were stained with a marker for CD3 (red) and blood vessels with a lectin staining (green). T-cells are marked with a *. Scale bars are 20µm. Images are representative for n = 3 per genotype.

OBSERVATION 4: Inhibition of the VWF A1 domain limits ischemic stroke brain injury

Given the central role of the VWF A1 domain in cerebral ischemia/reperfusion injury[4], we next wanted to unravel its potential inflammatory contribution in ischemic stroke. To this end, we used a nanobody (KB-VWF-006bv) that specifically binds the VWF A1 domain, inhibiting its interaction with the platelet receptor GPIb.[11] Intravenous treatment with 10mg/kg of the nanobody was started immediately after establishment of reperfusion. Mean residence time of the nanobody

is 3.5 hours and this allows blocking of the VWF-A1 domain during the acute reperfusion phase. As a control, a nonspecific nanobody (KB-VWF-004bv) was administered. Twenty-four hours after stroke, mice treated with the anti-VWF A1 nanobody KB-VWF-006bv had significantly less ischemic stroke brain damage compared to control-treated mice (Figure 4A and B). This translated in an improved motor score (Figure 4C) and neurological behavior (Figure 4D), although this difference was only statistically significant for the latter. Of note, no intracranial bleedings were observed in any of the mice treated with the VWF A1 nanobody. These data further corroborate the crucial involvement of the VWF-GPIb axis in cerebral ischemia/reperfusion injury.[6,7,12,13]

OBSERVATION 5: Inhibition of the VWF A1 domain reduces the recruitment of neutrophils, monocytes and T-cells

Targeting the VWF A1 domain also significantly reduced inflammatory cell recruitment to the ischemic brain (Figure 5). Indeed, similar to our results in VWF KO mice, flow cytometric analysis revealed that inhibition of VWF A1 also leads to a 2-fold reduction of immune cell recruitment in the brains of treated mice compared to control mice (7095 ± 2550 vs 16310 ± 3980; $p < 0.005$; Fig. 5A). Both myeloid (5195 ± 2259 vs 11978 ± 3322; $p < 0.05$; Fig. 5B) and lymphoid WBCs (1529 ± 269 vs 3017 ± 514; $p < 0.05$; Fig. 5C) were reduced in the ipsilateral hemispheres of VWF A1 nanobody treated mice. Specifically, inhibition of the VWF A1 domain reduced the amount of infiltrated inflammatory monocytes (3726 ± 1824 vs 8266 ± 2651; $p < 0.05$; Fig. 5D), neutrophils (304 ± 94 vs 1557 ± 317; $p < 0.0005$; Fig. 5E) and T-cells (487 ± 93 vs 1111 ± 248; $p < 0.05$; Fig. 5F) in the ipsilateral hemisphere of the brain, 24 hours after stroke. These data suggest that the inflammatory effect of VWF in ischemic stroke is mediated through the VWF A1 domain.

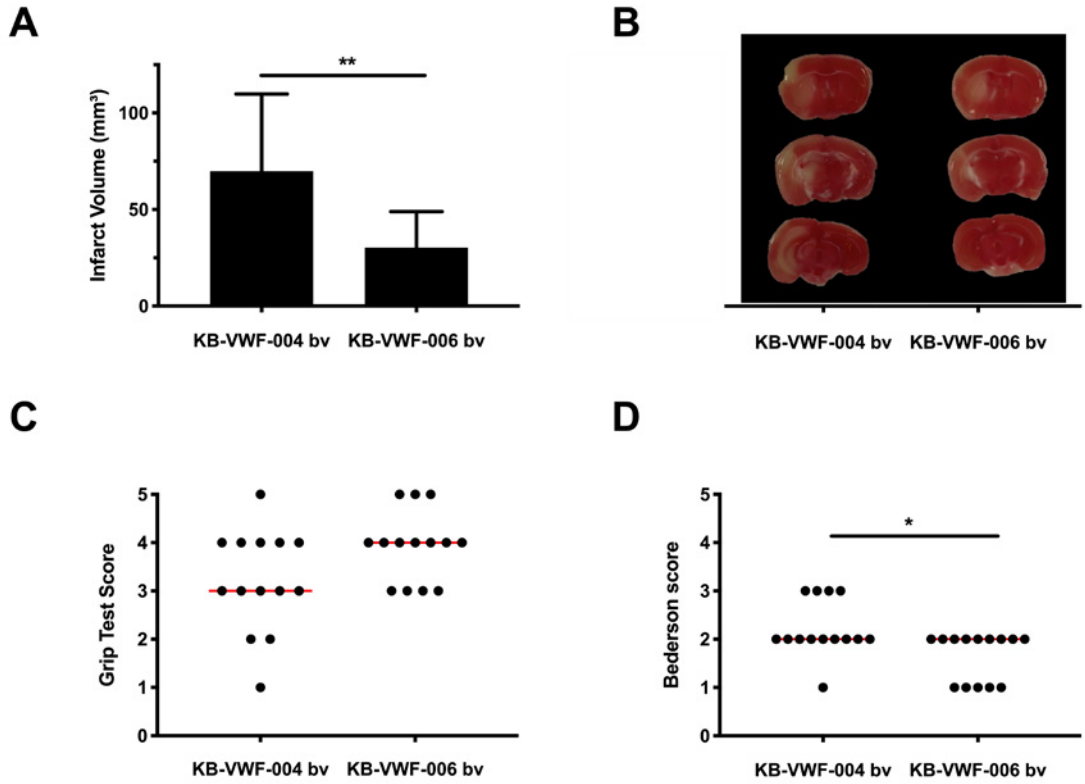

Figure 4: Inhibition of the VWF-A1 domain protects mice from acute ischemic stroke. Transient focal cerebral ischemia was induced by 60 minutes occlusion of the right middle cerebral artery (tMCAO), followed by 23 hours of reperfusion. Immediately at the start of reperfusion, mice were intravenously treated with 10 mg/kg of either control (KB-VWF-004 bv) or inhibitory anti-VWF A1 nanobody (KB-VWF-006 bv). **A.** Edema-corrected brain infarct volumes were quantified by planimetric analysis 24 hours after stroke. **B.** Representative TTC staining of 3 consecutive brain sections. **C.** Motor function was examined using the grip test. **D.** Neurological outcome 24 h after stroke was assessed using the Bederson test. Data are represented as scatter plots showing all data points and the median value, except for infarct size which is shown as mean ± standard deviation. *, $p<0.05$; **, $p<0.01$. (n = 10-11)

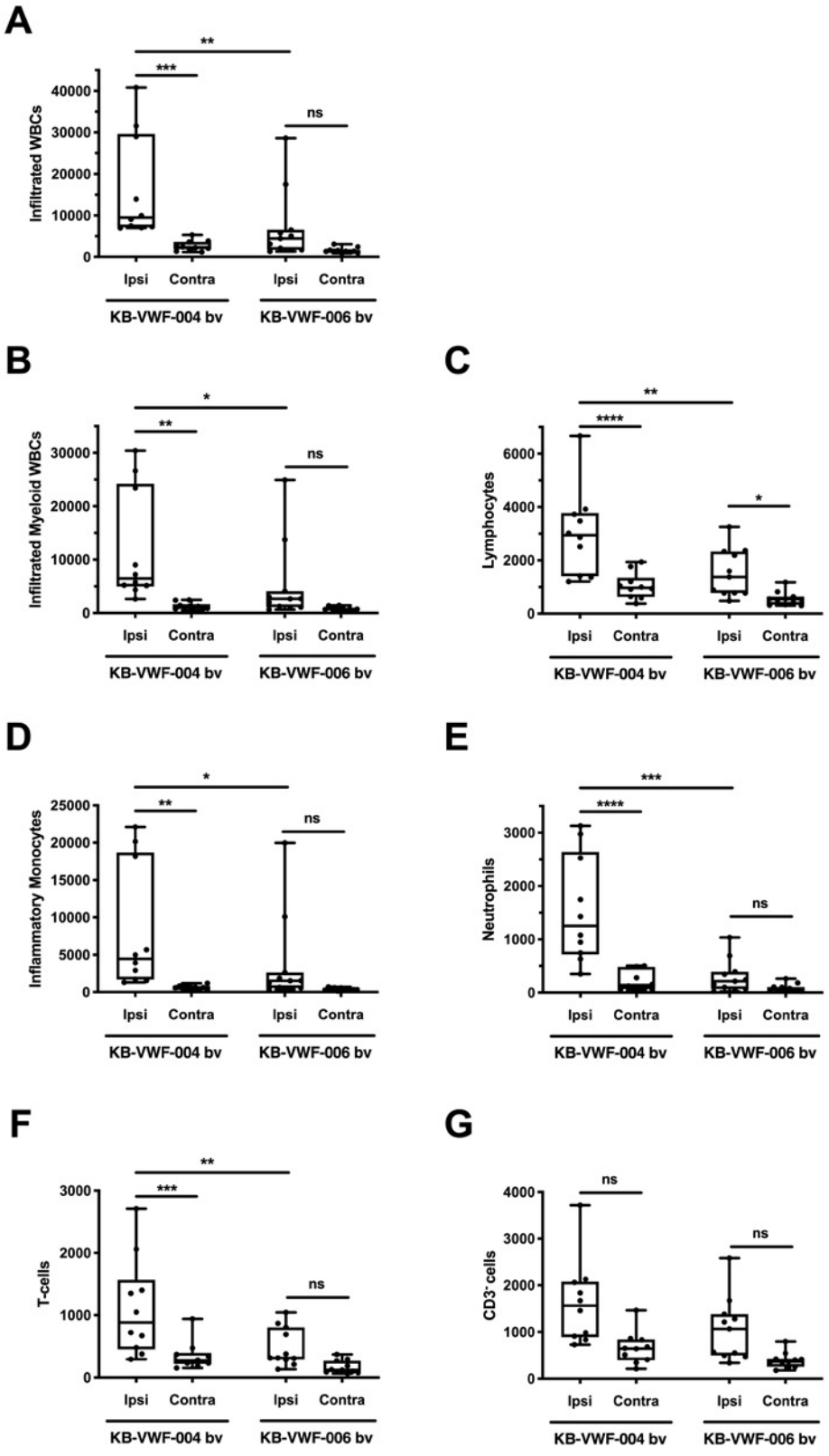

Figure 5: The VWF-A1 domain recruits monocytes, neutrophils and T-cells to the brain after acute ischemic stroke. Transient focal cerebral ischemia was induced by 60 minutes occlusion of the right middle cerebral artery (tMCAO), followed by 23 hours of reperfusion. Immediately at the start of reperfusion, mice were intravenously treated with 10 mg/kg of either control (KB-VWF-004 bv) or inhibitory anti-VWF A1 nanobody (KB-VWF-006 bv). Twenty-four hours after tMCAO, recruitment of specific subsets of WBC to each hemisphere was determined by flow cytometry. **A.** White blood cells ($CD45^{high}$). **B.** Myeloid white blood cells ($CD45^{high}$; $CD11b^{+}$). **C.** Lymphoid white blood cells ($CD45^{high}$; $CD11b^{-}$; $CD11c^{-}$). **D.** Inflammatory Monocytes ($CD45^{high}$; $CD11b^{+}$; $Ly6C^{+}$; $Ly6G^{-}$). **E.** Neutrophils ($CD45^{high}$; $CD11b^{+}$; $Ly6G^{+}$). **F.** T-cells ($CD45^{high}$; $CD11b^{-}$; $CD11c^{-}$; $CD3e^{+}$). **G.** CD3neg lymphocytes ($CD45^{high}$; $CD11b^{-}$; $CD11c^{-}$; $CD3e^{-}$). * $p < 0.05$; **, $p<0.01$; ***: $p < 0.005$; ****, $p<0.001$. (n = 10-11)

Conclusion and next steps in WP1

As the main finding from this work pacakge, we report that VWF mediates an inflammatory response during cerebral ischemia/reperfusion via the recruitment of inflammatory monocytes, neutrophils and T-cells, through a mechanism that is dependent on the VWF A1 domain. Blocking of the A1 domain reduced the inflammatory response and improved stroke outcome. This information offers novel treatment avenues for the treatment of ischemic stroke via Inhibition of VWF-mediated thromboinflammation, for example by blocking the VWF A1-GPIb interaction, or by cleaving VWF with ADAMTS13[3], both of which could become promising treatment strategies for the prevention of cerebral ischemia/reperfusion injury. In terms of translation to human therapy, it is encouraging that the first generation inhibitors of the VWF-GPIb interaction are currently enrolled in successful clinical studies for TTP, with the (Belgian) nanobody caplacizumab as the leading agent.[14] In addition, recombinant ADAMTS13 is currently being developed and shows promising results in first clinical TTP trials.[15] This work was published in the leading journal Haematologica' with GSKE acknowledgement. [16] In the next steps, we want to specifically focus on the thrombo-inflammatory aspects of VWF and neutrophil extracellular traps (NETs) in cerebral ischemia/reperfusion injury. We hypothesize that by recruiting neutrophils, VWF can also stimulate the formation of NETs in the brain (intravascular or extravascular) leading to further obstruction of the microcirculation or further tissue damage. Current experiments are dissecting the potential role of VWF in NETs-formation in this stroke model.

2.2. WP 2: 3D-microscopy to map VWF-mediated thrombo-inflammation in the brain

A light sheet microscope will be acquired and installed by the summer of 2021. Due to the covid-19 situation, the acquisition of this microscope has been delayed. In the meantime the optical clearing methods have been optimized to start 3D-analysis of the mouse brain after stroke.

3. Output

Papers with GSKE acknowledgement (2020):

- Denorme F, Martinod K, Vandenbulcke A, et al. The von Willebrand Factor A1 domain mediates thromboinflammation, aggravating ischemic stroke outcome in mice. *Haematologica*. 2020. In press.
- Staessens S, De Meyer SF. Thrombus heterogeneity in ischemic stroke. *Platelets*, 2020. In press.
- Senna Staessens, Frederik Denorme, Olivier François, Linda Desender, Tom Dewaele, Peter Vanacker, Hans Deckmyn, Karen Vanhoorelbeke, Tommy Andersson and Simon F. De Meyer. Structural analysis of ischemic stroke thrombi: histological indications for therapy resistance. *Haematologica*. 2020 In press.
- Staessens S, Fitzgerald S, Andersson T, Clarençon F, Denorme F, Gounis MJ, Hacke W, Liebeskind DS, Szikora I, van Es A, Brinjikji W, Doyle KM, **De Meyer SF.** Histological stroke clot analysis after thrombectomy: Technical aspects and recommendations. *Int J Stroke*. 2020 Jul;15(5):467-476
- Senna Staessens, Olivier François, Waleed Brinjikji, Karen Doyle, Peter Vanacker, Tommy Andersson, and Simon De Meyer. Studying stroke thrombus composition after thrombectomy: what can we learn? Submitted in the journal 'Stroke'

4. References

1. De Meyer SF, Denorme F, Langhauser F, et al. Thromboinflammation in Stroke Brain Damage. *Stroke*. 2016;47(4):1165–1172.
2. Mizuma A, You JS, Yenari MA. Targeting Reperfusion Injury in the Age of Mechanical Thrombectomy. *Stroke*. 2018;49(7):1796–1802.
3. De Meyer SF, Stoll G, Wagner DD, Kleinschnitz C. von Willebrand factor: an emerging target in stroke therapy. *Stroke*. 2012;43(2):599–606.
4. Denorme F, De Meyer SF. The VWF-GPIb axis in ischaemic stroke: lessons from animal models. *Thromb. Haemost.* 2016;116(4):597–604.
5. Kleinschnitz C, De Meyer SF, Schwarz T, et al. Deficiency of von Willebrand factor protects mice from ischemic stroke. *Blood*. 2009;113(15):3600–3603.
6. De Meyer SF, Schwarz T, Deckmyn H, et al. Binding of von Willebrand factor to collagen and glycoprotein Ibalpha, but not to glycoprotein IIb/IIIa, contributes to ischemic stroke in mice--brief report. *Arteriosclerosis, Thrombosis, and Vascular Biology*. 2010;30(10):1949–1951.
7. De Meyer SF, Schwarz T, Schatzberg D, Wagner DD. Platelet glycoprotein Ib is an important mediator of ischemic stroke in mice. *Exp Transl Stroke Med*. 2011;3(1):9.
8. Verhenne S, Denorme F, Libbrecht S, et al. Platelet-derived VWF is not essential for normal thrombosis and hemostasis but fosters ischemic stroke injury in mice. *Blood*. 2015;126(14):1715–1722.
9. Kleinschnitz C, Schwab N, Kraft P, et al. Early detrimental T-cell effects in experimental cerebral ischemia are neither related to adaptive immunity nor thrombus formation. *Blood*. 2010;115(18):3835–3842.
10. Jickling GC, Liu D, Ander BP, et al. Targeting neutrophils in ischemic stroke: translational insights from experimental studies. *J. Cereb. Blood Flow Metab.* 2015;35(6):888–901.
11. Aymé G, Adam F, Legendre P, et al. A Novel Single-Domain Antibody Against von Willebrand Factor A1 Domain Resolves Leukocyte Recruitment and Vascular Leakage During Inflammation-Brief Report. *Arteriosclerosis, Thrombosis, and Vascular Biology*. 2017;37(9):1736–1740.
12. Kleinschnitz C, Pozgajova M, Pham M, et al. Targeting platelets in acute experimental stroke: impact of glycoprotein Ib, VI, and IIb/IIIa blockade on infarct size, functional outcome, and intracranial bleeding. *Circulation*. 2007;115(17):2323–2330.
13. Li T-T, Fan M-L, Hou S-X, et al. A novel snake venom-derived GPIb antagonist, anfibatide, protects mice from acute experimental ischaemic stroke and reperfusion injury. *Br. J. Pharmacol.* 2015;172(15):3904–3916.
14. Scully M, Cataland SR, Peyvandi F, et al. Caplacizumab Treatment for Acquired Thrombotic Thrombocytopenic Purpura. *N. Engl. J. Med.* 2019;380(4):335–346.
15. Scully M, Knöbl P, Kentouche K, et al. Recombinant ADAMTS-13: first-in-human pharmacokinetics and safety in congenital thrombotic thrombocytopenic purpura. *Blood*. 2017;130(19):2055–2063.
16. Denorme F, Martinod K, Vandenbulcke A, et al. The von Willebrand Factor A1 domain mediates thromboinflammation, aggravating ischemic stroke outcome in mice. *Haematologica*. 2020;haematol, in press

Geneeskundige Stichting Koningin Elisabeth
Fondation Médicale Reine Elisabeth
Königin-Elisabeth-Stiftung für Medizin
Queen Elisabeth Medical Foundation

Progress report of the university research project of

Prof. dr. Lieve Moons &
Lies De Groef, MSc, PhD
Katholieke Universiteit Leuven (KU Leuven)

Prof. dr. Lieve Moons
Head Division Animal Physiology and Neurobiology (APN)
Head RU Neural Circuit Development and Regeneration (http://bio.kuleuven.be/df/LM/)
Department of Biology, KU Leuven
Zoological Institute, Naamsestraat 61, bus 2464
3000 Leuven

Phone: 32-16-32 39 91
E-mail: lieve.moons@kuleuven.be

Lies De Groef, MSc, PhD
Onderzoeksgroep neurale ontwikkeling en regeneratie premonstreit college
Naamsestraat 61 bus 2464 b-
3000 leuven
lies.degroef@kuleuven.be

Oligodendrocytes in Wolfram syndrome: bystanders or partners in crime?

1. Project aims

Wolfram syndrome is a rare hereditary disease, causing diabetes, blindness, deafness and other neurological problems in infants and young adults, and results in death around the age of 30 years. Wolfram patients carry recessive mutations in the WFS1 gene, resulting in loss of function of the WFS1 protein. Loss of WFS1 has been shown to result in ER stress, dysregulated Ca^{2+} homeostasis and mitochondrial dysfunction. Remarkably, in the brains of Wolfram patients, distinct white matter loss has been observed. Combining this with the observation that myelinating oligodendrocytes are especially sensitive to ER stress, we hypothesize that oligodendrocytes play an important role in the neurodegeneration seen in Wolfram patients. Therefore, in this project, we will investigate what the effect of these 'diseased' oligodendrocytes is on the function of 'healthy' neurons, focusing on ER stress, mitochondria and cell metabolism as potential underlying mechanisms. In addition, we will further unravel the function of the WFS1 protein by identifying its binding partners in this cellular model system. Finally, we will study the interplay between oligodendrocyte/myelin loss and neurodegeneration in a Wfs1 mouse model, and provide seeding evidence that interfering with the studied cellular processes and WFS1 binding partners can rescue the disease phenotype.

The concrete goals of this project are:

1. To perform a comprehensive study of the WFS1 binding partners.
2. To study *in vitro* which cellular processes are affected in Wolfram patient iPSC-derived oligodendroglia, thereby focusing on ER stress, mitochondrial function and metabolism; investigating the contributions of the newly identified WFS1 binding partners to these cellular processes; and studying the effect of 'diseased' oligodendroglia on wild-type 'healthy' neurons.
3. To study *in vivo* the changes in oligodendrocytes and neurons in the *Wfs1* KO mouse model, to compose a timeline of neuronal *versus* oligodendrocyte pathology.
4. To rescue the Wolfram syndrome phenotype in the *Wfs1* KO mice by interfering with the newly identified WFS1 binding partners or cellular processes.

2. Progress report

In the first year of the project –as planned in the original Gantt chart– we have focused on aims (ii) and (iii), thereby performing the first tasks of work packages II and III. We have performed an *in vitro* study of the effects of WFS1 deficiency in iPSC-derived oligodendroglia (task I.1), a morphological characterization of CNS integrity in Wfs1 KO mice (task III.1) as well as a functional characterization of CNS integrity in Wfs1 KO mice (task III.2). Experiments related to the study of the WFS1 binding partners (work package I) were postponed and instead more resources were invested into the functional characterization of CNS integrity in the Wfs1 KO mice –which will therefore be completed sooner. We believe that this will allow us to progress faster to a deeper understanding of the pathological processes underlying Wolfram syndrome and that this knowledge will advance the analysis of the planned proteomics study in WP I. Indeed, a better knowledge of the cell types and disease processes underlying Wolfram syndrome will aid the identification of relevant WFS1 binding partners and speed up their validation in task II.3.

2.1. Task I.1 *In vitro* study of the effects of WFS1 deficiency in iPSC-derived oligodendroglia

At the start of this project, two WFS1 patient iPSC lines, one isogenic control line and two commercially available control lines were available in house. Using the protocol published by García-León *et al.*[1] these **iPSC lines were differentiated into O4⁺ oligodendrocytes**. A first series of experiments with these iPSC-derived oligodendrocytes, however, revealed that differentiation into iPSC is suboptimal. Hence we switched to a newly developed protocol[2]which can subsequently myelinate neurons, both *in vitro* and in vivo. To date, OPCs have been derived from eight different hPSC lines including those derived from patients with spontaneous and familial forms of MS and ALS, respectively. hPSCs, fated for 8 d toward neural progenitors, are transduced with an inducible lentiviral vector encoding for SOX10. The addition of doxycycline for 10 d results in >60% of cells being O4-expressing OPCs, of which 20% co-express the mature OL marker myelin basic protein (MBP that uses genome engineering to deliver SOX10, the 'master' transcriptional regulator of the oligodendrocyte lineage, to iPSCs (Figure 1A-C). We found that iPSC-derived oligodendrocytes from this protocol show a better morphology, survival and tremendously increased oligodendrocyte maturation. Therefore, all patient and control iPSC lines were genome engineered according to this protocol, and also an additional isogenic control line was made using adenine base editing (ABE). A third patient iPSC line is currently being engineered.

Following quality checks with junction PCRs, southern blotting, GFP-based flow cytometry and qPCR for SOX10, these engineered iPSC lines were next differentiated into oligodendrocytes, which were then further characterized to **study pathological processes that have been linked to Wolfram syndrome**. While optimization of the yield of the O4+ oligodendrocytes is still ongoing, we already show that patient iPSC-derived oligodendrocytes at 37 days *in vitro* (DIV 37) are more vulnerable to tunicamycin-induced **ER stress** compared to controls, as evident from qPCR for the ER stress marker C/-EBP homologous protein (CHOP) (Figure 1D). Furthermore, this tunicamyin treatment also led to a **loss of myelin** basic protein (MBP) expression in the patient iPSC-derived oligodendrocytes, while oligodendrocytes differentiated from iPSC isogenic control lines kept their MBP levels (Figure 1E). Furthermore, staining with the mitochondrial membrane potential probe JC-1 on DIV 40 revealed **mitochondrial membrane depolarization** in patient iPSC-derived oligodendrocytes compared to isogenic controls (Figure 1F).

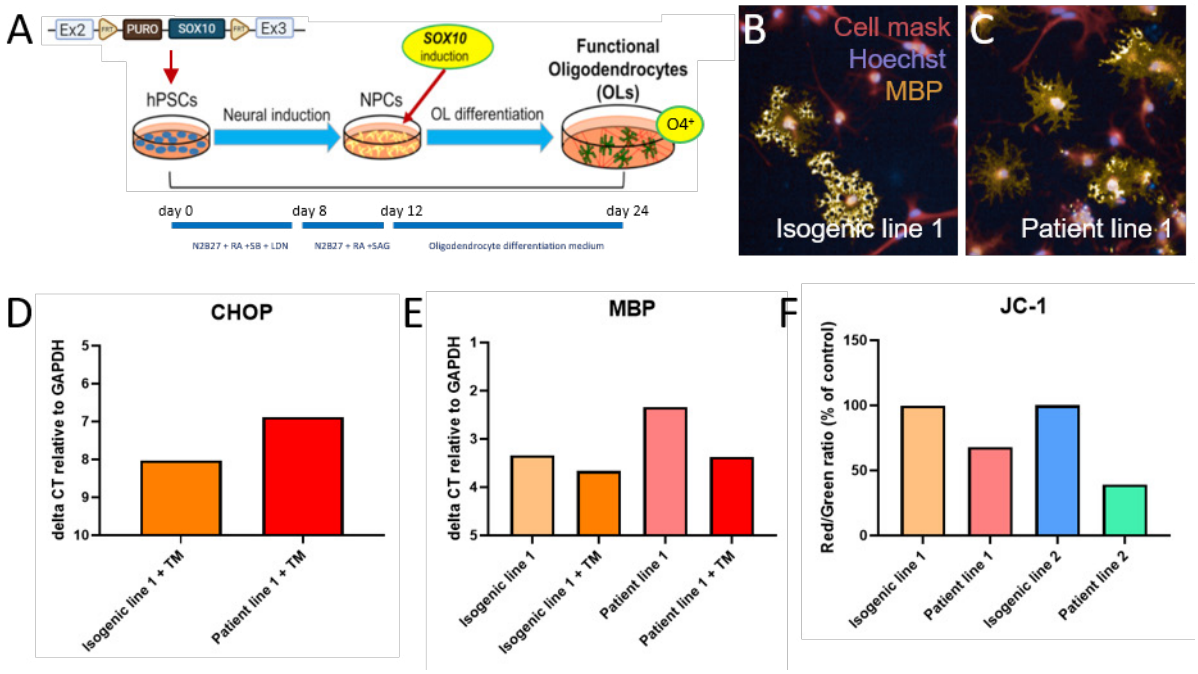

Figure 1. ER stress, oligodendrocyte maturation and mitochondrial changes in patient iPSC-derived oligodendrocytes. (A) Schematic overview of the protocol to generate oligodendrocytes from iPSCs. First, an inducible SOX10 cassette is introduced into the iPSC cell genome. Hereafter, neuronal precursor cells are formed and SOX10 expression is induced using doxycycline. After 24 days, O4$^+$ oligodendrocytes are generated. (B-C) Illustration of mature MBP$^+$ oligodendrocytes generated from iPSC isogenic line 1 (B) and patient line 1 (C), using this protocol. (D) After treatment with the ER-stress inducer tunicamycin (TM), CHOP expression is increased in patient line 1 iPSC-derived oligodendrocytes. (E) Treatment with TM lowers MBP expression more in patient line 1 compared to isogenic line 1 oligodendrocytes. (F) Staining with the JC-1 dye reveals mitochondrial depolarization in patient line 1 and 2 iPSC-derived oligodendrocytes.

Altogether these data suggest that iPSC-derived oligodendrocytes from Wolfram patients may be more vulnerable to ER stress and display signs of mitochondrial dysfunction. Replicate experiments are ongoing to confirm these findings, and additional studies of ER stress, mitochondrial function and cell metabolism are planned to elaborate on these findings. In parallel, we have also initiated the co-cultures of oligodendrocytes and neurons, thereby preparing a smooth start for task II.2.

2.2. Task III.1 Morphological characterization of CNS integrity in Wfs1 KO mice & Task III.2 Functional characterization of CNS integrity in Wfs1 KO mice

The eye, optic nerve and brain phenotype of Wfs1 KO mice and corresponding WT littermates was studied at 3, 4.5, 6 and 7.5 months of age. Besides elevated intraocular pressure (Figure 2A), Wfs1 mice display **reduced visual acuity (Figure 2B) and abnormal electrophysiological responses (pSTR) of their retinal ganglion cells (Figure 2C)** at 6 to 7.5 months of age. These functional deficits, however, were not reflected in the retinal morphology. No signs of retinal neurodegeneration were found. However, **neuroinflammation**, *i.e.* macro- and microglial reactivity, is apparent in the retina of Wfs1 KO at the age of 6 months, as shown via Western blot (Figure 2D-F) and immunohistochemistry for glial fibrillary acidic protein (GFAP), S100 calcium-binding protein B (S100B) and Ionized calcium binding adaptor molecule 1 (IBA1) (Figure 2 G-L).

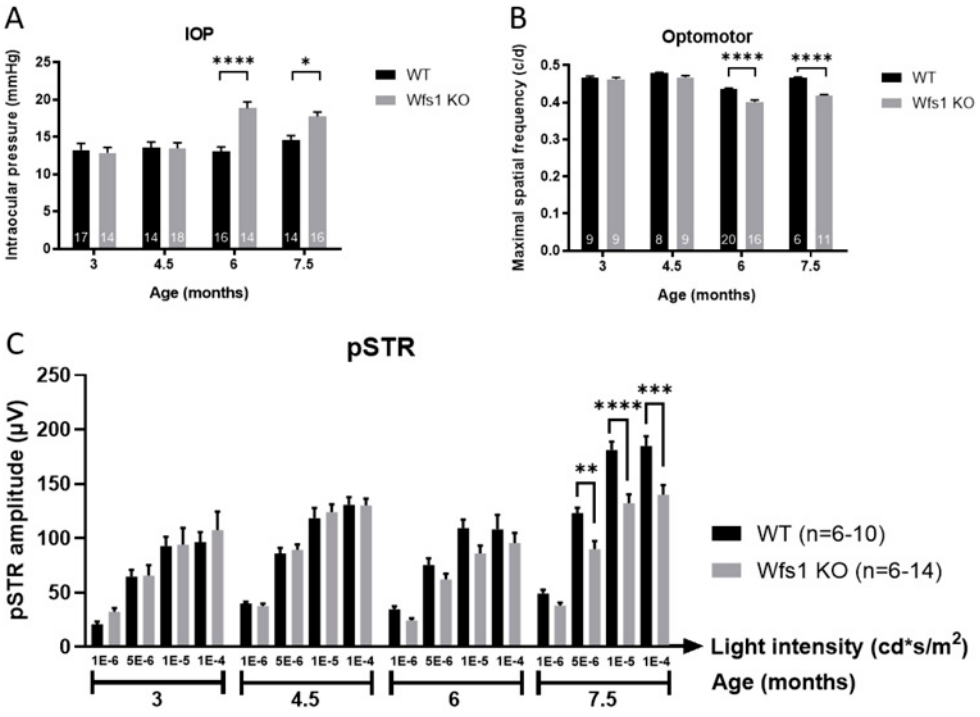
A
IOP
Intraocular pressure (mmHg)
****
*
WT
Wfs1 KO
Age (months)
B
Optomotor
Maximal spatial frequency (c/d)
****
****
WT
Wfs1 KO
Age (months)
C
pSTR
pSTR amplitude (µV)
**
****
***
WT (n=6-10)
Wfs1 KO (n=6-14)
Light intensity (cd*s/m2)
Age (months)

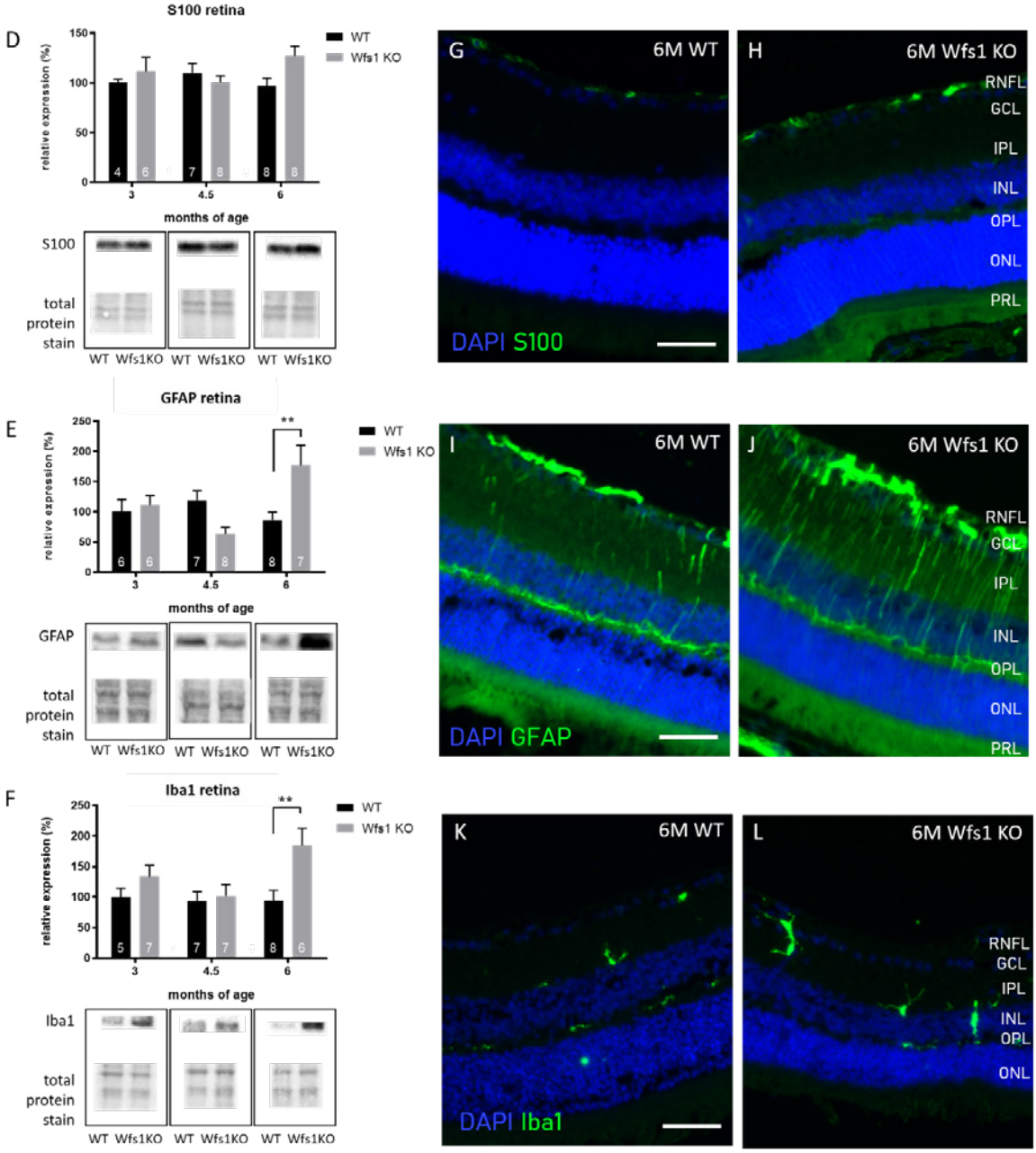

Figure 2. Wfs1 KO mice show reduced neuronal functionality and increased inflammation in the retina. (A) Wfs1 KO mice show a significant increased intraocular pressure (IOP) compared to WT mice starting at 6 months of age. (B) Visual acuity is decreased in Wfs1 KO mice compared to WT littermates starting at 6 months of age. (C) Reduced pSTR amplitudes are observed in Wfs1 KO compared to WT mice at 6 and 7.5 months of age. (D-F) Western blots for S100B (D), GFAP (E) and Iba1 (F) reveal that there is macro- and microgliosis in the retina of 6-month-old Wfs1 KO mice. (G-L) Representative images of immunostainings on retinal sections of 6-month-old Wfs1 KO and WT mice, show an increased S100B expression, an increased number of GFAP immunopositive fibers and an increase in microglia/infiltrating macrophage numbers in Wfs1 KO mice. Scale bar: 50 µm. NFL: nerve fiber layer, GCL: ganglion cell layer, IPL: inner plexiform layer, INL: inner nuclear layer, OPL: outer plexiform layer, ONL: outer nuclear layer, PL: photoreceptor layer. Two-way ANOVA, Sidak's post-hoc test; *, p<0.05; **, p<0.01; ***, p<0.001; ****, p<0.0001; the number of biological repeats/mice is included in the graphic.

In line with the results from these ocular/retinal phenotyping experiments, **optic nerve atrophy** was observed on toluidin blue-stained semi-thin sections of the optic nerve of Wfs1 KO mice at 6 months of age (Figure 3A). Furthermore, we found evidence for a **reduced action potential conduction in the optic nerve** of these mice, via *in vivo* measurements of visual evoked potentials (Figure 3B) as well as *ex vivo* recordings of compound action potentials in optic nerves from Wfs1 KO *versus* WT mice (Figure 3C-D. Transmission electron microscopy analyses of the optic

nerve revealed that WfS1 KO mice have more axons with a small diameter yet there were no over differences in the G-ratio (Figure 3E-F). Together, this suggests that, although the axonal conduction is affected, there are no changes in myelination in WfS1 KO mice.

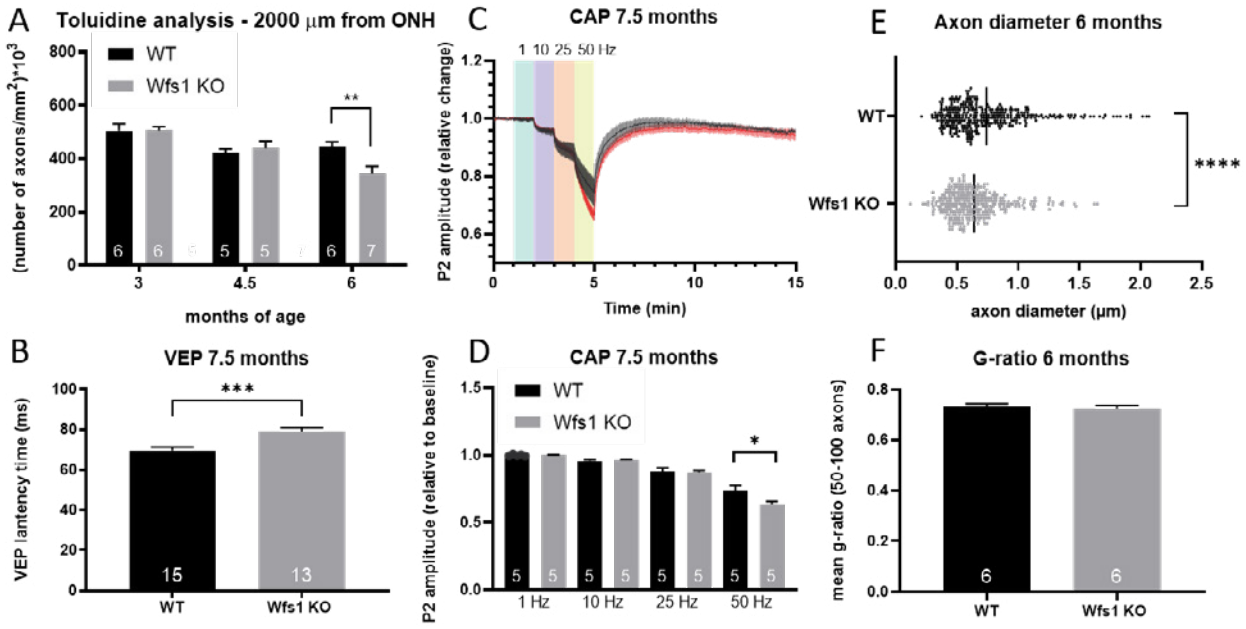

Figure 3. Optic nerve function and morphology is altered in Wfs1 KO mice. (A) Analysis of the number of axons on toluidine blue-stained sections at a distance of 2000 µm from the optic nerve head shows a decreased number of axons in 6-month-old Wfs1 KO mice as compared to WT littermates. (B) Visual evoked potential latency time, a measure for conduction speed and an indication for myelination status, is significantly elevated in 7.5-month-old Wfs1 KO compared to WT mice. (C-D) In addition, *ex vivo* compound action potential (CAP) measurements reveal a lower amplitude at the highest stimulation frequency (50 Hz) in 7.5-month-old Wfs1 KO mice compared to WT controls. (E) Measurements of individual axon diameters on transmission electron microscopy (TEM) images, reveal that the average axon diameter is smaller in Wfs1 KO mice compared to WT controls. (F) Measurements of the G-ratio of axons on TEM images show no difference in 6-month-old Wfs1 KO mice. Two-way ANOVA, Sidak's post-hoc test was used for the toluidine analysis; unpaired student's t-tests were used for the other graphs; *, p<0.05; **, p<0.01; ***, p<0.001; ****, p<0.0001; the number of biological repeats/mice is included in the graphic. TEM and CAP studies were performed in collaboration with Prof. E. Wolfs (Hasselt University) and Prof. A. Saab (Zürich University), respectively.

Finally, we assessed the neurodegeneration and -inflammation phenotype of the Wfs1 mouse in the **cerebellum, medulla and pons** – given that these regions are mostly affected in Wolfram patients. Here, we observed an early and severe phenotype in the cerebellum, with **neurodegeneration, astrogliosis and microglia** reactivity already at 3-6 months of age. Smaller and later changes were seen in the medulla and pons (Figure 4). To zoom in on this brain phenotype and expand our analysis to other brain regions, we next carried out a pilot **MRI study** of the optic nerve and brain, in collaboration with Prof. U. Himmelreich (MOSAIC, KU Leuven). MRI images have been acquired in 7.5-month-old Wfs1 KO and WT mice and are currently being analysed. We collected anatomical, T2-weighted and diffusion tensor images, to study neuroanatomy and -degeneration, iron accumulation and white matter microstructure, respectively. Such images will in a next phase also be acquired at younger ages, to study the course of neurodegeneration/demyelination in more detail. Based on these first MRI results, we will investigate neuronal cell numbers, myelination, oligodendrocyte differentiation, glial reactivity and inflammation within the different parts of the brain via follow-up immunohistological experiments and Western blot –for which sample collection has already been completed. Additionally, depending on the MRI results, functional tests assessing the cerebellum, limbic system and brainstem will be started in collaboration with Prof. R. D'Hooghe (KU Leuven).

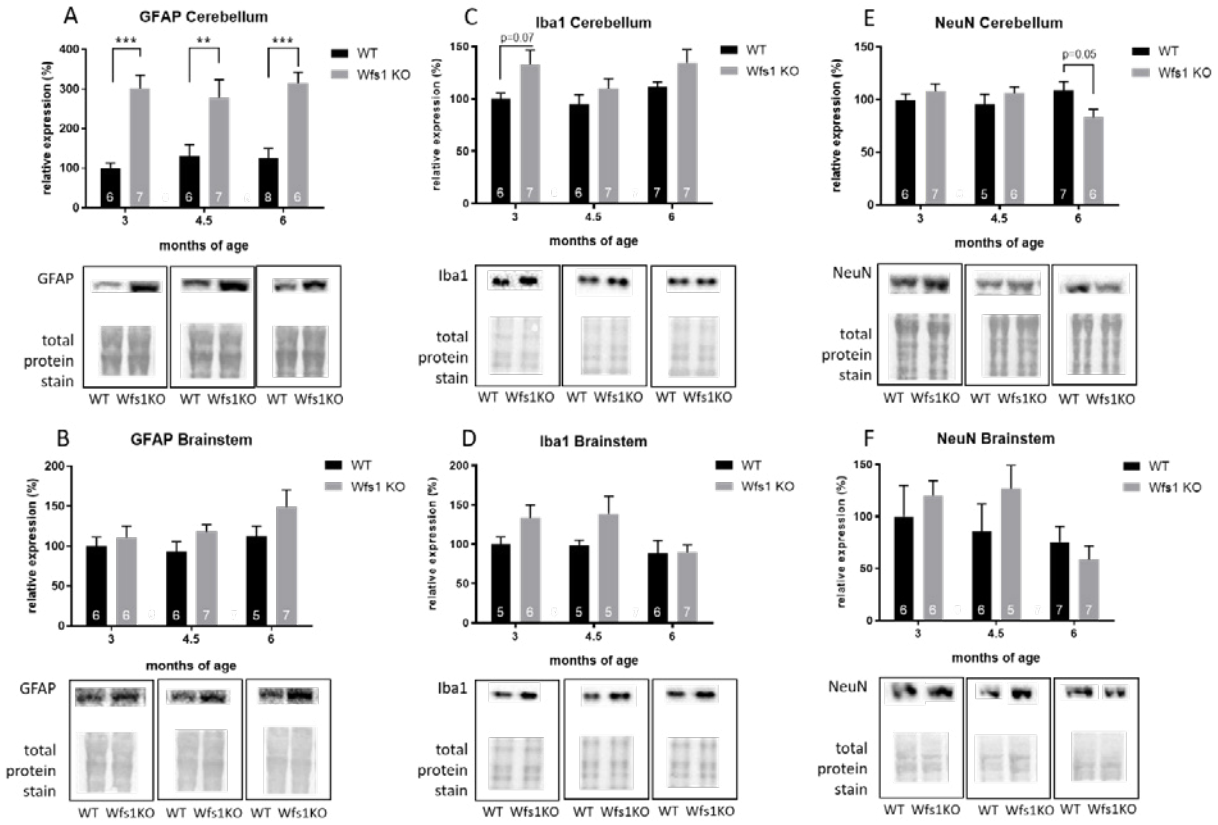

Figure 4. Wfs1 KO brains are characterized by neurodegeneration, astrogliosis and microgliosis. (A) Densitometric analysis of GFAP expression in the cerebellum shows a significant increase over time in Wfs1 KO mice. (B) In the brainstem, GFAP does not show distinct differences at any age in Wfs1 KO mice as compared to WT mice. (C,D) Densitometric analysis of Iba-1 shows upregulated expression levels in the cerebellum (C) but not in the brainstem (D). (E,F) Densitometric analysis of NeuN expression show significant differences between Wfs1 KO and WT mice at 6 months of age in the cerebellum (E), but not in the brainstem (F). Two-way ANOVA, Sidak's post-hoc test; **, p<0.01; ***, p<0.001; the number of biological repeats/mice is included in the graphic.

In conclusion, a pathological phenotype was observed in the retina, optic nerve and cerebellum in 6-month-old Wfs1 KO mice. This phenotype comprises axonal degeneration and hypomyelination, neuronal dysfunction and neuroinflammation. In a next step, we will focus on the temporal orchestration of these events and the interplay between neurons and oligodendrocytes. For the latter, we have also initiated the acquisition of WFS1 floxed mice, which will be cross-bred with cell type-specific Cre lines to further disentangle which cell types are the drivers of Wolfram syndrome pathology.

3. Conclusions and future planning

The data gathered within this project, in Wolfram syndrome patient iPSC-derived oligodendrocytes and a Wolfram syndrome mouse model point towards a critical role for oligodendrocytes in this neurodegenerative pathology. This supports the central hypothesis of the project, *i.e.* that oligodendrocytes rather than neurons might be the drivers of the disease processes that lead to neurodegeneration in Wolfram syndrome, and confirms that we are on track with the proposed research. Despite some delays due to COVID19, we can state that the work is ongoing according to the original plans and the goals set for the first year have largely been reached. As such, everything is in place for the successful continuation of the project in the coming years.

4. References

1. García-León, J. A. *et al.* SOX10 Single Transcription Factor-Based Fast and Efficient Generation of Oligodendrocytes from Human Pluripotent Stem Cells. *Stem Cell Reports* **10**, 655–672 (2018).
2. García-León, J. A. *et al.* Generation of oligodendrocytes and establishment of an all-human myelinating platform from human pluripotent stem cells. *Nat. Protoc.* **15**, 3716–3744 (2020).

Geneeskundige Stichting Koningin Elisabeth
Fondation Médicale Reine Elisabeth
Königin-Elisabeth-Stiftung für Medizin
Queen Elisabeth Medical Foundation

Progress report of the university research project of

Prof. Pierre Vanderhaeghen, MD, PhD (VIB)
Katholieke Universiteit Leuven (KU Leuven)

Prof. Pierre Vanderhaeghen, MD, PhD
Stem Cell and Developmental Neurobiology
Lab VIB-KU Leuven Center for Brain & Disease Research Department of Neurosciences,
Leuven Brain Institute IRIBHM / ULB Neuroscience Institute
pierre.vanderhaeghen@kuleuven.be

Deciphering the mechanisms underlying intellectual deficiency and autism spectrum disorders by cellular modelling in human neurons in vivo.

1. State of the art and objectives

Neurodevelopmental disorders (NDDs), including intellectual disability (ID) and autism spectrum disorders (ASD) present a major challenge in clinical genetics and medicine. The advent of novel genomic technologies has led to the identification of many underlying genetic defects [1,2]. However, before tailored therapies can be developed, one needs to decipher the exact underlying pathophysiology.
To this aim, most of the studies on NDD have relied on animal models, which has led to substantial progress thanks to the evolutionary conservation of many signaling pathways. However there are also important evolutionary differences in brain development, so that the exact impact of NDD mutations in human neurons remains unknown, as well as the translatability of preclinical findings. This is particularly relevant for ID and ASD, which are mostly linked to alterations of the cerebral neocortex, the most evolutionary divergent structure in the human brain.

Given the the difficulty to study the brain of patients at the cellular level, the advent of human pluripotent stem cell (PSC) has offered new opportunities [3]. While *in vitro* PSC-based models have been used successfully to model several NDD, *in vivo* elements are crucially missing from these approaches, which thus display serious limitations to model faithfully all aspects of ID/ASD. For this reason we have started to develop models of xenotransplantation, where PSC-derived human neurons are transplanted into the mouse cortex [4,5]. Following transplantation in the mouse neonatal cortex, the PSC-derived pyramidal neurons develop like endogenous cortical neurons, and integrate functionally in the host brain, following their species-speciifc time-line.

In this project we aim to determine the pathophysiological mechanisms of ID/ASD conditions linked to mutations in *SYNGAP1* and *MEF2C*, through the *in vivo* study of human neurons displaying clinically relevant mutations. The project is based on the following objectives:
***Aim1.* Development of fully validated *in vitro* PSC models for *SYNGAP1* and *MEF2C* related disorders.**
***Aim2.* Characterization of SYNGAP1 and MEF2C loss of function in human cortical neurons *in vivo*.**

2. Results

2.1. WP1. Generating human cortical neurons displaying specific NDD mutations.

The first step of the project is to generate isogenic PSC lines displaying specific mutations of *SYNGAP1* and *MEF2C* using directed genomic engineering. We have now generated these lines for SYNGAP1, including several lines harbouring homozygote or heterozygote mutations.
Briefly, human embryonic stem cell (ESC) lines (using H9 line routinely used in our lab) were disrupted for SYNGAP1 using CRISPR/Cas9 technology. A pair of single guide RNAs (sgRNA) was used to target and delete exon 8, which was chosen because it is common to all *SYNGAP1* alternate transcripts, and is located upstream of the functionally most important functional domains (***Figure 1***). To generate SYNGAP1 heterozygote lines we have relied on a knock-in

approach to ensure that only one allele is targeted. Following selection several clones were differentiated into cortical pyramidal neurons and tested by Western blotting for SYNGAP1 expression. This confirmed loss of expression in homozygote mutants, and reduction to 50% expression in heterozygote lines, as expected. Moreover analysis of canonical markers of corticogenesis did not reveal any differtence between the lines, indicating that the early step of cortical neurons generation and differentation appear to be normal following SYNGAP1 loss of function.
A similar approach is ongoing for MEF2C.

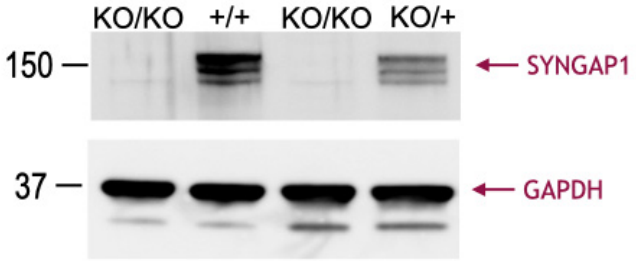

Figure 1: *Western blot immunodetection of SYNGAP1 and GAPDH in cortical neurons differentiated from human ESC, control (+/+), homozygote (KO/KO) or heterozygote (KO/+) mutants for SYNGAP1.*

2.2. WP2. *In vivo* characterization of SYNGAP1 loss of function in human cortical neurons.

Following *in vitro* validation, human differentiated cortical neurons from mutant and control cell lines are now routinely transplanted into neonatal mice. Specifically we will rely on a system that we pioneered, revealing species-specific patterns of development of human cortical pyramidal neurons and their maturation up to physiological functional responses indistinguishable from host mouse neurons.

WP2.1 Synaptic function and plasticity of mutant human cortical neurons in vivo.

Control and mutant cortical cells were differentiated *in vitro* and infected by lentiviruses prior to transplantation with fluorescent reporters markers (tdTomato or Venus).
Ex vivo brain slices were prepared from transplanted mice and examined by patchclamp recording focused on GFP-labelled transplanted neurons (***Figure 2***). The intrinsic electrophysiological properties of grafted neurons were determined, as well as the existence of functional synaptic inputs from host to transplanted neurons.
Remarkably this analysis revealed a striking increase in synaptic activity and maturation in SYNGAP1 mutants (both homos and heteros), while intrinsic neuronal properties appear to be normal. This important dataset thus constitutes a first direct evidence that SYNGAP1 los of function leads to accelerated synaptogenesis in human neurons.

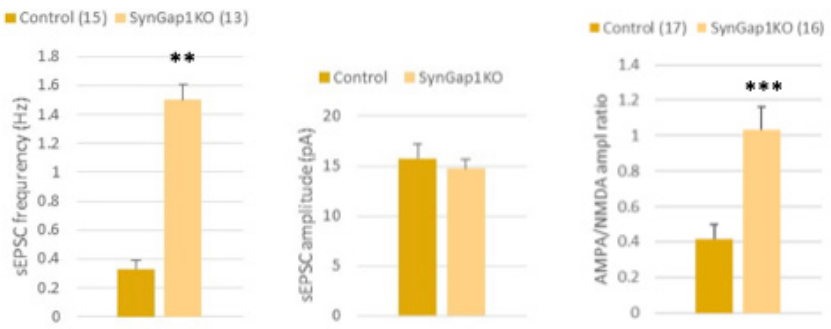

Figure 2: *Patch-clamp recordings of human neurons (control and SYNGAP1 KO) in ex vivo slices from xenotransplanted mice at 4.5 months post-transplantation. SYNGAP1KO neurons display increased frequency of synaptic activity and increased AMPA/NMDA ratios, indicative of greater maturation.*

WP2.2. Neuronal morphogenesis of mutant human cortical neurons in vivo.
Following recordings, the cells were filled with biocytin to study their detailed morphology using confocal imaging and 3D reconstruction. This analysis revealed increase density of the spines in the mutant neurons, further confirming increased maturation rates in the mutant cells (data not shown).

WP2.3. Live characterization of mutant neurons using in vivo imaging.
Finally, have started *in vivo* multiphoton imaging to characterize in *live* animals the developmental dynamics and function of human neurons. For developmental dynamics focused on dendritic spines, as a *proxy* of synapse formation, using standard imaging of fluorescently labeled neurons. Briefly, the transplanted animals undergo specific surgery for cranial window at 3MPT or 6MPT, enabling the identification of the human neurons. Then the same neuron are repetitively imaged over a period of up to six weeks, enabling to reveal dendritic spines with high spatial and temporal resolution (***Figure 3***). This has revealed a striking increase of dendritic spine density in both homozygote and heterozygote neurons, together with increased rates of spine formation.
For functional analysis, we will use GCAMP functional calcium imaging that we have successfully implemented to human neurons transplanted in the mouse visual cortex, enabling to reveal specific functional responses of these neurons following physiological visual stimuli in awake animals. The analysis of the mutant neurons is currently ongoing at relevant developmental timepoints.

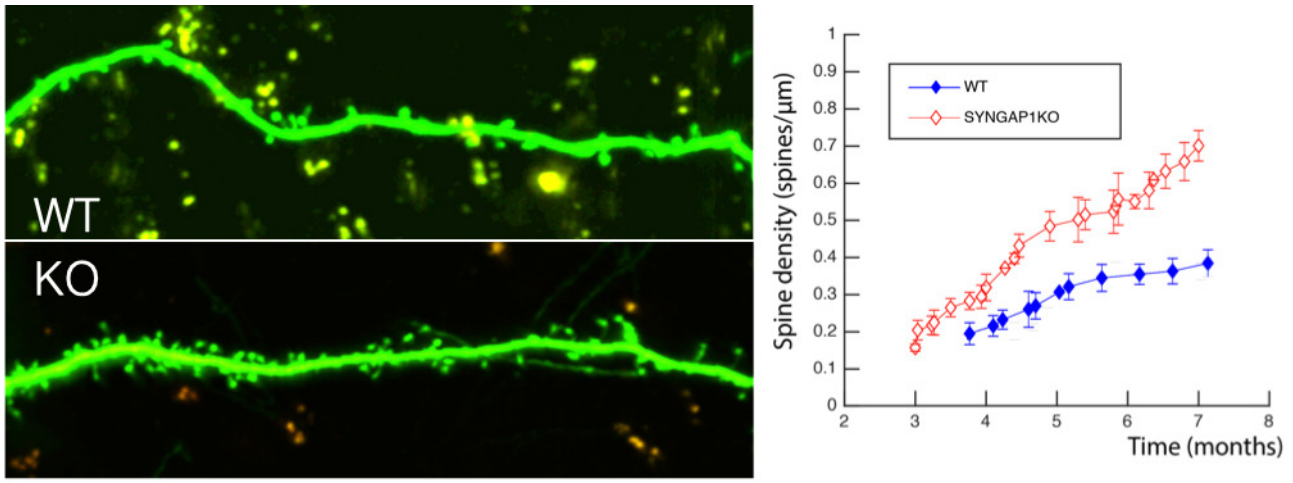

Figure 3: *In vivo imaging of dendritic spines of control and SYNGAP1KO neurons in xenotranspanted neurons reveals increased spine density and increased rates of dendritic spine outgrowth in SYNGAP1 KO neurons.*

Collectively, the experiments that we have performed so far thus enabled us to establish an in vivo neuronal model of SYNGAP1-related neurodevelopmental disorders. Moreoever our data obtained so far all converge on a striking acceleration of synaptic maturation in the mutant neurons, thus revealing a first potential physiopathological mechanism of this disease.

We will now pursue these experiments, focusing on function of mutant cells and extending to MEF2C and other pathologies in which we suspect that NDD is caused by disrupted cortical neuronal development, including diseases striking mitochondria, which we recently found to be instructive for proper corticogenesis [6].

3. References

1. Walsh, C. A., Morrow, E. M. & Rubenstein, J. L. Autism and brain development. *Cell* **135**, 396–400 (2008).
2. Zoghbi, H. Y. & Bear, M. F. Synaptic dysfunction in neurodevelopmental disorders associated with autism and intellectual disabilities. *Cold Spring Harb Perspect Biol* **4**, (2012).
3. Brennand, K. J. K. J. *et al.* Creating Patient-Specific Neural Cells for the In Vitro Study of Brain Disorders. *Stem Cell Reports* **5**, 933–945 (2015).
4. Espuny-Camacho, I. *et al.* Pyramidal Neurons Derived from Human Pluripotent Stem Cells Integrate Efficiently into Mouse Brain Circuits In Vivo. *Neuron* **77**, 440–456 (2013).
5. Linaro, D. *et al.* Xenotransplanted Human Cortical Neurons Reveal Species-Specific Development and Functional Integration into Mouse Visual Circuits. *Neuron* **104**, 972-986.e6 (2019).
6. Iwata, R., Casimir, P. & Vanderhaeghen, P. Mitochondrial dynamics in postmitotic cells regulate neurogenesis. *Science (80-.).* **862**, 858–862 (2020).

4. Publications in 2020

Mitochondria dynamics in postmitotic cells regulate neurogenesis.
Iwata R, Casimir P, **Vanderhaeghen P**.
Science 2020, 369 (6505):858-862.

Tempus fugit: How time flies during development.
Iwata R, **Vanderhaeghen P**.
Science 2020 369 (6510):1431-1432.

Geneeskundige Stichting Koningin Elisabeth
Fondation Médicale Reine Elisabeth
Königin-Elisabeth-Stiftung für Medizin
Queen Elisabeth Medical Foundation

Progress report of the university research project of

Prof. dr. Thomas Voets (VIB)
Katholieke Universiteit Leuven (KU Leuven)

Prof. dr. Thomas Voets
Laboratory of Ion Channel Research
VIB-KU Leuven Center for Brain & Disease Research
KU Leuven, Department of Cellular and Molecular Medicine
Herestraat 49 bus 801
3000 Leuven
Tel: +32 16 33 02 17
Thomas.voets@kuleuven.vib.be

Table of contents

Unraveling the cellular and molecular basis of noxious cold sensing

1. Background

Noxious cold and noxious heat have detrimental effects on key biological macromolecules, and thus on the integrity of cells, tissues and organisms[1]. Thanks to the action of a subset of somatosensory neurons, mammals can swiftly detect noxiously cold or hot objects or environments. These temperature-sensitive nociceptor neurons become activated when the temperature at their free endings in the skin or mucosae reaches noxious levels, provoking acute pain and initiating avoidance reflexes[2].

In the last two decades, several ion channels of the transient receptor potential (TRP) superfamily have been put forward as key molecular sensors in somatosensory neurons, involved in various aspects of temperature sensing and pain[1-3]. In a recent key paper from our research group, with the support of the Queen Elisabeth Medical Foundation, we uncovered the molecular basis of noxious heat detection, by showing that acute heat-induced pain depends on three TRP channels (TRPV1, TRPM3 and TRPA1), acting as redundant heat sensors in nociceptor neurons[4]. We found that simultaneous elimination of all three TRP channels fully eliminates heat responses in isolated sensory neurons, and completely abolishes heat-induced pain responses in mice[4].

In contrast, the molecular basis of noxious cold sensing remains unresolved[1]. Several studies, including work from our research group, have revealed that TRPM8 and TRPA1 act as molecular cold sensors involved in different aspects of innocuous and noxious cold sensing[5-13] . However, a subset of sensory neurons remains cold sensitive after combined elimination of both channels, and *Trpm8*$^{-/-}$/*Trpa1*$^{-/-}$ double knockout mice still exhibit a robust pain response to noxious cold[11, 14]. Thus, the cellular and molecular basis of noxious cold sensing remains essentially unknown[1]. The aim of the proposed research is therefore to unravel the cellular and molecular mechanisms underlying cold-induced pain, by identifying the mechanisms underlying TRPM8- and TRPA1-independent cold sensing.

Elucidating the basis of cold-induced pain not only addresses a fundamental question in sensory neurobiology, but may also have important medical applications. About one in five of adult Europeans suffer from moderate-to-severe chronic pain, and despite the fact that access to adequate pain management is considered a Fundamental Human Right[15], half of these chronic pain sufferers report inadequate pain control with available analgesic treatments[16, 17]. Cold allodynia, the condition where non-noxious cool stimuli evoke pain, is a frequent aspect of chronic pain and represents one of the hallmarks of neuropathic pain following nerve injury or chemotherapy[18]. Unfortunately, there are currently no safe and efficient therapies to treat cold allodynia. We anticipate that novel insights into the mechanisms of cold-induced pain may fuel the development of novel targeted pain therapies.

2. Scientific objective

In earlier work, we and others identified a subset sensory neurons exhibiting robust TRPM8- and TRPA1-independent Ca^{2+}-influx in response to cold[11, 19, 20]. As the origin of their cold sensitivity is unknown, we will name this subset of sensory neurons **O**rphan **C**old **N**eurons (OCNs). We hypothesize that these OCNs play a central role in cold pain, and express at least one type of cold sensor of unknown molecular identity. We intend to characterize these OCNs and identify the molecular basis of their cold sensitivity.

3. Results

3.1. Functional characterization and transcriptome analysis of cold-sensitive sensory neurons

A number of recent studies have reported RNA-seq-based single-cell transcriptome analyses of mouse DRG neurons, leading to hierarchical clustering of neurons into 11-18 subtypes[21-23]. However, how this transcriptome-based classification relates to the functional properties of sensory neurons is poorly understood. By performing Fura-2-based Ca^{2+}-imaging experiments followed by single-cell sequencing, we generated an approach that combines functional information with the cell's transcriptional fingerprint.

Our published and unpublished results indicate that approximately 8% of DRG neurons can be classified as M8-CNs an approximately 15% as A1-CNs; between 3 and 7% of all DRG neurons are OCNs[11]. In order to properly identify OCNs and exclude TRPA1 and TRPM8-cold mediated responses, we used *TRPA1*$^{-/-}$ knockout mice and excluded all neurons that reacted to the cooling agent menthol (TRPM8 agonist). Therefore, all DRG neurons that responded to cooling but failed to react to menthol (200 μM) stimulation were identified as OCNs. Once we identified by Ca^{2+}-imaging all OCNs, menthol sensitive neurons and neurons that did not respond to colling, we individually harvested the neurons of interest. For this, we used microcapillary pipettes connected to a micromanipulator to aspirate single cells under visual control. Individually harvested neurons had their transcriptome profile unraveled by Smart-seq 2 technology. Smart-seq2 is the preferred approach as it provides good coverage of the transcriptome, including rarer transcripts and splice variants [24]. To date, we collected and fully sequenced a total of 46 cells (20 OCNs, 4 menthol sensitive cells and 22 cells that do not respond to cooling). An average of approximately 8.000 genes was identified per cell. The marker genes used to identify cell types were: neurons = Rbfox3, endothelial = Cldn5, macrophages = Mrc1, glia = Mbp and fibroblasts = Mgp. All the collected samples presented a high expression of the neuronal marker Rbfox3 (Figure 1A), indicating that we successfully harvested sensory neurons. Most samples also showed some expression of the glial cell marker Mbp (Figure 1A). DRGs contain a unique type of glia cells, known as satellite glia cells, which form a sheath around the cell body of DRG neurons (generally, one neuron is wrapped by several SGCs), which may explain the presence of the glial marker in many of the neuronal samples (Figure 1B).

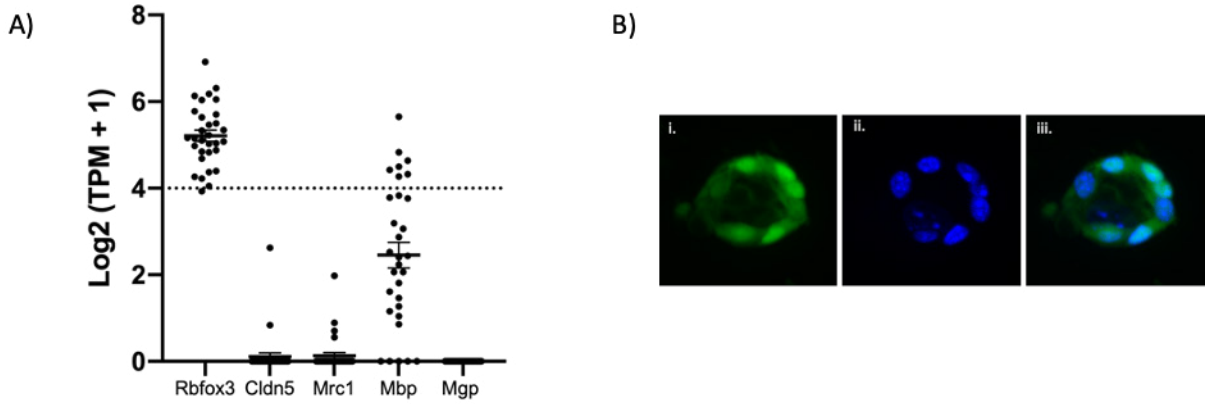

Figure 1: Cell subtype identification in DRG culture. (A) RNA seq data showing DRG cell subtype marker gene expression. Marker genes: Rbfox3 = neurons, Cldn5 = endothelial, Mrc1 = macrophages, Mbp = glia and Mgp = fibroblasts. (B) Satellite glia cells wrapping DRG neurons in a standard DRG culture. Cells were loaded with the calcium indicator Fluo-4 AM (green) and cell nuclei were stained with Hoechst® 33342 dye (blue). Images were made using confocal microscope. i. Fluo-4 AM, ii. Hoechst® 33342 and iii. overlay of the two channels.

The functional data obtained by Fura-2-based Ca^{2+}-imaging experiments presented a good correlation with the transcriptome data (Figure 2). The collected neurons that were sensitive to both menthol (TRPM8 agonist) and cooling stimulation (Figure 2A) turned out to have high expression levels of TRPM8 ion channels (Figure 2B). On the other hand, neurons that did not respond to menthol stimulation (Figure 2A) had no reads corresponding to TRPM8 transcripts (Figure 2B).

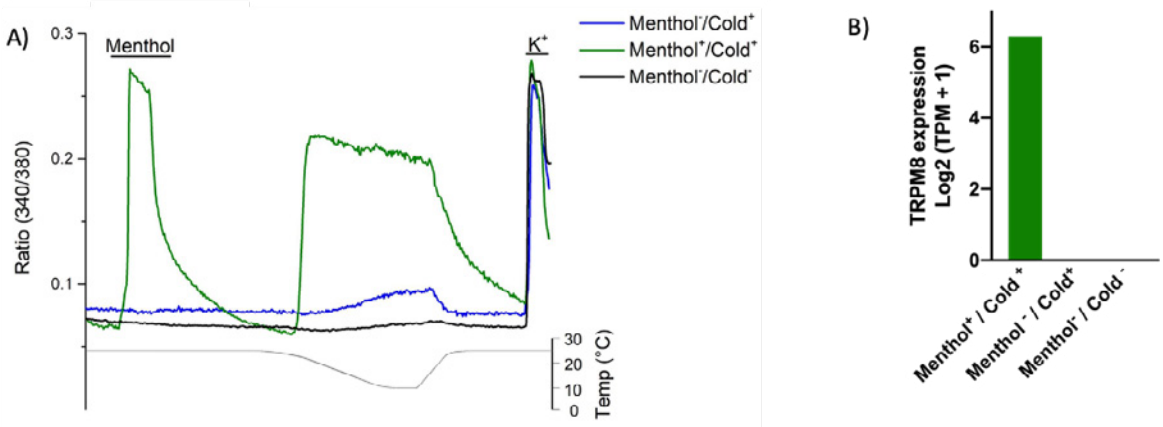

Figure 2: Functional and molecular characterization of DRG neurons. (A) Ratiometric measurement of changes in intracellular Ca^{2+} in response to menthol (200 μM) and cooling stimulation. The traces represent individual responses of 3 distinct neurons. (B) RNA seq data showing TRPM8 expression levels of the cells functionally characterized in panel A. Gene expression is given as log2(TPM+1).

3.2. Identification of candidate genes underlying cold responses in OCNs

For further characterization of OCNs and identification of genes that may underlie their cold sensitivity, we compared the transcriptomes of the identified OCNs and those from cells insensitive to cooling stimulation. Our data revealed 315 genes that are differentially expressed between the two groups of cells (Figure 3). Of these 315 genes, 171 are significantly upregulated in OCNs, and thus may contribute to their "orphan" cold sensitivity. As ion channels and membrane receptors represent prime candidate cold sensors, we will initially focus on genes that encode proteins with at least one transmembrane domain and select either proteins with unknown function or known ion channels. Among the 171 upregulated genes in OCNs, 12 have known transmembrane ion transporter activity (Figure 3). These possible candidates include ion channels permeable for sodium, potassium and calcium ion, as well as solute transporters and pumps.

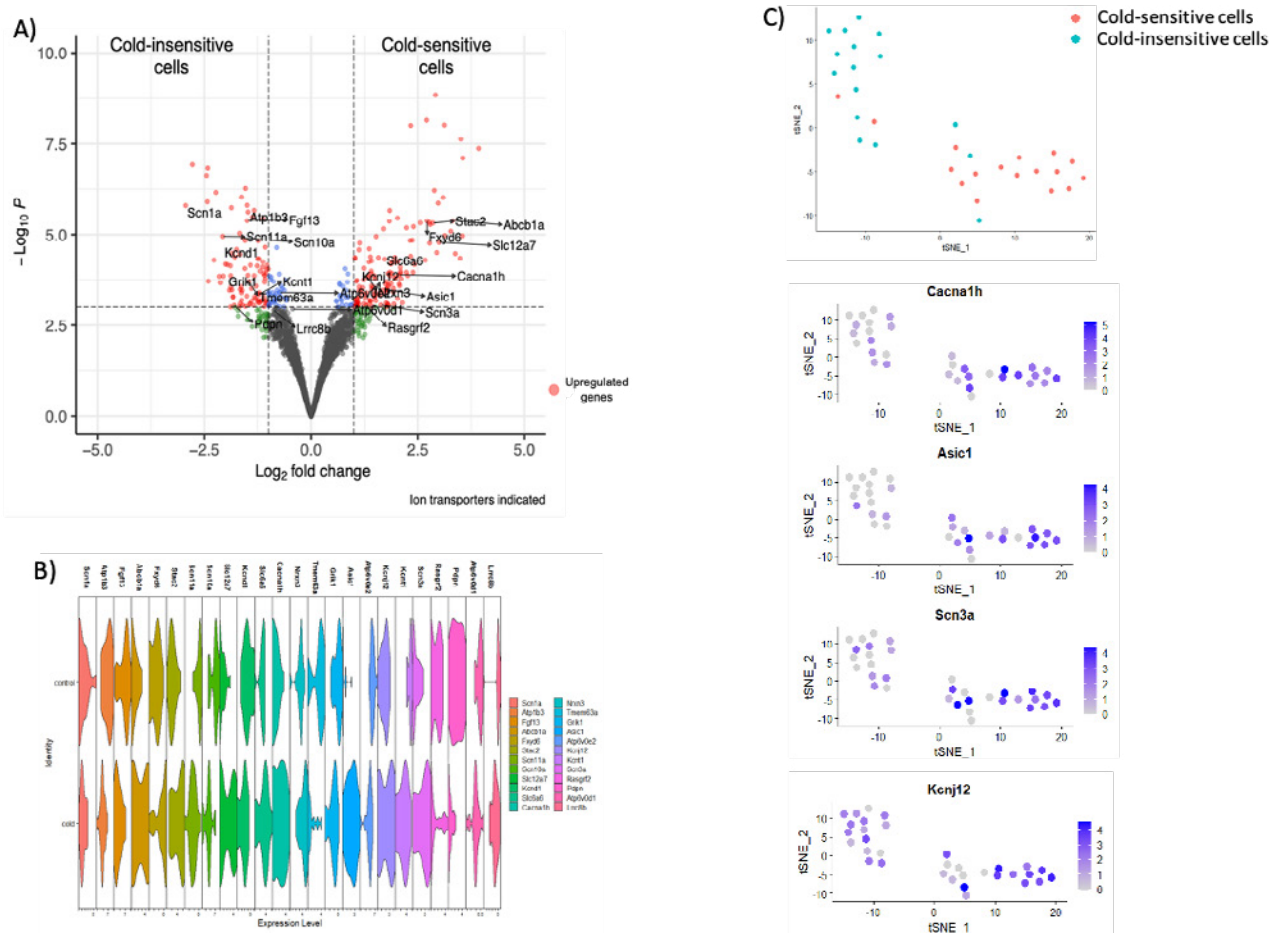

Figure 3: Gene expression analysis of scRNA-seq data. (A) Volcano plot displaying differentially expressed genes of cold sensitive and insensitive cells. Genes that have a P value smaller than 0.05 and an absolute value of log (fold change) larger than 1 are considered significant. Up-regulated genes in cold sensitive and insensitive cells are colored in red. Significantly upregulated ion transporters are indicated. (B) Overview of the expression levels of ion channel transporters between the 2 groups: Control (cold-insensitive cells) and cold (cold sensitive cells). (C) Expression levels of some of the upregulated calcium, sodium and potassium ion channels found in OCNs represented per cell collected.

4. Outlook and budget

With the financial support of the GSKE, we have been able to establish an approach to obtain a detailed transcriptome analysis of functionally characterized sensory neurons, and provide part of the salary of a dedicated postdoctoral researcher, Dr. Ana Freitas. This has allowed us to identify a set of candidate genes that may contribute to "orphan" cold responses. We are currently refining the candidate selection based on further electrophysiological characterization of OCNs, combine Fura-2-based Ca^{2+}-imaging experiments with whole-cell patch-clamp recordings.

Interestingly, amongst the top candidates is ASIC1, well known as an acid-activated ion channel although. Our preliminary data suggest that it may contribute to cold responses in sensory neurons. ASIC1-deficient mice are available from a commercial source (The Jackson Laboratory; strain 013733), so we are currently looking out to purchase a breeder pair, which we can cross to TRPA1 and TRPM8 deficient mice that are already available in our team. This will allow us to directly test whether ASIC1 contributes cold-induced pain. The additional cost associated with the purchase and breeding of these lines amount to 20 kEuro.

5. Recent papers (published in 2020-21) mentioning financial support of GSKE

- A.C.N. Freitas, **T. Voets**, Why the emperor penguin reigns where elephants shiver, Cell Calcium 91 (2020) 102263.
- K. Held, V.D. Aloi, A.C.N. Freitas, A. Janssens, A. Segal, J. Przibilla, S.E. Philipp, Y.T. Wang, **T. Voets**, J. Vriens, Pharmacological properties of TRPM3 isoforms are determined by the length of the pore loop, Br J Pharmacol (2020).
- B. Kelemen, S. Pinto, N. Kim, E. Lisztes, M. Hanyicska, A. Vladar, A. Olah, Z. Penzes, B. Shu, J. Vriens, T. Biro, T. Rohacs, **T. Voets***, B.I. Toth, The TRPM3 ion channel mediates nociception but not itch evoked by endogenous pruritogenic mediators, Biochem Pharmacol 183 (2021) 114310.
- M. Mulier, N. Van Ranst, N. Corthout, S. Munck, P. Vanden Berghe, J. Vriens, **T. Voets***, L. Moilanen, Upregulation of TRPM3 in nociceptors innervating inflamed tissue, Elife 9 (2020).
- M. Mulier, I. Vandewauw, J. Vriens, **T. Voets**, Reply to: Heat detection by the TRPM2 ion channel, Nature 584(7820) (2020) E13-E15.
- E. Persoons, K. De Clercq, C. Van den Eynde, S. Pinto, K. Luyten, R. Van Bree, C. Tomassetti, **T. Voets**, J. Vriens, Mimicking Sampson's Retrograde Menstrual Theory in Rats: A New Rat Model for Ongoing Endometriosis-Associated Pain, Int J Mol Sci 21(7) (2020).
- L. Vangeel, M. Benoit, Y. Miron, P.E. Miller, K. De Clercq, P. Chaltin, C. Verfaillie, J. Vriens, **T. Voets**, Functional expression and pharmacological modulation of TRPM3 in human sensory neurons, Br J Pharmacol 177(12) (2020) 2683-2695.
- (*Corresponding and shared last author)

6. References

1. F. Viana, T. Voets, Heat Pain and Cold Pain, in: J.N. Wood (Ed.), The Oxford Handbook of the Neurobiology of Pain, Oxford University Press, Oxford, 2019.
2. J. Vriens, B. Nilius, T. Voets, Peripheral thermosensation in mammals, Nat Rev Neurosci 15(9) (2014) 573-89.
3. M.J. Caterina, M.A. Schumacher, M. Tominaga, T.A. Rosen, J.D. Levine, D. Julius, The capsaicin receptor: a heat-activated ion channel in the pain pathway, Nature 389(6653) (1997) 816-24.
4. I. Vandewauw, K. De Clercq, M. Mulier, K. Held, S. Pinto, N. Van Ranst, A. Segal, T. Voet, R. Vennekens, K. Zimmermann, J. Vriens, T. Voets, A TRP channel trio mediates acute noxious heat sensing, Nature 555(7698) (2018) 662-666.
5. D.D. McKemy, W.M. Neuhausser, D. Julius, Identification of a cold receptor reveals a general role for TRP channels in thermosensation, Nature 416(6876) (2002) 52-8.
6. A.M. Peier, A. Moqrich, A.C. Hergarden, A.J. Reeve, D.A. Andersson, G.M. Story, T.J. Earley, I. Dragoni, P. McIntyre, S. Bevan, A. Patapoutian, A TRP channel that senses cold stimuli and menthol, Cell 108(5) (2002) 705-15.
7. K. Obata, H. Katsura, T. Mizushima, H. Yamanaka, K. Kobayashi, Y. Dai, T. Fukuoka, A. Tokunaga, M. Tominaga, K. Noguchi, TRPA1 induced in sensory neurons contributes to cold hyperalgesia after inflammation and nerve injury, J Clin Invest 115(9) (2005) 2393-401.
8. D.M. Bautista, S.E. Jordt, T. Nikai, P.R. Tsuruda, A.J. Read, J. Poblete, E.N. Yamoah, A.I. Basbaum, D. Julius, TRPA1 mediates the inflammatory actions of environmental irritants and proalgesic agents, Cell 124(6) (2006) 1269-82.
9. R.W. Colburn, M.L. Lubin, D.J. Stone, Jr., Y. Wang, D. Lawrence, M.R. D'Andrea, M.R. Brandt, Y. Liu, C.M. Flores, N. Qin, Attenuated cold sensitivity in TRPM8 null mice, Neuron 54(3) (2007) 379-86.
10. A. Dhaka, A.N. Murray, J. Mathur, T.J. Earley, M.J. Petrus, A. Patapoutian, TRPM8 is required for cold sensation in mice, Neuron 54(3) (2007) 371-8.
11. Y. Karashima, K. Talavera, W. Everaerts, A. Janssens, K.Y. Kwan, R. Vennekens, B. Nilius, T. Voets, TRPA1 acts as a cold sensor *in vitro* and in vivo, Proc Natl Acad Sci U S A 106(4) (2009) 1273-8.
12. C. Gentry, N. Stoakley, D.A. Andersson, S. Bevan, The roles of iPLA2, TRPM8 and TRPA1 in chemically induced cold hypersensitivity, Mol Pain 6 (2010) 4.
13. P. Uvin, J. Franken, S. Pinto, R. Rietjens, L. Grammet, Y. Deruyver, Y.A. Alpizar, K. Talavera, R. Vennekens, W. Everaerts, D. De Ridder, T. Voets, Essential role of transient receptor potential M8 (TRPM8) in a model of acute cold-induced urinary urgency, Eur Urol 68(4) (2015) 655-61.
14. W.M. Knowlton, A. Bifolck-Fisher, D.M. Bautista, D.D. McKemy, TRPM8, but not TRPA1, is required for neural and behavioral responses to acute noxious cold temperatures and cold-mimetics in vivo, Pain 150(2) (2010) 340-50.
15. D. Lohman, R. Schleifer, J.J. Amon, Access to pain treatment as a human right, BMC medicine 8 (2010) 8.
16. K.J. Reid, J. Harker, M.M. Bala, C. Truyers, E. Kellen, G.E. Bekkering, J. Kleijnen, Epidemiology of chronic non-cancer pain in Europe: narrative review of prevalence, pain treatments and pain impact, Current medical research and opinion 27(2) (2011) 449-62.

17. L. Colloca, T. Ludman, D. Bouhassira, R. Baron, A.H. Dickenson, D. Yarnitsky, R. Freeman, A. Truini, N. Attal, N.B. Finnerup, C. Eccleston, E. Kalso, D.L. Bennett, R.H. Dworkin, S.N. Raja, Neuropathic pain, Nat Rev Dis Primers 3 (2017) 17002.
18. T.S. Jensen, N.B. Finnerup, Allodynia and hyperalgesia in neuropathic pain: clinical manifestations and mechanisms, Lancet Neurol 13(9) (2014) 924-35.
19. C. Munns, M. AlQatari, M. Koltzenburg, Many cold sensitive peripheral neurons of the mouse do not express TRPM8 or TRPA1, Cell Calcium 41(4) (2007) 331-42.
20. T. Memon, K. Chase, L.S. Leavitt, B.M. Olivera, R.W. Teichert, TRPA1 expression levels and excitability brake by KV channels influence cold sensitivity of TRPA1-expressing neurons, Neuroscience 353 (2017) 76-86.
21. C.L. Li, K.C. Li, D. Wu, Y. Chen, H. Luo, J.R. Zhao, S.S. Wang, M.M. Sun, Y.J. Lu, Y.Q. Zhong, X.Y. Hu, R. Hou, B.B. Zhou, L. Bao, H.S. Xiao, X. Zhang, Somatosensory neuron types identified by high-coverage single-cell RNA-sequencing and functional heterogeneity, Cell Res 26(8) (2016) 967.
22. D. Usoskin, A. Furlan, S. Islam, H. Abdo, P. Lonnerberg, D. Lou, J. Hjerling-Leffler, J. Haeggstrom, O. Kharchenko, P.V. Kharchenko, S. Linnarsson, P. Ernfors, Unbiased classification of sensory neuron types by large-scale single-cell RNA sequencing, Nat Neurosci 18(1) (2015) 145-53.
23. A. Zeisel, H. Hochgerner, P. Lonnerberg, A. Johnsson, F. Memic, J. van der Zwan, M. Haring, E. Braun, L.E. Borm, G. La Manno, S. Codeluppi, A. Furlan, K. Lee, N. Skene, K.D. Harris, J. Hjerling-Leffler, E. Arenas, P. Ernfors, U. Marklund, S. Linnarsson, Molecular Architecture of the Mouse Nervous System, Cell 174(4) (2018) 999-1014 e22.
24. S. Picelli, O.R. Faridani, A.K. Bjorklund, G. Winberg, S. Sagasser, R. Sandberg, Full-length RNA-seq from single cells using Smart-seq2, Nat Protoc 9(1) (2014) 171-81.

Geneeskundige Stichting Koningin Elisabeth
Fondation Médicale Reine Elisabeth
Königin-Elisabeth-Stiftung für Medizin
Queen Elisabeth Medical Foundation

Progress report of the university research project of

Prof. dr. Sarah Weckhuysen, MD, PhD
Universiteit Antwerpen (UAntwerpen)

Prof. dr. Sarah Weckhuysen, MD, PhD
Applied&Translational Neurogenomics Group
VIB-UAntwerp Center for Molecular Neurology
UAntwerp-CDE
Parking P4, Building V
Universiteitsplein 1, 2610 Antwerpen
Belgium
uantwerpen.vib.be

Neurology Department
Antwerp University Hospital
Drie Eikenstraat 655, 2650 Edegem
Belgium
www.uza.be/neurologie

Study and targeted treatment development for epileptic encephalopathies using 2D and 3D human induced plupripotent stem cell-derived neuronal cultures

1. Background

The **developmental and epileptic encephalopathies (DEEs)** are a debilitating subgroup of the epilepsies, characterized by frequent and often treatment resistant seizures with early onset, and developmental delay. The majority of patients have a genetic cause. Current treatments for DEE focus on seizure control using anti-epileptic drugs. However, even though some patients do become seizure free, most patients with genetic DEEs still suffer from severe developmental delay. Many lines of evidence suggest that the developmental and the epileptic features are both, at least partially, an independent result of the underlying genetic defect. There is thus a strong need for new therapies that not only treat seizures, but also target the developmental aspects of DEEs.
The prototype and most common genetic form of neonatal DEE, illustrating many of the characteristics of genetic DEEs, is **KCNQ2 encephalopathy (KCNQ2-E)**. This disorder, described by our group in 2012, is caused by ***de novo* missense mutations** in the gene *KCNQ2* encoding the Kv7.2 subunit of the tetrameric M channel, a voltage gated potassium channel that is widely expressed throughout the brain, in excitatory and inhibitory neurons at the axon initial segment (AIS), nodes of Ranvier, presynaptic terminals and the soma, as well as in astrocytes. The M-current is responsible for repolarization of the membrane, dampening of repetitive firing and **controlling neuronal excitability**. Both a severe lack and excess of channel function can result in the development of KCNQ-E, due to heterozygous dominant negative or gain of function mutations respectively. Seizures in children with KCNQ-E often respond poorly to anti-epileptic drugs, and more importantly, therapies for the developmental problems are currently unavailable.

With the financial support of the GSKE, we plan to develop 2D and 3D human induced Pluripotent Stem Cell (hIPSC)-derived neuronal cultures starting from patient peripheral blood mononuclear cells, as a model of KCNQ2-E, and perform multimodal characterization using electrophysiology and (high-content) microscopy. We will then use the characterized model to provide proof-of-concept for mutant allele silencing as a treatment strategy for KCNQ2-E, using antisense oligonucleotides as a therapeutic tool.

2. Progress made in 2020

The COVID-19 pandemic unfortunately did have an impact on our research work, as during the months of March until June access to the lab has been severely restricted and no new experiments were allowed. Also in the second half of the year, access to the cell culture lab has been limited to two persons at a time for the whole department. Nevertheless, despite these limitations, we did manage to proceed with the project and generate significant results as illustrated below.

2.1. Optimization of the protocol to generate iPSC derived excitatory neurons and astrocytes

iPSC lines of 5 patients with KCNQ2-E (carrying three dominant negative mutations, and two gain of function mutations), and two control individuals were already available in our lab. In addition, we have two iPSC lines of patients with a self-limiting epilepsy disorder (Benign Familial Neonatal Seizures) due to mutations in KCNQ2 (KCNQ2-B).
In the last year, we have successfully set up and optimized the protocols for generation of excitatory neurons in our own laboratory. To generate **excitatory neurons** we have used a TALEN approach, to stably integrate the hNGN donor construct in the CLYBL safe harbor locus, as optimized by Prof. M. Ward (Fig1A). Compared to lentiviral transduction, this approach has the advantage that it allows selection of clones with homozygous insertions, assuring an equal expression of hNGN1 and hNGN2, in all the lines. Equal TF expression levels, together with the use of cytosine b-D-arabinofuranoside (Ara-C), an anti-mitotic compound that increases the developmental synchronicity of the neuronal cultures, reduces variability within and between neuronal cultures. The donor construct, as shown in Fig1A, contains both hNGN1 and hNGN2 under a doxycycline inducible promoter, as well as a CAG promoter driving constitutive expression of the reverse tetracycline transactivator (rtTA3G), and the EF-1 promoter driving constitutive expression of mCherry. So far, we have generated stable lines for all the aforementioned iPSC lines (Fig1B,C). Taking advantage of the IncuCyte live cell imaging system (Sartorius) to measure neurite length of cultured cells, differentiation efficiency of the stable iPSC lines can be validated in real time (Figure 1D). 3DIV iNeurons were frozen and will be thawed and plated for future experiments (survival and differentiation efficiency of thawed frozen iNeurons has been tested and confirmed, Figure 1D), enabling the initiation of experiments with multiple lines at the same time. In addition, using the protocol of Tcw J *et al*, we have also successfully generated iPSC-derived **astrocytes**, as shown in figure 1E.

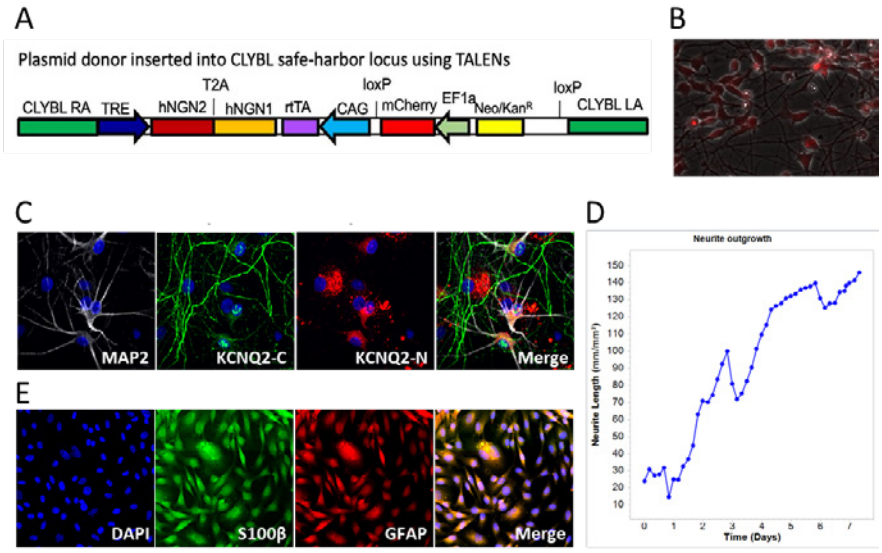

7u

Figure 1: Generation and validation of excitatory iNeurons and iAstro. (A) Schematic representation of the CLYBL-TALEN donor vector. (B) 100% mCherry positive neuronal culture. (C) Immunostaining of iNeurons, 25 days *in vitro* (DIV). MAP2+ neurons (gray), the canonical KCNQ2 isoform (green) and all KCNQ2 isoforms (red). (D) Validation of differentiation efficiency via Neurite outgrowth using Incucyte technology. (E) iAstro, 18 DIV, positive for the astrocyte marker S100 **(green)** and GFAP (red).

In February-March of this year, my PhD student Nina Dirkx also did an additional training with the group of Prof. A. George (Northwestern University, Chicago, USA) in patch clamping of iPSC-derived neuronal cultures. Prof. A. George has a long-standing experience in the study of the function of ion channels, including those involved in genetic epilepsies. During this research stay, Nina was able to grow co-cultures of excitatory neuron and rodent glia and study one of our KCNQ2-B lines (variant R547W). Current-clamp recordings were acquired using a Multiclamp 700B amplifier (Molecular Devices, USA) and digitized at 10kHz (filtered at 3kHz) with the neurons held at -65mV (Vh). Resting membrane potential (RMP) was measured immediately after establishing the whole-cell patch clamp configuration. Data were analyzed using custom MATLAB protocols. Figure 2A shows the preliminary current clamp data generated from wild-type (WT) and KCNQ2-R547W lines, 25 days after differentiation (DIV). No difference in action potential (AP) firing was observed at this time point, however, intrinsic properties show a significant decrease in AP amplitude in the KCNQ2-R547W neurons (WT=95Vm vs GOF=85Vm, adjusted P value = 0,000185 using multiple t-test).

Finally, we also used a multielectrode array (MEA) using a MaxTwo multiwell High density CMOS MEA system available at our institute to measure bursting patterns of our excitatory neuron of the R201H-GOF line vs WT. Results from this preliminary experiment show an increased mean firing rate in the GOF line (figure 2B). Interestingly, the increased firing is due to an increased activity within the bursts (spikes within burst; WT=24,9% *vs* GOF=37.2%), which is also reflected in an increase in the burst peak and spikes per burst. Furthermore, a decreased in the interburst interval is observed in the GOF. (No statistical analysis was performed on this data set yet, as the data was generated from a single differentiation.)

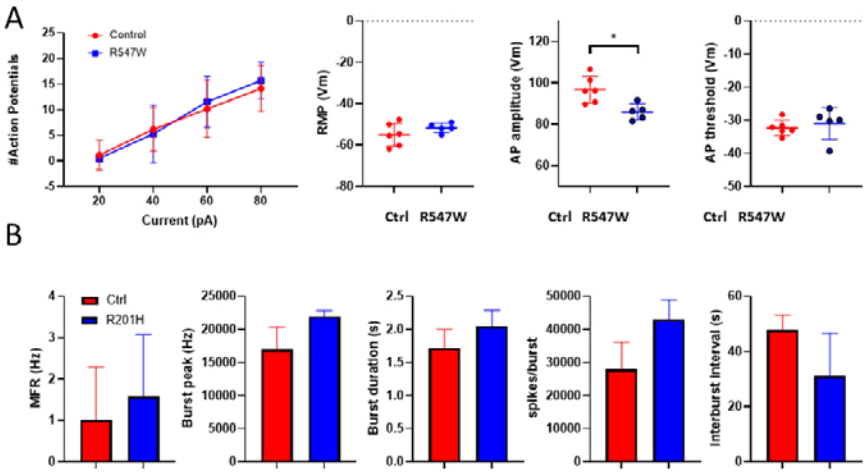

Figure 2: Preliminary electrophysiological characterization. (A) Patch clamp data of BFNE-R547W *vs* WT excitatory neurons, 25 DIV. WT neurons = 6 and BFNE neurons = 5. (B) CMOS MEAs data of GOF-R201H vs WT, 25 DIV. 150*10³ neurons/MEA, 1 differentiation. Values displayed represent mean +/- SD. * p<0.001

In summary, with the work we did this year, we show that in our lab we are able to generate electrically active excitatory iNeurons expressing *KCNQ2,* and provide preliminary evidence of electrophysiological differences between network activity of WT neurons *versus* at least one of the *KCNQ2* mutation types.

2.2. Generation of two isogenic control lines

With the support of the GSKE, we were able to have two isogenic lines generated, an essential element for our further experiments. One isogenic line was generated from an iPSC line from a patient with a dominant negative KCNQ2 variant, and one from a patient with a gain of function KCNQ2 variant.
Isogenic lines were generated as a service by the stem cell core at the ICM institute in Paris, France (https://celis.institutducerveau-icm.org/service/service-1/).

3. Additional funding acquired

The GSKE funding allowed us to generate the necessary high-quality preliminary data (as described above) to acquire additional funding to expand the iPSC culture work on neurodevelopmental and epileptic encephalopathies in our research group. More in particular, we were granted funding from the European EJP-RD program for our project "TreatKCNQ" of which Prof. Dr. Sarah Weckhuysen will be the coordinator. In this project, our group will develop iPSC derived neuronal cultures of different KCNQ gene related neurodevelopmental disorders and use them to identify and validate novel targeted treatments that have the potential to improve the developmental outcome of KCNQ-E.

Geneeskundige Stichting Koningin Elisabeth
Fondation Médicale Reine Elisabeth
Königin-Elisabeth-Stiftung für Medizin
Queen Elisabeth Medical Foundation

Projecten jonge onderzoekers 2020-2022 gefinancierd door de G.S.K.E.

Projets de recherche de jeunes chercheurs 2020-2022 subventionnés par la F.M.R.E.

Research projects of young researchers 2020-2022 funded by the Q.E.M.F.

Universiteiten met onderzoeksprogramma's die gesteund worden door de G.S.K.E.

Universités ayant des programmes de recherche subventionnés par la F.M.R.E.

Universities having research programs supported by the Q.E.M.F.

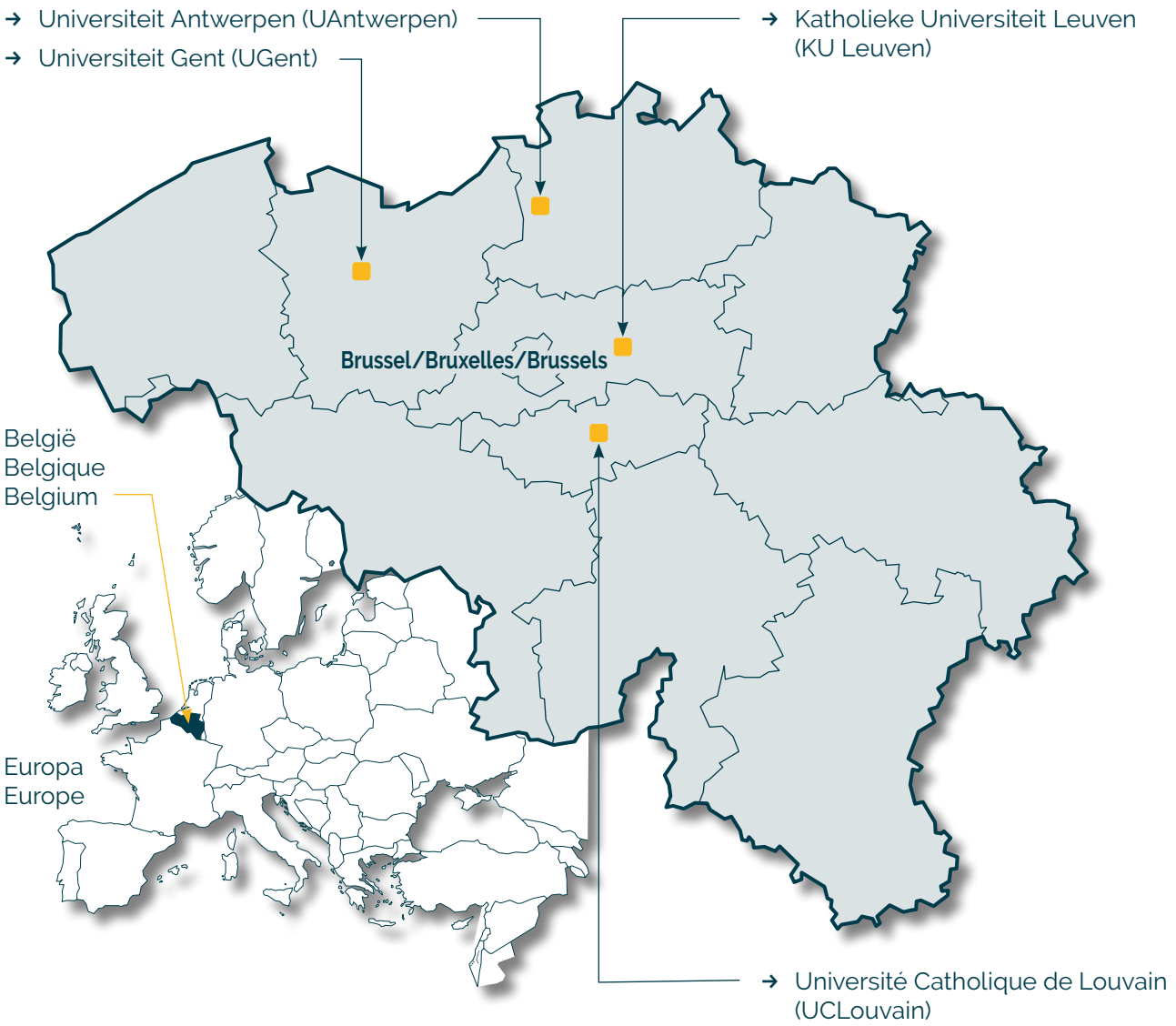

Projecten jonge onderzoekers 2020-2022 gefinancierd door de G.S.K.E.

Projets de recherche de jeunes chercheurs 2020-2022 subventionnés par la F.M.R.E.

Research projects of young researchers 2020-2022 funded by the Q.E.M.F.

UGent

Dr. Lars Emil Larsen, PhD
Closed loop precision therapy for epilepsy using photopharmacology

Prof. dr. Evelien Carrette (UZ Gent)
Novel interventions for patients with drug resistant epilepsy and cognitive decline: neuromodulatory effects of combined transcutaneous vagal nerve stimulation and cognitive therapy

UAntwerpen

Eline Wauters, PhD (VIB)
Onset age variability in GRN-associated frontotemporal lobar degeneration: identification of a functional onset age modifier

KU Leuven

Dr. Valerie Uytterhoeven
Molecular mechanisms and inducers of chaperone mediated Tau autophagy in Alzheimer's Disease

Aya Takeoka, PhD (IMEC)
Learning to walk without the brain: Determining cellular signatures underlying age-dependent spinal cord plasticity

UCLouvain

Prof. Bernard Hanseeuw, PhD

Biochemical mechanisms of regional tau protein aggregation in the human brain

Dr. Emanuel Vandenbroeke

The involvement of top-down facilitatory serotonergic pathways in nocebo- induced pain hypersensitivity

Prof. Riëm El Tahry, MD, PhD

Optimization Vagus nerve stimulation for refractory epilepsy

Geneeskundige Stichting Koningin Elisabeth
Fondation Médicale Reine Elisabeth
Königin-Elisabeth-Stiftung für Medizin
Queen Elisabeth Medical Foundation

Progress report of the research project of the young researcher

Prof. dr. Evelien Carrette
(UZ Gent)

Prof. dr. Evelien Carrette
Beleidsmedewerker
Neurologie | Neuroscience@U(Z)Gent

Universitair Ziekenhuis Gent | C. Heymanslaan 10 | 9000 Gent
T +32 9 332 45 40
evelien.carrette@uzgent.be
Skype eveliencarrette
Ingang 12 | Route 1556 | uzgent.be |

Novel interventions for patients with drug resistant epilepsy and cognitive decline: neuromodulatory effects of combined transcutenaous vagal nerve stimulation and cognitive therapy.

Our goal is to investigate the efficacy and underlying mechanism of action of transcutaneous vagal nerve stimulation (t-VNS), a non-invasive neurostimulation approach, and cognitive therapy (CT) for patients with DRE and memory problems in a collaborative setting of the Reference Center for Refractory Epilepsy at Ghent University Hospital and ULB Erasme.
We hypothesize that combined tVNS-CT is able to improve the memory performance of these patients better than CT alone by affecting neuronal cortical plasticity networks and aim to demonstrate this by electrophysiological co-registration.

1. Achieved results 2020

In the past years we have started with evaluating the effect of tVNS in healthy subjects (both in young and older participants).

1.1. STUDY 1: Effect of tVNS on memory via Word Recognition Tasks

Invasive vagus nerve stimulation (VNS) improves word recognition memory in patients with epilepsy. Recent studies with transcutaneous VNS (tVNS) have also shown positive effects on various subdomains of cognitive functioning in healthy volunteers.

We performed a randomized, controlled, crossover study, in which we investigated the effect of tVNS on a word recognition memory paradigm in healthy volunteers to further investigate the potential of tVNS in the treatment of cognitive disorders.

For this study we included 41 healthy participants aged between 18 and 30 years (young age group) and 24 healthy participants aged between 45 and 80 years (older age group). Each participant completed a word recognition memory paradigm during three different conditions: true tVNS, sham, and control. During true tVNS, stimulation was delivered at the cymba conchae. Sham stimulation was delivered by stimulating the earlobe. In the control condition, no stimulation was given.
In each condition, participants were asked to remember highlighted words from three test paragraphs. Accuracy scores were calculated for immediate recall after each test paragraph and for delayed recognition at the end of the paradigm. We hypothesized that highlighted words from paragraphs in the true tVNS condition would be more accurately recalled and/or recognized compared to highlighted words from paragraphs in the sham or control condition (see figure below).

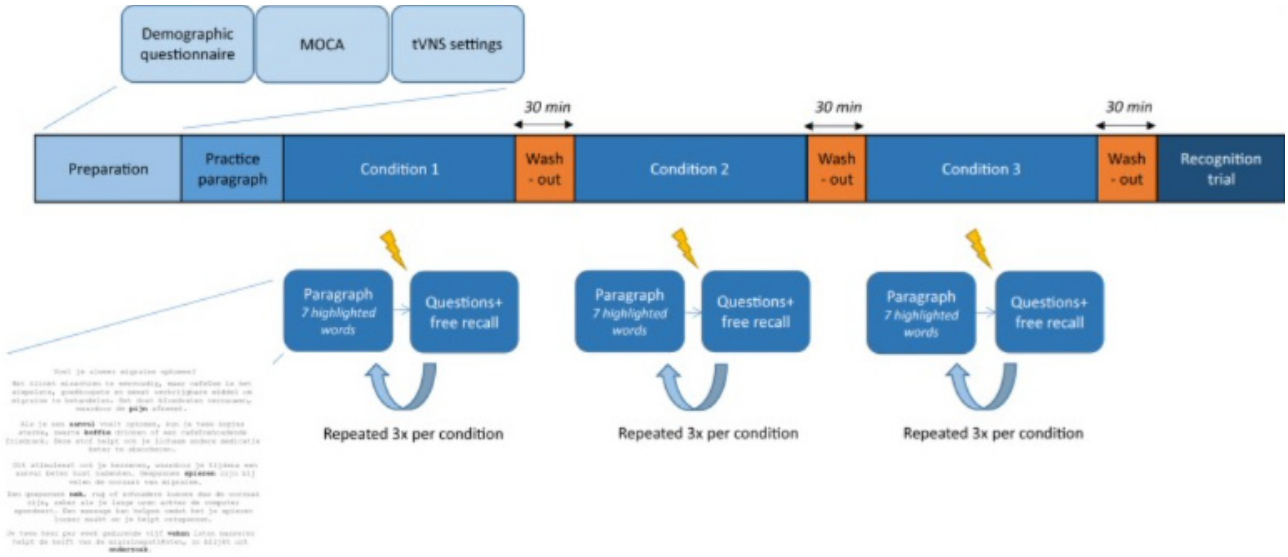

In this randomized study, tVNS did not affect the accuracy scores for immediate recall or delayed recognition in both age groups. The younger group did show significantly higher accuracy scores than the older group. The accuracy scores improved over time, and the most recently learned words were better recognized. Moreover participants rated true tVNS as significantly more painful; however, pain was not found to affect accuracy scores.

In this study, tVNS did not affect verbal memory performance in healthy volunteers. Our results could not replicate the positive effects of invasive VNS on word recognition memory in epilepsy patients.

Based on these results we concluded that future research with the aim of improving cognitive function should focus on the rational identification of optimized and individualized stimulation settings primarily in patients with cognitive deficits.

(Mertens A, Naert L, Miatton M, Poppa T, Carrette E, Gadeyne S, Raedt R, Boon P, Vonck K. Transcutaneous Vagus Nerve Stimulation Does Not Affect Verbal Memory Performance in Healthy Volunteers. Front Psychol. 2020 Apr 15;11:551. doi: 10.3389/fpsyg.2020.00551. PMID: 32351421; PMCID: PMC7174665.)

1.2. STUDY 2: Can we find an electrophysiological biomarker for effective tVNS stimulation in healthy volunteers using a cognitive ERP?

For invasive VNS it has been shown that the stimulation of vagal nerve fibers in the neck region, which are connected to the locus coeruleus (LC) neurons in the brainstem, provokes cortical noradrenaline (NA) release. This pathway is one the mechanisms of action trying to explain the effect of VNS.
The objective of this study was to investigate whether tVNS is able to modulate the P3b component of the P300, a cognitive event related potential (ERP) reflecting NA brain activation under control of the LC and therefore a (bio)marker for non-invasive LC activation via tVNS .

For this study 39 healthy volunteers were included in a randomized, single-blind, sham-controlled cross-over study. Volunteers were again randomly assigned to three consecutive different intervention conditions with no stimulation, sham tVNS (earlobe) and true tVNS (cymba concha) while performing a three-stimulus auditory oddball task. Stimulation output current was gradually increased until the individual subject's threshold (30 Hz, 500 µs, 7s ON/18s OFF).

P3b amplitude and latency, as well as behavioral outcome parameters were measured in each condition and mean values were compared between the three conditions using linear mixed models.

The amplitude and latency of the P3b during tVNS did not differ significantly from sham or control.

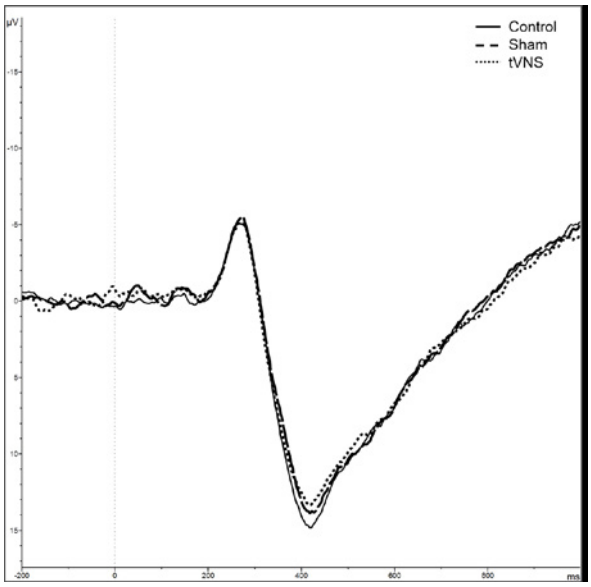

Figure: Grand average P3b plot at electrode Pz showing no significant difference between the three stimulation conditions

The order in which the oddball tasks were carried out, did had a significant effect on several outcome parameters. Reaction time shortened and latency was prolonged with each next attempt of the oddball task.

So, with this study we were able to show that using stimulation parameters based on preclinical research that were shown to increase NA release, we were unable to target cognitive evoked potentials by means of tVNS in a large homogeneous group of healthy volunteers.

Using other stimulation paradigms and/or targeting a diseased population may be strategies to further investigate whether tVNS is able to change objective electrophysiological parameters reflecting cognitive functioning in the brain.

(Stefanie Gadeyne, Evelien Carrette, Ann Mertens , Freek Van Den Bossche, Paul Boon, Robrecht Raedt and Kristl Vonck. Can we target cognition in healthy volunteers using transcutaneous auricular vagus nerve stimulation? (Paper in preparation))

Based on both studies described above, it has become clear that targeting vagal nerve fibres by means of a non-invasive transcutaneous approach, is not able to improve memory performance or to modulate a cognitive ERP (i.e. reflecting an absence of noradrenergic brain activity modulation with the applied stimulation paradigms) in healthy participants.

The stimulation parameters used and the short-term delivery of tVNS may have been insufficient to activate vagal fibres and adequately modulate the LC or on the other hand, the normal functioning memory and LC-NE system in healthy volunteers may simply not be receptive for modulation, in contrast to diseased states in patients with epilepsy, memory problems or depression, in whom a disbalanced LC-NE system may be more prone for improvement.

1.3. STUDY 3: Transcranial Magnetic Stimulation as a tool for the Evaluation of Neuromodulatory Effects of tVNS

The goal of this third study is to provide more insight into the underlying effect of tVNS on brain neurophysiology not taking the effect on memory performance or the LC-NE system as a read-out.

By combining transcranial magnetic stimulation (TMS) with EMG and EEG, we can study the modulation of Motor Evoked Potentials (MEPs) and TMS Evoked Potentials (TEPs). As these MEPs and TEPS are reproducible within subjects, they can be useful to study the effect of neuromodulatory interventions, like tVNS.

We performed a prospective cross-over study in which 15 healthy male subjects underwent 2 sessions, at least one week apart. During each session, tVNS or sham stimulation was delivered at the maximum tolerated amplitude during one hour. The resting motor threshold, MEPs and TEPs were measured before and after the intervention. For these measurements, 120 single TMS pulses, 120 paired TMS pulses with a short interstimulus interval and 120 paired TMS pulses with a long interstimulus interval were delivered over the motor hotspot. To assess the effect of tVNS on MEP morphology, we measured the average latency and amplitude of all MEPs for each condition and each pulse type. Intracortical inhibition after paired pulses was assessed by expressing the amplitude of the paired pulse response as a percentage of the amplitude of the single pulse response. MEP latency, amplitude and percentage were then compared at the single subject level before and after each intervention. Statistical analysis was conducted by means of a two-way repeated measures ANOVA. TMS-EEG data was preprocessed offline using the TESA toolbox in Matlab. A cluster based permutation statistical analysis was conducted.

The resting motor threshold showed no significant change after real tVNS compared to sham stimulation. MEP data analysis showed no significant change in mean amplitude after real tVNS compared to sham stimulation for both single pulses and paired pulses. Only a trend could be found towards decreased amplitude of MEPs evoked by short interval paired pulses after real tVNS. Intracortical inhibition produced by paired pulses also showed no statistically significant change. Regarding onset latency, a significant effect of timing, but not intervention was found, showing an increase in latency for both interventions.

However an association was found between tVNS output current and MEP outcome measures indicating a decrease in cortical excitability as tVNS output current increased. A subanalyis of participants stimulated with tVNS output current ≥ 2.5mA showed a significant increase of resting motor threshold, decrease of MEP amplitude and modulation of P70 and P180 TEP components. This study demonstrates the potential of tVNS to modulate specific markers of cortical excitability when high output currents are used. These findings stimulate the development of appropriate stimulation protocols for future studies investigating the effect of tVNS in epilepsy patients.

So far, in contrast to previous research, our results show that active tVNS, as compared to sham stimulation, did not modify cortical excitability measured by single and paired pulse TMS-EMG for the whole group, however we did show the potential of tVNS to modulate specific markers of cortical excitability when high output currents are used.

(TMS-EEG data analysis is currently ongoing and will be described in a next progress-report.)

→ These findings stimulate the development of appropriate stimulation protocols for future studies investigating the effect of tVNS in patients (MCI or other diseases).

(Ann Mertens, Debby Klooster, Sofie Carrette, Emma Lescrauwaet, Evelien Carrette, Robrecht Raedt, Kristl Vonck, Paul Boon. High output current transcutaneous vagus nerve stimulation modulated cortical excitability in healthy participants: a TMS-EMG/EEG study. (Paper in preparation))

2. Future Experiments

Based on the findings in the healthy subjects, we feel that it is necessary to first conduct some additional studies including more fundamental research to elucidate the mechanism-of-action or to identify a biomarker to tailor the stimulation parameters to.
Via setting-up new collaborations we are investing in this goal, beyond the goals set in advance:

- FUTURE STUDY: Early detection of cognitive decline from EEG responses in AD risk group
  Via a collaboration with Prof. Van Hulle and dr. Khachatryan (KULeuven) a study in individuals with high and low risk of Alzheimer Disease (AD) development will start soon (as soon as COVID-19 measures will allow this).
  In this study it will be determined which Event Related Potential (ERP) components differ between healthy controls, subjective cognitive decline (SCD) individuals at high and low risk of AD development, MCI and early-AD patients (research question 1). Candidate ERP components were already identified in a pilot study on healthy individuals. We will use the known risk factors (e.g., APOE 4 genotype) and the collected structural and molecular neuroimaging data (PET/MR) from all participants as our ground truth when assessing which ERP components differ between the mentioned subject groups.
  For our second objective, we reverse research question 1 and want to show that we can differentiate between the tested groups based on the ERP components we identified (research question 2). We will conduct the ROC analysis, as well as evaluate positive and negative predictive values for studied ERP components. We will do this by using the latest statistical techniques of classification.

  At the same time these selected patients will undergo the same study paradigm as the one described in study 1 and 2, but that at that time was performed in healthy participants. This way we can evaluate the effect of tVNS on working memory and on P3b in patients with memory complaints.

- FUTURE STUDY: Non-pharmacological interventions to promote sleep and memory in ageing: a multimodal approach
  Via a collaboration with Prof. Peigneux and Dr. Alison Mary (ULB) a project will be set-up combining our expertise on tVNS with their expertise on sleep and memory. Understanding how cognitive functions can be maintained at old age is an increasingly important societal issue. Indeed, substantial changes in cognitive functions occur with age, memory decline being the most frequent complaint in the elderly. In this project the goal is to evaluate the effect of tVNS in healthy ageing to induce neuroplastic changes in brain regions that have been shown to play a crucial role on memory processes. These effects will be investigated via a multimodal approach, combining high-density electroencephalography (hdEEG), functional magnetic resonance imaging (fMRI) and diffusion-weighted magnetic resonance imaging (DWI). This multimodal project will shed light on the brain mechanisms of induced-memory enhancement and may offer new therapeutic interventions to restore sleep and improve memory that may reduce the risk of cognitive impairment in ageing.

3. Networking

In addition to the experimental work that we have conducted so-far and the plans we have for the future (described above), we are formal partners in the Network for Transcutenous Vagus Nerve Stimulation Research supported via an endorsed and supported Scientific Research Network of FWO.
Evelien Carrette was personally involved in the organization and moderated this (virtual) meeting (program in attachment – attachment 1). We plan follow-up meetings every 3 months during the 4 years to come (and potentially extended) and will take a leading role within the consortium.
Our research group has also been involved in the writing of a guideline in Frontiers in Human Neuroscience within the tVNS-Consensus-group. Prof. Kristl Vonck has been listed as an author from 4BRAIN (see below).

4. Publications

- Mertens A, Naert L, Miatton M, Poppa T, Carrette E, Gadeyne S, Raedt R, Boon P, Vonck K. Transcutaneous Vagus Nerve Stimulation Does Not Affect Verbal Memory Performance in Healthy Volunteers. Front Psychol. 2020 Apr 15;11:551. doi: 10.3389/fpsyg.2020.00551. PMID: 32351421; PMCID: PMC7174665
- On behalf of tVNS-ConsensusGroup – Farmer AD, et al. International Consesnus Based Review and Recommendations for Minimum Reporting Standards in Research on Transcutaneous Vagus Nerve Stimulation (Version 2020). Frontiers in Human Neuroscience
- Stefanie Gadeyne, Evelien Carrette, Ann Mertens , Freek Van Den Bossche, Paul Boon, Robrecht Raedt and Kristl Vonck. Can we target cognition in healthy volunteers using transcutaneous auricular vagus nerve stimulation? (Paper in preparation).
- Ann Mertens, Debby Klooster, Sofie Carrette, Emma Lescrauwaet, Evelien Carrette, Robrecht Raedt, Kristl Vonck, Paul Boon. High output current transcutaneous vagus nerve stimulation modulated cortical excitability in healthy participants: a TMS-EMG/EEG study. (Paper in preparation)

5. First tVNS research network meeting – Jan 25, 2021

5.1. Attendees

KU Leuven, Faculty of Psychology and Educational Sciences, BE
- Ilse Van Diest, Prof. Dr. Health Psychology Research group
- Andreas M. Burger, Dr. Health Psychology Research group
- Andreas von Leupoldt, Prof. Dr. Health Psychology Research group
- Johan Vlaeyen, Prof. Dr. Health Psychology Research group
- Martina D'Agostini, PhD student Health Psychology Research group
- Valentina Jelinčić, PhD student Health Psychology Research group

Ghent University Hospital, Faculty of Medicine and Health Sciences, BE
- Kristl Vonck, Prof. Dr. 4Brain
- Evelien Carrette, Dr. 4Brain
- Robrecht Raedt, Prof. Dr. 4Brain
- Marijke Miatton, Prof. Dr. 4Brain
- Ann Mertens, Dr. 4Brain

Vrije Universiteit Brussel, Faculty of Medicine and Farmacy, BE
- Marijke De Couck Mental Health and Wellbeing Research Group

Leiden University, The Faculty of Social and Behavioural Sciences, NL
- Bart Verkuil, Prof. Dr. Institute of Psychology
- Sander Nieuwenhuis, Prof. Dr. Institute of Psychology

University of Potsdam, Faculty of Human Sciences, DE
- Mathias Weymar, Prof. Dr. Department of Biological Psychology and Affective Science
- Carlos Ventura-Bort, Dr. Department of Biological Psychology and Affective Science
- Manon Giraudier, PhD student Department of Biological Psychology and Affective Science

Queen Mary University of London, Blizard Institute - Barts and The London, UK
- Qasim Aziz, Prof. Dr. Wingate Insitute of Neurogastroenterology
- Kazuya Takahashi, Dr. Wingate Insitute of Neurogastroenterology

University of Texas at Dallas, USA
- Christa McIntyre, Prof. Dr. Texas Biomedical Device Center
- Crystal Engineer, Prof. Dr. Texas Biomedical Device Center
- Rimenez Rodrigues de Souza, Dr. Texas Biomedical Device Center

University Hospital Heidelberg, Centre for Psychosocial Medicine, DE
- Julian Koenig, Prof. Dr. Department of Child and Adolescent Psychiatry

University of Greifswald, University Medicine, DE
- Taras Usichenko, Prof. Dr. Department of Anesthesiology

5.2. Program

1:30 - 1:45 PM

- *Introduction on the research network's goals, partners, possibilities*

Prof. Dr. Ilse Van Diest, Health Psychology Research Group, Faculty of Psychology and Educational Sciences KU Leuven, BE

1:45 PM - 2:30 PM

- *Invited lecture*

Towards International Consensus Based Recommendations for Minimum Reporting Standards in Research on Transcutaneous Vagus Nerve Stimulation

Prof. Dr. Julian Koenig, Department of Child and Adolescent Psychiatry, Centre for Psychosocial Medicine, University of Heidelberg, DE

2:30 - 3:30 PM: Pitch Round 1

- *Pitch 1 – 10 min*

Effects of invasive VNS on plasticity and behavior in rats

Prof. Dr. Christa McIntyre, Texas Biomedical Device Center, University of Texas at Dallas, USA

- *Pitch 2 – 10 min*

tVNS research at the Health Psychology Research Group, KULeuven: history, findings and struggles

Prof. Dr. Ilse Van Diest, & Martina D'Agostini, Health Psychology Research Group, Faculty of Psychology and Educational Sciences KU Leuven, BE

- *Pitch 3 – video clip – 10 min*

Learning from and with tVNS in Leiden

Prof. Dr. Bart Verkuil, Institute of Psychology, The Faculty of Social and Behavioural Sciences, Leiden University, NL

- *Pitch 4 – 10 min*

tVNS, arousal, and memory

Prof. Dr. Mathias Weymar, Department of Biological Psychology and Affective Science, Faculty of Human Sciences, University of Potsdam, DE

- *Discussion (3:10 - 3:30)*

3:30 - 3:50 PM

- *Break*

3:50 – 5:00 PM: Pitch round 2
- *Pitch 5 – 10 min*

VNS @4BRAIN, studying the effect tVNS in epilepsy and its co-morbidities

Prof. Dr. Kristl Vonck, 4Brain, Faculty of Medicine and Health Sciences, Ghent University Hospital, BE

- *Pitch 6 – 10 min*

tVNS and pain

Prof. Dr. Taras Usichenko, Department of Anesthesiology, University Medicine, University of Greifswald, DE

- *Pitch 7 – 10 min*

tVNS in visceral pain - success and challenges

Prof. Dr. Qasim Aziz, Wingate Insitute of Neurogastroenterology, Blizard Institute - Barts and The London, Queen Mary University of London, UK

- *Pitch 8 – 10 min*

tVNS in child psychiatry

Prof. Dr. Julian Koenig, Department of Child and Adolescent Psychiatry, Centre for Psychosocial Medicine, University of Heidelberg, DE

- *Pitch 9 – 10 min – video clip*

Non-invasive neurostimulation of the autonomic nervous system

Prof. Dr. Sue Deuchars & Prof. Dr. Jim Deuchars, Faculty of Biological Sciences, University of Leeds, UK

- *Discussion (4:40 – 5:00)*

5:00 - 5:25 PM
- *Break*

5:25 - 5:45 PM: Closing Discussion
- *Wrap up & Where to go next?*

Prof. Dr. Ilse Van Diest, Health Psychology Research Group, Faculty of Psychology and Educational Sciences KU Leuven, BE

Prof. Dr. Kristl Vonck, 4Brain, Faculty of Medicine and Health Sciences, Ghent University Hospital, BE

5.3. Contacts

In case of technical problem with zoom or other unforeseen issues, contact Martina D'Agostini: +39 3461639141

Geneeskundige Stichting Koningin Elisabeth
Fondation Médicale Reine Elisabeth
Königin-Elisabeth-Stiftung für Medizin
Queen Elisabeth Medical Foundation

Progress report of the research project of the young researcher

Prof. Riëm El Tahry, MD, PhD
Université Catholique de Louvain (UCLouvain)

Prof. Riëm El Tahry, MD, PhD
Chef de Clinique Adjointe
Neurologie, Centre de référence pour l'épilepsie réfractaire
Tel.: +32 2 764 28 55

Secrétariat:
Tel.: +32 2 764 10 82 / +32 2 764 33 09
Fax: +32 2 764 36 79

Avenue Hippocrate 10
1200 Brussels
Belgium
Tel.: +32 2 764 11 11
www.saintluc.be

Optimization Vagus nerve stimulation for refractory epilepsy

1. Progress report

As requested, we are sending you a report of our scientific activities performed in 2020.

As notified earlier, we have decided to postpone the use of the FMRE budget until 1 November 2022, as it was initially foreseen to finance the salary of Anton Kavaldzhiev, PhD student working on chronic recording of vagus nerve activity for seizure detection. Mr Kavaldzhiev is actually paid by the starting grant of the Fond de Recherche Clinique from the Cliniques Universitaires Saint Luc. His second year of PhD is financed through an obtained FSR grant from the UCLouvain. For this reason, we have asked permission to postpone the first utilization of the grant by November 2022 and extend its use until 30 September 2024.

In meanwhile, the following scientific goals were achieved:

Our manuscript entitled "Transcutaneous VNS applied to experimental pain: a paired EEG and behavioral study using thermonociceptive CO2 laser" was accepted with major revision in the journal PLOS ONE (IF 2.7). A second manuscript entitled: "A vagus nerve electroneurogram based seizure detection algorithm" is in preparation to be submitted to International journal of neural systems (IF 6.5). A third manuscript " Automated low-density Electrical source Imaging to characterize insular irritative zone: an ESI/SEEG comparison", is in preparation for submission to Epilepsia (IF: 5.5)

1.1. The following manuscripts were published as last or first author:

- Vespa et al. Ictal EEG source imaging and connectivity to localize the seizure onset zone in extratemporal lobe epilepsy, Seizure (IF:2)
- El Tahry et al. Additional clinical value of voxelbased morphometric MRI postprocessing for MRInegative epilepsies: a prospective study, Epileptic Disorders (IF:2)
- Stumpp, et al. Recording of spontaneous vagus nerve activity during Pentylenetetrazol-induced seizures in rats, Journal of neuroscience methods (IF:2.7)

1.2. The following manuscripts were published as co-author:

- Vanabelle et al. Epileptic seizure detection using EEG signals and extreme gradient boosting, The Journal of Biomedical Research (IF:1)
- Tassigny et al. Anterior Thalamic Nucleus Deep Brain Stimulation for Refractory Epilepsy: Preliminary results in our first 5 patients, Neurochirurgie.

1.3. Two abstracts were presented at the virtual American Epilepsy Congress 2020:

- Automated low-density Electrical Source Imaging to characterize insular irritative zone: an ESI/SEEG comparison Riëm El Tahry, Simone Vespa, Vénéthia Danthine, Amir G. Baroumand, Gert van Hollebeke, Gregor Strobbe, Geraldo Ribeiro Vaz, Pieter van Mierlo, Susana Ferrao Santos. These results were also presented by orally at a neurophysiology platform presentation 6/12/2020 by myself.
- Effect of Vagus Nerve Stimulation on EEG oscillations and connectivity. Simone Vespa, Youssef Agram, Federico Lucchetti, Susana Ferrao Santos, Antoine Nonclercq, Riëm El Tahry

In addition, we succeeded in finishing a first prototype of a video EEG vagus nerve electroneurgram recording system for rats and are now developing new strategies to manufacture our own custom made vagus nerve electrodes for rats. Considering our human experiments, we adapted our protocol for pupil experiments in VNS patients and expect to test new patients beginning of 2021. Alexandre Berger, bioengineer, started to work at our institute and will focus on locus coerelus imaging in VNS patients. He is financed by the Walloon Region ("doctorat en enterprise" with a company called Synergia Medical).

We would like to thank la fondation Médicale Reine Elisabeth for its contribution in our research.

Sincerely yours

Riëm El Tahry

Geneeskundige Stichting Koningin Elisabeth
Fondation Médicale Reine Elisabeth
Königin-Elisabeth-Stiftung für Medizin
Queen Elisabeth Medical Foundation

Progress report of the research project of the young researcher

Prof. Bernard Hanseeuw, PhD
Université Catholique de Louvain (UCLouvain)

Prof. Bernard Hanseeuw, PhD

Postdocs
Lisa Quenon

PhD students
Imaging
- Vincent Malotaux
- Lise Colmant
- Thomas Gérard

Biological analyses (CSF)
- Nathalie Nyalu Ngoie

Main collaborators
Adrian Ivanoiu, MD PhD (Neurology)
Renaud Lhommel, MD (Nuclear Medicine)
Laurence Dricot, Ir PhD (Radiology)
Vincent van Pesch, MD PhD (Neurochemistry)
Yves Sznajer, MD (Neurogenetics)
Didier Vertommen, PhD (Mass Spectrometry)

Website
https://uclouvain.be/fr/instituts-recherche/ions/neur/the-louvain-aging-brain-lab.html

Contact
recherche-alzheimer@uclouvain.be
bernard.hanseeuw@uclouvain.be

Biochemical mechanisms of regional tau protein aggregation in the human brain

The **Human Tau study** evaluates the manifestations related to pathological aging, such as that caused by Alzheimer's disease (AD) and related disorders, called tauopathies. These disorders all involve biochemical alterations in the tau protein. We relate brain damage disclosed by imaging techniques (MRI, tau-PET using [18F]-MK6240) and biological changes observed in the cerebrospinal fluid (CSF) to cognitive changes measured using neuropsychological testing. Our research targets are patients with mild cognitive impairment who consult the Memory Clinic, normal subjects at family risk for developing Alzheimer's disease and healthy control subjects, young and old.

In 2019, we have acquired the first tau-PET images in French-speaking Belgium (see below). Three imaging PhD students are funded by the FNRS. The support of the Queen Elisabeth Medical Foundation has allowed me to expand this research program and hire a biochemical PhD student.

She was funded during her first year (2019-2020) by the Fonds de Recherche Clinique from UCLouvain and will be funded the next two years (2021-2022) by the QEMF. Despite the pandemics, she could develop an immuno-precipitating protocol isolating the tau protein from the CSF and brain samples. By analyzing the protein with mass spectrometry, she has achieved to identify tau isoforms (3R vs 4R) and several phosphorylation sites. By late 2022, we hope to (1) distinguish different tauopathies based on isoform detection, and (2) study the relationships between tau phosphorylation in the CSF and tau propagation to different brain regions (using MK6240 tau-PET).

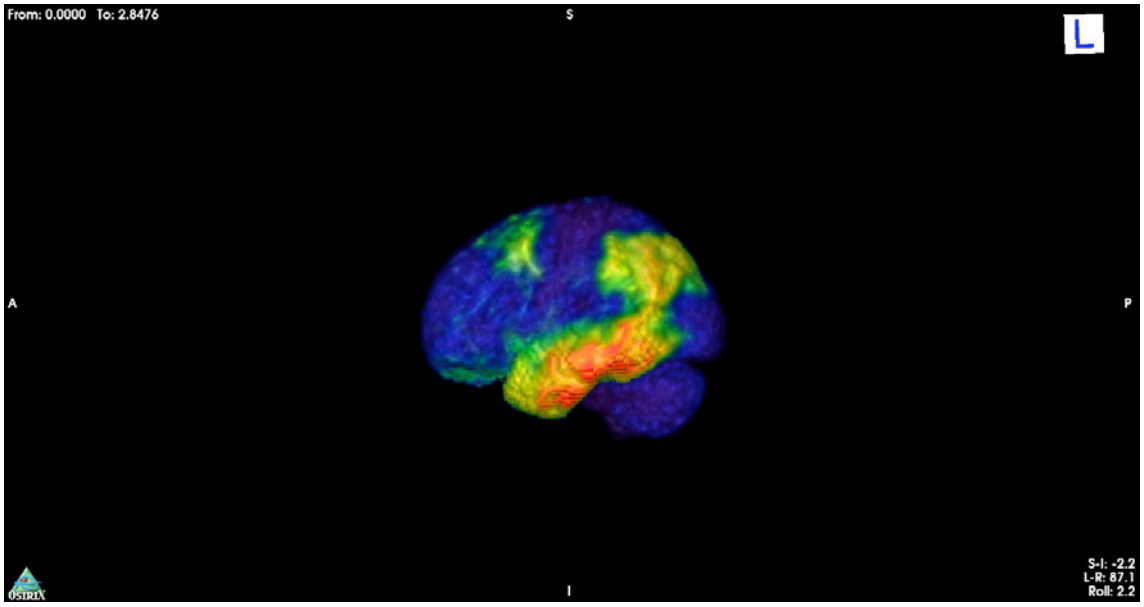

Tau-PET image of a patient with mild cognitive impairment. MMSE = 26/30. Free recall = 0/3. The temporal lobe is strongly affected by tau pathology, the parietal lobe to a lesser extent, but the frontal and occipital lobes are still largely preserved, consistent with the preservation of executive and visuospatial functions. We aim to investigate which biochemical alterations of tau are associated with a certain level of tau propagation in the brain.

1. Key recent publications

- *Hanseeuw, B. J., Malotaux, V., Dricot, L., Quenon, L., Sznajer, Y., Cerman, J., Woodard, J. L., Buckley, C., Farrar, G., Ivanoiu, A., & Lhommel, R. (2020). Defining a Centiloid scale threshold predicting long-term progression to dementia in patients attending the memory clinic : An [18F] flutemetamol amyloid PET study.* ***European Journal of Nuclear Medicine and Molecular Imaging****.*
- *Mormont, E., Bier, J.-C., Bruffaerts, R., Cras, P., De Deyn, P., Deryck, O., Engelborghs, S., Petrovic, M., Picard, G., Segers, K., Thiery, E., Versijpt, J., & Hanseeuw, B. (2020). Practices and opinions about disclosure of the diagnosis of Alzheimer's disease to patients with MCI or dementia : A survey among Belgian medical experts in the field of dementia.* ***Acta Neurologica Belgica****.*
- *Hanseeuw, B. J., Scott, M. R., Sikkes, S. A. M., Properzi, M., Gatchel, J. R., Salmon, E., Marshall, G. A., & Vannini, P. (2020). Evolution of anosognosia in alzheimer's disease and its relationship to amyloid.* ***Annals of Neurology****, 87(2), 267280.*
- *Hanseeuw, B. J., Betensky, R. A., Jacobs, H. I. L., Schultz, A. P., Sepulcre, J., Becker, J. A., Cosio, D. M. O., Farrell, M., Quiroz, Y. T., Mormino, E. C., Buckley, R. F., Papp, K. V., Amariglio, R. A., Dewachter, I., Ivanoiu, A., Huijbers, W., Hedden, T., Marshall, G. A., Chhatwal, J. P., … Johnson, K. (2019). Association of Amyloid and Tau With Cognition in Preclinical Alzheimer Disease : A Longitudinal Study.* ***JAMA Neurology****, 76(8), 915.*

Geneeskundige Stichting Koningin Elisabeth
Fondation Médicale Reine Elisabeth
Königin-Elisabeth-Stiftung für Medizin
Queen Elisabeth Medical Foundation

Progress report of the research project of the young researcher

Dr. Lars Emil Larsen, PhD
Universiteit Gent (UGent)

Dr. Lars Emil Larsen, PhD
Postdoctoral Researcher
4Brain/MEDISIP
Ghent University

Campus UZ
Corneel Heymanslaan 10,
Entrance 36 - Ground floor
9000 Gent
Belgium

Closed loop precision therapy for epilepsy using photopharmacology

1. Year overview

The principal goal of this project is to develop and provide a proof of concept for closed-loop precision therapy for epilepsy using photopharmacology. Our first objective was to study seizures in the intrahippocampal kainic-acid model in mice, a model which our laboratory has abundant experience with (Desloovere, Boon et al. 2019). We envisioned doing so using high-density multisite electrophysiology, which our laboratory has experience with through previous collaborations with international experts in extracellular in vivo electrophysiology (Neumann, Raedt et al. 2017). Completing this experiment, however, relied on the delivery of a new state-of-the-art electrophysiology acquisition system (https://open-ephys.org/next-gen-acquisition-system) utilizing light-weight implants enabling up to 64 electrode contacts in mice. This system was scheduled for delivery in the first quarter of 2020. A slight delay, combined with the covid-19 pandemic unfolding world-wide in 2020 led to a delay in the delivery of several components of the system, meaning that delivery has been postponed till the first quarter of 2021. The covid-19 pandemic also exerted a significantly halting impact on our experimental activities, which included a temporary ban for new experiments in the facilities of Ghent University from mid-March 2020 till the end of May 2020.

Despite these circumstances, we have still been able to make significant progress on the topic of photopharmacology for epilepsy via alternative routes, which is presented in the following. More specifically, we have identified and selected a very interesting photopharmacological ligand, coumarin-caged A1 agonist N^6-cyclopentyladenosine (cCPA), which is an adenosine-1 (A1) receptor agonist once uncaged by exposure to UV-light (wavelength ~405 nm). Adenosine analogs are interesting candidates for seizures as adenosine signaling, particularly through inhibitory A1-receptors, is one of the most potent seizure suppressing mechanisms. Build up of adenosine in relation to seizure activity is in fact believed to be one of the key endogenous mechanisms for seizure termination. Our laboratory, in particular my colleague, drs. Jeroen Spanoghe, dedicated a majority of the experimental downtime caused by the covid-19 pandemic to write a review on the A1-receptor signaling in the context of seizures and epilepsy, which was recently published in International Journal of Molecular Sciences (Spanoghe, Larsen et al. 2020). Due to non-specific off target side effects, which in worst case are lethal, adenosine analogs have not seen any clinical use yet. With photopharmacology, however, we have a unique possibility to exploit the pronounced inhibitory potency of adenosine and restrict its effects in space and time. In the final half of 2020, significant progress was made on adapting and validating this photosensitive A1 receptor agonist, through *in-vitro* and preliminary *in-vivo* experimentation, results of which are presented in the following.

1.1. Validation of CPA in brain slices of mice of the intrahippocampal kainic acid model for epilepsy

In initial experiments, we assess the effects of the native CPA compound on synaptic transmission and epileptiform activity in brain slices of both healthy control mice and epileptic mice. The rationale of doing so was 1) to establish a robust experimental setup with the native CPA compound before investigating the photocaged compound and 2) to assess whether targeting A1-receptors is equally effective in healthy vs. epileptic tissue. The latter objective was addressed in the light of previous observations of compromised adenosine signaling in epileptic tissue. Mice

were injected intrahippocampally with either kainic acid (200 ng in 50 nL of saline) for induction of status epilepticus, leading to development of spontaneous seizures in the weeks following. As controls, a subset of mice were injected with a vehicle solution (a corresponding volume of saline). After at least 4 weeks, mice were euthanized and slices were prepared for *in vitro* electrophysiological measurements. Slices were placed on a 60-channel multielectrode array (MEA), which allowed both acquisition of extracellular field potentials and electrical stimulation. In this way, electrical stimulation was delivered to a contact placed in the Schaffer Collaterals, which are afferent projections to the CA1 region, where the resulting response was measured as an evoked potential (EP), of which the dominating component was a field excitatory post synaptic potential (fEPSP) reflecting depolarization of CA1 neurons in response to the Schaeffer Collateral input. Our initial measurements have indicated a dose-dependent suppression of synaptic transmission in the CA1 by CPA, which is equally potent in epileptic and healthy brain slices (**Figure 1**).

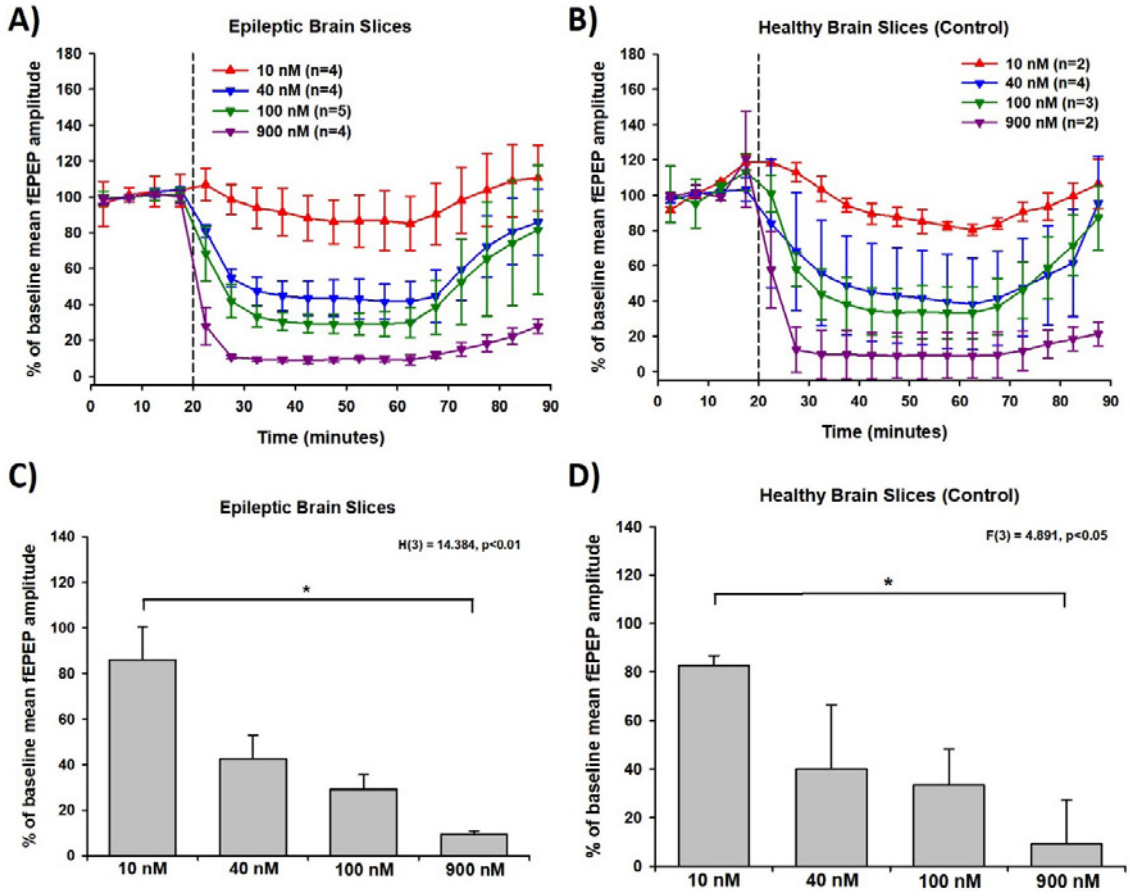

Figure 1: CPA application induces a dose dependent inhibition of the amplitude of field excitatory post synaptic potentials (fEPSP) in the CA1 of both epileptic and healthy brain slices. CPA was infused on the slices following 20 minutes of baseline recordings (A and B). After 10 minutes of infusion of CPA, there was a significant reduction in fEPSP amplitude in both epileptic and healthy control slices (C and D).

In a second preliminary experiment, the anticonvulsant efficacy of CPA was tested in slices perfused with 4-aminopyridine (4AP). 4AP is known to evoke a characteristic epileptiform pattern in hippocampal slices. Application of 900 nM CPA decreased epileptiform spiking activity in a manner consistent with previous reports in literature.

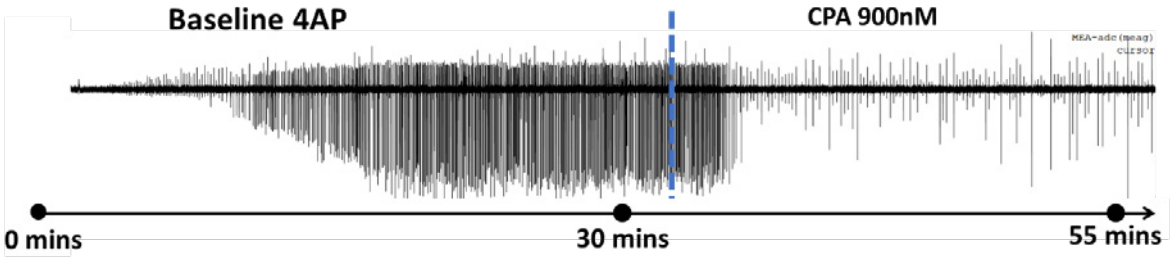

Figure 2: Application of CPA (900 nM) decreases spiking activity in the hippocampal field induced by 4AP *in vitro*

These experiments have thus demonstrated that despite indications of altered adenosine signaling in epilepsy, CPA is equally effective in inhibiting evoked activity and suppressing epileptiform activity of slices obtained from chronically epileptic mice as in healthy brain slices. As we will be using the same model for epilepsy going forward, and for our eventual proof of concept trial, this information is crucial. Before doing so, however, we will repeat many of the same experiments, using the photocaged CPA compound.

1.2. Validation of photocaged CPA in healthy rat brain slices

Initial exploration of the inhibitory potential of caged CPA has been done in hippocampal slices of the healthy rat brain. Following euthanasia, healthy rat brain slices were prepared and placed on a 60-channel multielectrode array (**Figure 3A**), following which a series of EP recordings were performed. Infusion of 3µM photocaged CPA into the MEA well had no influence on the amplitude or slope of the fEPSP. Application of short light pulses (500 ms, 1000 ms, 2000 ms; **Figure 3C**), however, was associated with strong inhibition of the fEPSP, following which a gradual return towards baseline levels was observed. Repeated application of short light pulses led to repeated fEPSP inhibition, followed by repeated fading of effects, demonstrating the potential of integrating this therapeutic modality into a closed-loop system, which is the principal goal of this project.

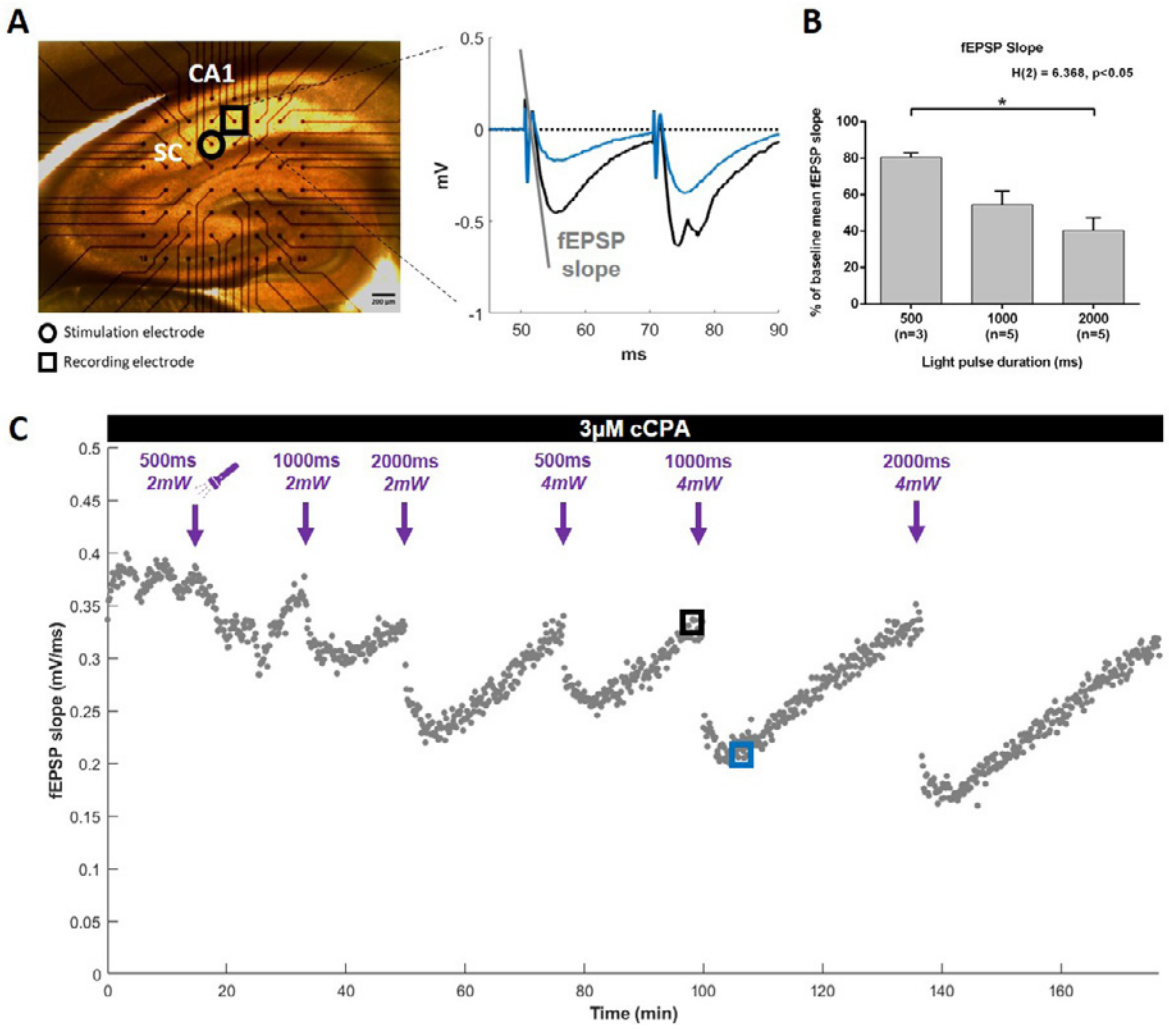

Figure 3: A) hippocampal slice positioned on a 60-channel multielectrode array (MEA). Electrical stimulation is applied to Schaffer Collaterals (SC) (black circle) and the evoked fEPSP response in the CA1 area (black square) is visualised. B) Percentage fEPSP slope relative to baseline recordings for different light pulse durations. Data are visualized as a bar plot with mean ± SEM. C) Representative trace of fEPSP slope over time of one MEA channel with multiple light pulse durations and varying light intensity.

These promising observations have encouraged the immediate parallel initiation of *in-vivo* experiments with photocaged CPA, which will be one of our key objectives for the first half of 2021.

1.3. In-vivo validation of inhibitory potential of CPA in the healthy mouse brain

Since our initial results in our *in-vitro* models with both CPA and caged CPA provided convincing proof of being able to both inhibit evoked activity and epileptiform activity, we set up an initial trial in which we tested the native CPA compound *in vivo* in anesthetized mice. For this experiment, mice were anesthetized with isoflurane (5% for induction, 2% for maintenance) and fixed in a stereotactic frame. Stainless steel wire electrodes were implanted in the hilus of the dentate gyrus for registration of dentate gyrus EPs and spontaneous local field potentials (LFPs). A bipolar stimulation electrode was implanted in the perforant path, the principal afferent input tract to the dentate gyrus, allowing the acquisition of dentate gyrus EPs. A Hamilton neurosyringe, was lowered to the level of the lateral ventricle contralateral to the site from which EPs and spontaneous hippocampal LFPs where acquired, which allowed the infusion of either CPA (low = 0.25 µg or high dose 1.25 µg, both dissolved in 5 µL of saline with 0.25% DMSO) or a vehicle solution (control condition). Following administration of CPA, there was a dose dependent suppression of

both fEPSP amplitude and the population spike of the dentate gyrus EPs (**Figure *4***) and a strong suppression of LFP power (**Figure 5**). Considering that the results obtained from this *in vivo* trial, though preliminary, clearly indicate similarly inhibitory potency of CPA as observed in our *in vitro* trials, we have the experimental setup in place to validate our photocaged CPA compound *in vivo* in the near future.

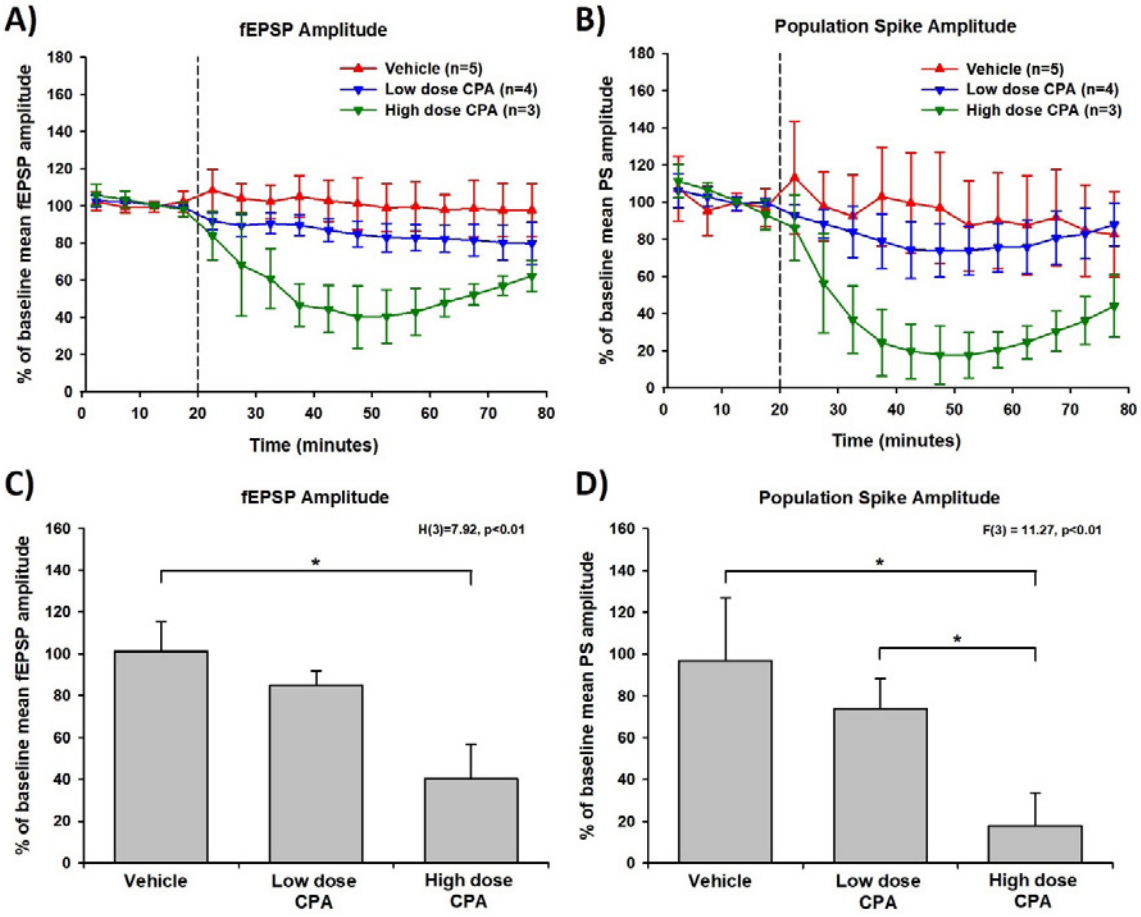

Figure 4: CPA administered intraventricularly induces a dose-dependent inhibition of dentate gyrus EPs, reflected by a gradual reduction in both field excitatory postsynaptic potential (fEPSP) amplitude and population spike amplitude (A and B), which was significant 30 minutes after administration of CPA (C and D).

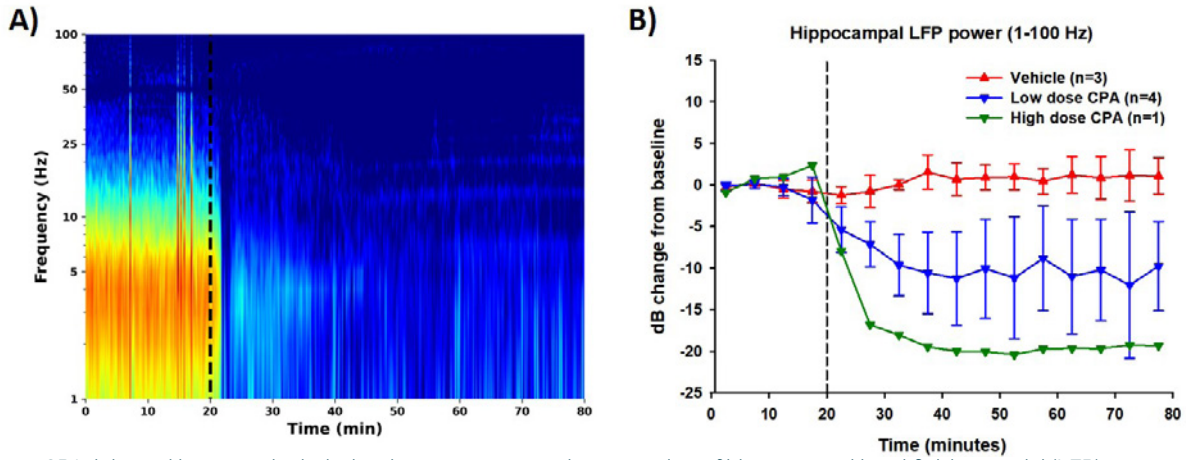

Figure 5: CPA, injected intraventricularly, leads to a pronounced suppression of hippocampal local field potential (LFP) power across most frequencies in the hippocampal LFP spectrogram (A). Total power appears to be affected in a dose-dependent manner, though only one animal has been studied for the high dose condition so far.

2. Scientific output

Recently, a review was published related to this project:
*Spanoghe, J., L. E. Larsen, E. Craey, S. Manzella, A. Van Dycke, P. Boon and R. Raedt (2020). "The Signaling Pathways Involved in the Anticonvulsive Effects of the Adenosine A1 Receptor." Int J Mol Sci **22**(1).*

In addition, an abstract has been submitted to the Gottingen Meeting of the German Neuroscience Society, based on preliminary data obtained from our *in vitro* slice experiments, which we aim to publish in full manuscript form in the course of 2021.

3. Perspectives for 2021

Considering these exciting results, we are doing everything we possibly can to move towards a closed-loop proof of concept trial as soon as possible. As seen above, our initial promising results have already encouraged us to initiate many of the planned experiments in parallel. Our first priority is to finish the experiments above and move towards publication of these results in the course of 2021. Although, high-density electrophysiology in epileptic mice in order to identify targets for precision intervention is still a goal of ours towards optimizing the concept of closed loop precision interventions, we are likely going to move straight to a proof of concept trial by simply targeting the lesion site (i.e. region injected with kainic acid). Though this may not be the best strategy, it has previously proven effective (Krook-Magnuson, Armstrong et al. 2013) and thus likely also sufficient to provide an initial proof of concept before moving towards optimization. We aim to initiate such trial towards the end of 2021.

4. References

- Desloovere, J., P. Boon, L. E. Larsen, C. Merckx, M. G. Goossens, C. Van den Haute, V. Baekelandt, D. De Bundel, E. Carrette, J. Delbeke, A. Meurs, K. Vonck, W. Wadman and R. Raedt (2019). "Long-term chemogenetic suppression of spontaneous seizures in a mouse model for temporal lobe epilepsy." Epilepsia **60**(11): 2314-2324.
- Krook-Magnuson, E., C. Armstrong, M. Oijala and I. Soltesz (2013). "On-demand optogenetic control of spontaneous seizures in temporal lobe epilepsy." Nat Commun **4**: 1376.
- Neumann, A. R., R. Raedt, H. W. Steenland, M. Sprengers, K. Bzymek, Z. Navratilova, L. Mesina, J. Xie, V. Lapointe, F. Kloosterman, K. Vonck, P. Boon, I. Soltesz, B. L. McNaughton and A. Luczak (2017). "Involvement of fast-spiking cells in ictal sequences during spontaneous seizures in rats with chronic temporal lobe epilepsy." Brain **140**(9): 2355-2369.
- Spanoghe, J., L. E. Larsen, E. Craey, S. Manzella, A. Van Dycke, P. Boon and R. Raedt (2020). "The Signaling Pathways Involved in the Anticonvulsive Effects of the Adenosine A1 Receptor." Int J Mol Sci **22**(1).

Geneeskundige Stichting Koningin Elisabeth
Fondation Médicale Reine Elisabeth
Königin-Elisabeth-Stiftung für Medizin
Queen Elisabeth Medical Foundation

Progress report of the research project of the young researcher

Aya Takeoka, PhD (IMEC)
Katholieke Universiteit Leuven (KU Leuven)

Aya Takeoka PhD
Principal Investigator at NERF, a joint research initiative by imec, VIB and KU Leuven
Assistant Professor, Department of Neuroscience @ KU Leuven
T +32 16 28 31 14
aya.takeoka@nerf.be
www.nerf.be
twitter.com/TakeokaLab

Learning to walk without the brain: Determining cellular signatures underlying age-dependent spinal cord plasticity

1. Aims

Adult rodents with complete spinal cord transection (cSTX) at the thoracic level do not regain the capacity to walk spontaneously. Nevertheless, mice receiving the same injury at early post-natal period (post-natal day 5, P5), exhibit proficient hindlimb locomotion on a motorized treadmill as adult. This is achieved despite the spinal cord circuits controlling hindlimb movements are functionally isolated from the brain. With support from GSKE/FMRE, **we have made a concerted effort to unravel circuit signatures that define age-dependent plasticity of spinal locomotor circuits (**Bertels et al., *manuscript in preparation*). In the first year of this funding cycle, we have narrowed down on spinal interneuron populations that define proficient circuit functions after neonatal injury and the essential role of proprioception in facilitating remodeling of local spinal circuits. We found that **gene expression and connectivity of excitatory interneurons to be key characteristics that define age of injury dependent locomotor plasticity.**

1.1. Finding 1. Proprioception maintains the balance of neuronal transmitter phenotype after neonatal injury.

Give that somatosensory afferents are the only external input to the local spinal cord circuits after the complete spinal cord transection, we hypothesized that proprioceptive afferents (PAs), a somatosensory modality important for spinal circuit development, and their activity feeding into the spinal cord circuits is the key determinant for shaping the neurotransmitter (NT) phenotype signature. Using an established intersectional approach (Takeoka and Arber, 2019), we removed PAs at the time of neonatal injury (Figure 1). This intervention prevents the spinal cord to develop its capacity to walk without the brain as an adult. Using multiplex *in-situ hybridization* method, we determined abundance and position of spinal interneurons with excitatory (vGlut2^{ON}), inhibitory (VGAT^{ON}), or double (vGlut2^{ON} /VGAT^{ON}) neurotransmitter (NT) expression. In intact adult spinal segments in which motor neurons that innervate that hindlimb muscles reside, we found majority of interneurons express single NT, with minor proportion with both excitatory and inhibitory NT phenotype. In the adult spinal cords that received neonatal injury exhibited similar NT balance while ones with adult injury contained significantly higher proportion of double NT phenotype interneurons. Given that we observed no change in abundance of VGAT^{ON} interneurons but decrease in vGlut2^{ON} counterpart, we conclude that it is the vGlut2^{ON} interneurons that acquire inhibitory NT phenotype after injury as adults.

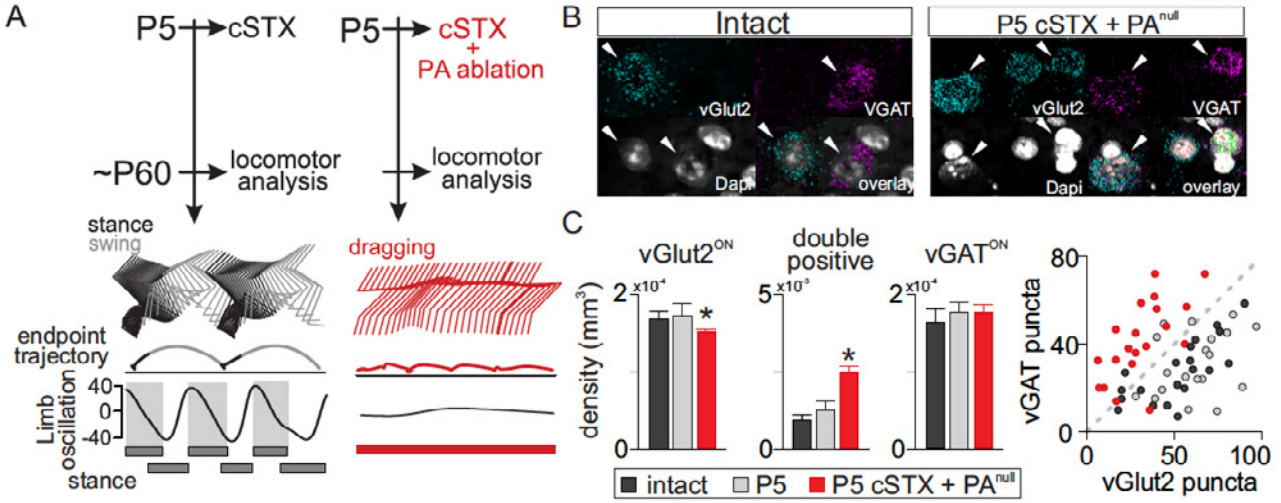

Figure 1. (A) Experimental timeline and locomotor kinematics of spinal cord injured mice as neonates, with or without proprioception. (B) Representative image of excitatory and inhibitory neurotransmitter expression in intact and neonatally injured + proprioceptive afferent (PA) ablated spinal cords. (C) Density of neurons with vGlut2 only, vGlut2/VGAT double positive, and VGAT only gene expressions. Right panel shows quantification of vGlut2 and VGAT transcripts of double positive neurons. Overall, neonatal injury combined with PA ablation leads to inverse relationship of vGlut2 and VGAT transcripts compared to intact or neonatal injury only. Asterisks indicate statistically significant difference to intact spinal cord.

1.2. Finding 2. Spinal excitatory neurons acquire inhibitory neurotransmitter phenotype after spinal cord injury as adults but not after neonatal injury.

We also found that the spinal cord without PAs after injury exhibited NT expression pattern that resemble that of after adult injury, in which dorsal and intermediate vGlut2^{ON} interneurons acquire inhibitory NT phenotype (Figure 2). These experiments provide compelling evidence that age-dependent plasticity in "brain-less" locomotion reflects fundamental differences in gene expression patterns within the spinal cord below lesion.

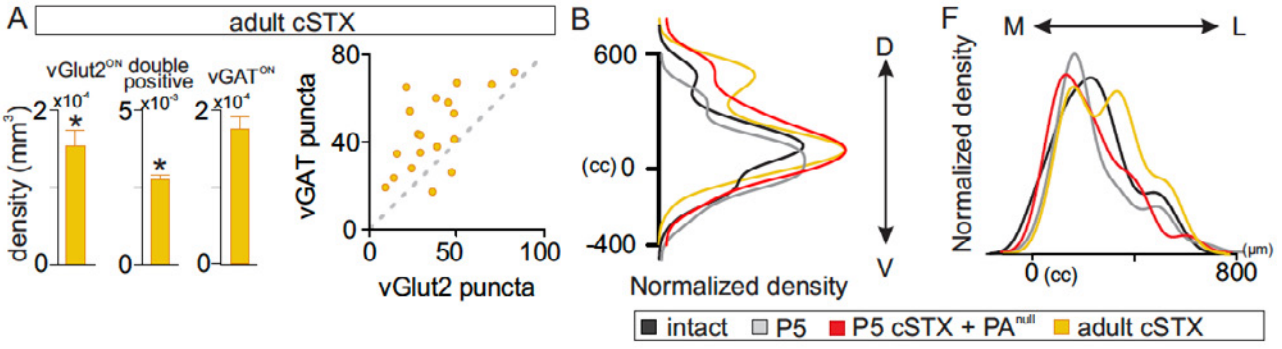

Figure 2. (A) Density of neurons with vGlut2 only, vGlut2/VGAT double positive, and VGAT only gene expressions in spinal cords injured as adults. Right panel shows quantification of vGlut2 and VGAT transcripts of double positive neurons. Transcript balance of vGltu2 and VGAT transcripts in the spinal cord injured as adults resemble condition with neonatal injury combined with PA ablation (Figure 1C). Asterisks indicate statistically significant difference to intact spinal cord. (B, C) Distribution of vGlut2/VGAT double positive neurons in the spinal cord, along Dorsal-ventral axis and medial-lateral axis. The results indicate many of double positive neurons reside in the dorsal half of the spinal cord, regardless of injury condition.

1.3. Finding 3. Injury has a selective effect on synaptic profile from excitatory interneurons to motor neurons that innervate hindlimb muscles.

As we observed in gene expression analysis that excitatory neurons that acquire inhibitory NT are predominantly residing in the dorsal half of the spinal cord, we determined whether and how that is reflected at the protein level and synaptic connectivity, in excitatory subpopulation-specific manner. For this purpose, we chose to disentangle three different excitatory neuronal

populations that are derived from a specific Progenitor domain (PD) during development and occupy distinct position along the dorsal-ventral axis, dI3 and dI5 (*Tlx3* ^{ON}), V2a (*Shox2*^{ON}), and V3 (*Sim1* ^{ON}) populations (Figure 3). We crossed PD^{cre} driver lines with *Tau*$^{LSL\text{-}SynGFP}$ mice to selectively visualize synaptic output derived from a specific PD population, and to quantify the number of SynGFP^{ON} input to motor neurons (MNs) that innervate hindlimb muscles. In addition, we marked SynGFP^{ON} terminals with vGlut2 or VGAT protein using immunohistochemistry. Our findings are two-folds. We detected no change in NT phenotype of synaptic terminals after neonatal injury, while we observed significant increase in the proportion of inhibitory terminals among *Tlx3*- and *Shox2*-SynGFP^{ON} input to MNs after adult injury. Concomitantly, number of synaptic appositions from dorsal and intermediate excitatory interneurons to MNs was significantly larger after neonatal injury compared to intact spinal cord while it was unaltered after adult injury. Interestingly, abundance of *Sim1*-GFP^{ON} synapses nor its neurotransmitter composition was altered. Complementary to gene expression analysis (Finding 1), injury or age of injury did not affect NT phenotype or abundance of synaptic innervation from inhibitory interneurons to MNs. We found that age of injury-dependent circuit plasticity mediated via the two distinct mechanisms, NT phenotype switch and axonal sprouting, leads 1) overall increase in excitatory drive after neonatal injury, and 2) decrease in excitatory drive after adult injury, to motor neurons innervating hindlimb muscles.

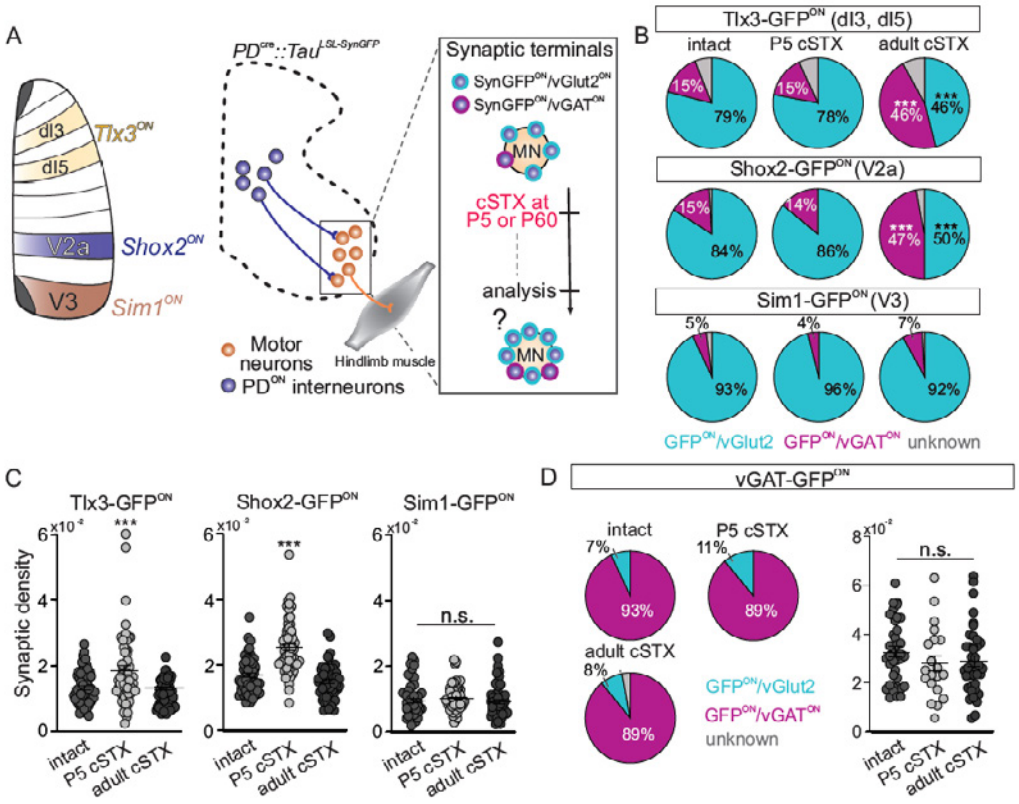

Figure 3. (A) Different transcription factors that mark distinct subpopulations of excitatory spinal interneurons, and experimental scheme. PD: progenitor domain. (B) Synaptic profiles categorized via neurotransmitter phenotype per PD interneurons, per injury condition examined. (C) Synaptic density calculated by SynGFP apposition onto MNs that innervate hindlimb muscles. (D) Inhibitory spinal interneurons do not exhibit either NT phenotype switch, or synaptic sprouting.

2. Summary of findings and Ongoing work

We found two distinct mechanisms that underlie spinal circuit reorganization that is dependent on age of injury. Currently, we are performing virus-mediated gain-of-function experiments in which excitatory interneurons to gain inhibitory neurotransmitter phenotype after a neonatal injury. This approach will allow us to determine whether maintenance of excitatory phenotype by excitatory interneurons is 1) indeed an essential feature of the capacity to walk without the brain, and 2) determine the extent of synaptic proliferation to motor neurons.

3. Planned manuscript submission with GSKE/FMRE support

Bertels H., Ortiz-Vicente G., El Khanbi K., Takeoka A. Spinal excitatory interneurons define age-dependent locomotor circuit plasticity after spinal cord injury. *manuscript in preparation*.

Geneeskundige Stichting Koningin Elisabeth
Fondation Médicale Reine Elisabeth
Königin-Elisabeth-Stiftung für Medizin
Queen Elisabeth Medical Foundation

Progress report of the research project of the young researcher

Dr. Valerie Uytterhoeven
Katholieke Universiteit Leuven (KU Leuven)

Dr. Valerie Uytterhoeven
Staff Scientist
Center for Brain & Disease Research, VIB-KU Leuven
Laboratory of neuronal communication
Herestraat 49 bus 602
3000 Leuven
Belgium
Tel: +32 16 37 61 03

Molecular mechanisms and inducers of chaperone mediated Tau autophagy in Alzheimer's disease

1. Summary research program

Tau's primary localization and function is in the axons of neurons. There, Tau binds microtubuli and stabilizes them. Many of the pathogenic mutations interfere with the attachment of Tau to the microtubuli resulting in the relocation of Tau to different neuronal compartments, including the presynapse. Our lab has shown in fruit flies and primary mouse neurons that Tau interacts with presynaptic vesicles via the synaptic vesicle protein, Synaptogyrin-3 and that in pathogenic conditions excessive Tau levels at presynapses results in the sequestration of synaptic vesicles compromising neurotransmission. This pathogenic action of Tau at presynapses can be reverted when Synaptogryin-3 levels are reduced [1,2]. In addition, we showed that lowering Synaptogyrin-3 expression rescues Tau-mediated memory defects and synapse loss in TauP301L mutant mice [3]. Although, the interaction of Tau with synaptic vesicles is reduced with lowering Synaptogyrin-3 expression, Tau continues to accumulate at presynapses. To circumvent the accumulation of Tau, we tested if we can increase the turnover of Tau by increasing endosomal microautophagy by the expression of Hsc70-4 [4] in fly neurons expressing pathogenic Tau. We succeeded to reduce presynaptic TauP301L levels and restore normal synaptic vesicle mobility and neurotransmission by increasing endosomal microautophagy. However, increasing endosomal microautophagy is not effective in lowering presynaptic Tau in TauV337M mutant neurons. Using a fluorescent timer attached to Tau, we show that older Tau is present in TauV337M compared to TauP301L mutant presynapses indicating that the turnover of TauV337M is hindered. In addition, with a fluorescence recovery after photobleaching assay, we show that both TauP301L and TauV337M are more mobile in axons compared to wild type Tau but is more severe for TauP301L indicating that TauP301L detaches more easily from the microtubuli. Together, these data show that both the detachment of Tau from microtubuli and defective turnover of Tau at presynapses contribute to the accumulation of Tau at presynapses and depending on the pathogenic mutation one of the two pathways plays a more prominent role in the accumulation of Tau at presynapses. These observations pave the way towards precision dementia medicine.

2. Results

2.1. Increased endosomal microautophagy reduces pathogenic TauP301L levels at fly presynapses

In our previous publication [5], we showed that endosomal microautophagy is fundamental at presynapses for the turnover of cytosolic synaptic proteins harboring a KFERQ-motif. Hsc70-4 is a rate controlling factor in this pathway as increased expression of Hsc70-4 boosts the degradation of KFERQ-motif containing presynaptic proteins [5]. Tau contains two of these motifs and was shown to be degraded via endosomal microautophagy [6]. Given that the expression of pathogenic Tau in neurons results in the accumulation of Tau at presynapses inducing presynaptic dysfunction [1,2] we tested if increasing endosomal by the expression of Hsc70-4 is effective in reducing presynaptic Tau levels. The expression of Hsc70-4 in Tau P301L mutant neurons significantly reduced presynaptic Tau levels (Figure 1). In addition, the expression of chaperone defective (D10N) [7] but not endosomal microautophagy defective (3KA) Hsc70-4 reduces presynaptic TauP301L levels, indicating that the reduction of TauP301L is a result of increased endosomal microautophagy and not a result of increased Hsc70-4's chaperone function

(Figure 1). Moreover, these results show that reduction of presynaptic TauP301L is not a dilution effect of the Tau mutant phenotype by saturizing the gene expression system used to express human TauP301L and Hsc70-4 simultaneously. Thus, pathogenic TauP301L can be reduced at presynapses by stimulating endosomal microautophagy via the expression of Hsc70-4.

2.2. TauP301L mediated presynaptic dysfunction is rescued with increased endosomal microautophagy

High Tau levels at presynapses sequesters synaptic vesicles resulting in reduced synaptic vesicle mobility and reduced neurotransmission [1,2]. To test if endosomal microautophagy mediated reduction of Tau rescues reduced vesicle mobility at TauP301L mutant presynapses, we performed a fluorescence recovery after photobleaching (FRAP) assay in TauP301L mutant presynapses with or whithout increased endosomal microautophagy. In this FRAP assay, a defined area with fluorescently labeled synaptic vesicles are photobleached and the recovery of fluorescence is recorded over time. The rate of fluorescence recovery in the photobleached area is a measure for the mobility of synaptic vesicles [1,2,8]. At TauP301L mutant presynapses, the recovery rate of fluorescence after photobleaching is significantly slower compared to control presynapses that do not express human Tau. This defect is rescued by the expression of wild type Hsc70-4 in Tau mutant neurons. Accordingly to the rescue of Tau levels at presynapses, the expression of chaperone defective Hsc70-4 (D10N) rescues the reduced FRAP rate in Tau mutant presynapses, indicating that the chaperone activity of Hsc70-4 does not contribute to the rescue of vesicle mobility in TauP301L mutant. Further, the expression of endosomal microautophagy defective (3KA) Hsc70-4 does not restore the FRAP rate in TauP301L mutant neurons (Figure 2 A and B). Hence, increasing endosomal microautophagy by the expression of Hsc70-4 in TauP301L mutant neurons restores the reduced mobility of synaptic vesicles at mutant presynapses to levels comparable to wild type presynapses.

Reduced synaptic vesicle mobility hampers replenishment of synaptic vesicles in the vesicle cycle and neurons are not able to sustain neurotransmission during high frequency (10Hz) stimulation [1,2]. Given that synaptic vesicle mobility is rescued upon increased endosomal microautophagy we also measured neurotransmission during high frequency at TauP301L mutant presynapses. In accordance with the resuce of synaptic vesicle mobility, the expression of wild type or chaperone defective Hsc70-4 rescues defective neurotransmission during high frequency (10Hz) stimulation in TauP301L mutant presynapses. In contrast the expression of microautophagy dead Hsc70 (3KA) does not rescue neurotransmission (Figure 2 C and D). Hence, these data show that the reduction of presynaptic TauP301L by increasing endosomal microautophagy is sufficient to rescue Tau mediated functional defects.

2.3. Rescue of TauP301L mediated presynaptic dysfunction prevents Tau mediated neurodegeneration in the fly brain.

Synaptic dysfunction and loss are key steps in the process of neurodegeneration (reviewed in Selkoe 2002; Jackson, 2019) [9,10]. In different animal models expressing pathogenic Tau, including fly tauopathy models, Tau mediated changes in synaptic function contribute to brain neurodegeneration [11–15]. Neurodegeneration in the adult fly brain manifests as vacuoles and these are easily visualized in haematoxylin and eosin stained paraffin sections of the adult fly brain. Young control flies and young flies expressing TauP301L panneuronally do not show signs of neurodegeneration (Figure 3 A and B). Neurodegeneration is more prevalent with aging and is significantly increased in 40-day old TauP301L mutant flies compared to 40-day old control flies, as quanitified as vacuole area (Figure 3 C and D). This increase in neurodegeneration in TauP301L mutant flies is significantly reduced comparable to control levels with the expression of wild type or chaperone dead Hsc70-4 (Figure 3 C and D). Together, the rescue of Tau mediated

synaptic dysfunction with increased endosomal microautophagy prevents neurodegeneration of the adult fly brain.

2.4. Increasing endosomal microautophagy is not effective in neurons expressing Tau with tampered KFERQ-motifs.

Endosomal microautophagy turns over proteins that harbour at least one KFERQ-motif. To test if the reduction of TauP301L via the expression of Hsc70-4 is truly based on KFERQ-motif selectivity, we generated transgenic flies that express Tau with mutated KFERQ-motifs. In both KFERQ-motifs we substitued glutamine and the hydrophobic residue with alanines (TauAA). These mutations did not block the expression of Tau protein but resulted in the accumulation of TauAA at presynapses to the same extent as mutant TauP301L (Figure 4 A and B). Thus the mutations in the KFERQ-motifs are sufficient to drive the accumulation of Tau at presynapses. This allowed us to quantify the effect of increased Hsc70-4 expression on presynaptic TauAA levels. The expression of wild type nor chaperone dead Hsc70-4 in TauAA mutant flies resulted in a reduction of Tau levels at presynapses (Figure 4 C and D). Thus, the reduction of Tau at presynapses by increasing the expression of Hsc70-4 is KFERQ-motif selective.

Pathogenic mutations in both Tau KFERQ-motifs are identified. In previous work, we showed that the V337M mutation in the second KFERQ-motif of Tau is sufficient for Tau to accumulation at presynapses [1,2]. Similar to mutant TauAA presynapses, increasing endosomal microautophagy with the expression of wild type or chaperone dead Hsc70-4 has no effect on presynaptic TauV337M levels. In addition, the expression of microautophagy dead Hsc70-4 either has no effect on TauV337M levels at presynapses (Figure 4 E and F). Together, our results show that disrupted KFERQ-motifs interfere with the Hsc70-4 mediated recognition of Tau for degradation via endosomal microautophagy.

Similar to TauP301L, TauV337M interacts with synaptic vesicles and reduces their mobility at presynapses resulting in reduced neurotransmission [1,2]. In contrast to TauP301L, TauV3737M is not reduced with increasing endosomal microautophagy at presynapses as shown in Figure 4. Further, expression of Hsc70-4 wild type nor chaperone dead (D10N) rescues reduced FRAP rates of Syt-GFP at TauV337M mutant presynapses (Figure 5 A-C). In addition, the expression of microautophagy dead Hsc70-4 has no effect either on reduced vesicle mobility at TauV337M mutant presynapses (Figure 5 D). Because synaptic vesicle mobility is essential for neurotransmission, neurotransmission is not sustained over time with a high frequency (10Hz) stimulation paradigm in TauV337M mutant neurons with increased expression of wild type or chaperone dead (D10N), similar to TauV337M mutant neurons (Figure 5 E and F). Hence, our results show that whenever increased Tau levels at presynapses are not reduced with increasing endosomal microautophagy, Tau mediated presynaptic dysfunction is not restored

2.5. Defective Tau identification for endosomal microautophagy and increased Tau mobility in axons mediate accumulation of pathogenic Tau at presynapses.

We show that with the expression of Hsc70-4 we can reduce presynaptic TauP301L (Figure 1) but not TauV337M (Figure 4). This result suggests that a defect in the recognition of TauV337M for endosomal microautophagy contributes to the accumulation of TauV337M at presynapses. To test the turnover rate of Tau at presynapses, we generated transgenic flies that express pathogenic Tau linked to a fluorescent timer. A fluorescent timer is a modified GFP that shifts from blue to red over time and the red/blue intensity ratio is a measure of how equal the mix of old and young Tau protein is. An increased red/blue ratio indicates an older Tau protein pool and vice versa. We measured an increased red/blue ratio in TauV337M and TauAA mutant presynapses compared to TauP301L mutant presynapses (Figure 6 A and B) indicating that the turnover of TauV337M and

TauAA is reduced compared to TauP301L at presynapses. Given that presynaptic Tau levels are equal in TauP301L, TauAA and TauV337M mutant presynapses (Figure 5A and [1]) and that the turnover of TauV337M and TauAA is decreased compared to TauP301L, indicates that another mechanism contributes to the accumulation of TauP301L at presynapses. The literature shows us that pathogenic mutations in Tau interfere with microtubuli binding. However, a strong consensus on the impact of different pathogenic Tau mutations on Tau-microtubuli interactions has not yet been reached [16–20]N279K, ΔSK280, P301L, V337M, R406W. Using FRAP of Tau-GFP in axons we measured the mobility of mutant Tau (P301L, V337M and AA). Tau-GFP FRAP in TauP301L axons is significantly increased compared to TauV337M and TauAA axons (Figure 6 C and D). These results show that in TauV337M mutants defective turnover dominates the accumulation of Tau at presynapses on the other hand in TauP301L mutants the decreased affinity of Tau for microtubuli results in the accumulation of Tau at presynapses. Hence, the nature of the Tau mutation defines the molecular route of Tau accumulation at presynapses.

3. Future perspectives

The next step is to validate our fruit fly results shown here in human neurons. First, we will differentiate iPSC generated from patients with a TauP301L or V337M mutation, which we recently received from the Neuronal stem cell Institute in New York and the Karch lab from Washington University [21]presenilin 1 (PSEN1, to mature neurons to confirm the increase of Tau levels at presynapses and reduction of synaptic vesicle mobility. Afterwards, we will increase endosomal microautophagy by lentiviral –mediated expression of Hspa8, the human homologue of Hsc70-4 in the patient-derived human neurons and measure the effect on Tau levels and vesicle mobility at presynapses *in vitro*. In addition, we will inject human neurons with increased endosomal microautophagy in Alzheimer's diseased mouse brain to test if the human neurons survive the pathogenic environment. In this human-mouse chimeric mouse AD model human neurons are exposed to the pathogenic environment, accumulate pathogenic Tau and degenerate. With this model we can test *in vivo* if increasing endosomal microautophagy has a positive effect on the survival of human neurons in pathogenic conditions.

Because TauV337M is not reduced by increasing endosomal microautophagy via the expression of Hsc70-4, we are developing a peptide that forces the sorting of TauV337M for endosomal microautophagy and this peptide will be further tested for its efficacy in rescuing Tau-mediated presynaptic defects in our fruit fly models and patient-derived human neurons.

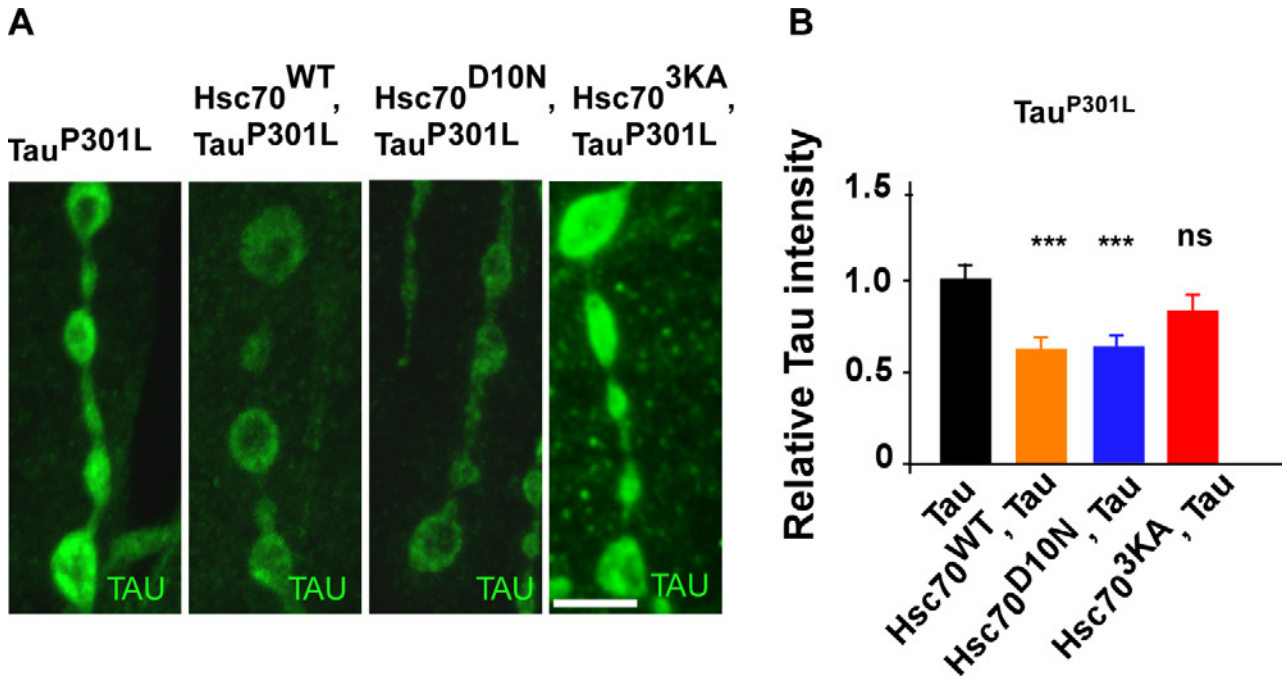

Figure 1. TauP301L mutant protein is reduced at presynapses after upregulation of endosomal microautophagy
A) Representative images of Tau intensities at neuromuscular junction of TauP301L mutant neurons (D42-GAL4>TauP301L) or TauP301L mutant neurons that express wild type((D42-GAL4> Hsc70WT, TauP301L), chaperone dead (D42-GAL4> Hsc70D10N, TauP301L) or endosomal microautophagy dead (D42-GAL4> Hsc703KA, TauP301L) Hsc70-4 **D)** Quantification of Tau intensities at presynapses of TauP301L mutant neurons or TauP301L mutant neurons expressing wild type (WT), chaperone dead (D10N) or endosomal microautophagy dead (3KA) Hsc70-4. Scale bar is 5µm. Bar graphs depict mean ± SEM. Number of larvae is 8 per genotype. An ordinary one-way ANOVA with Dunnett's correction for multiple comparisons was performed to determine significance levels between genotypes; ns is not significant, *** $p<0.001$.

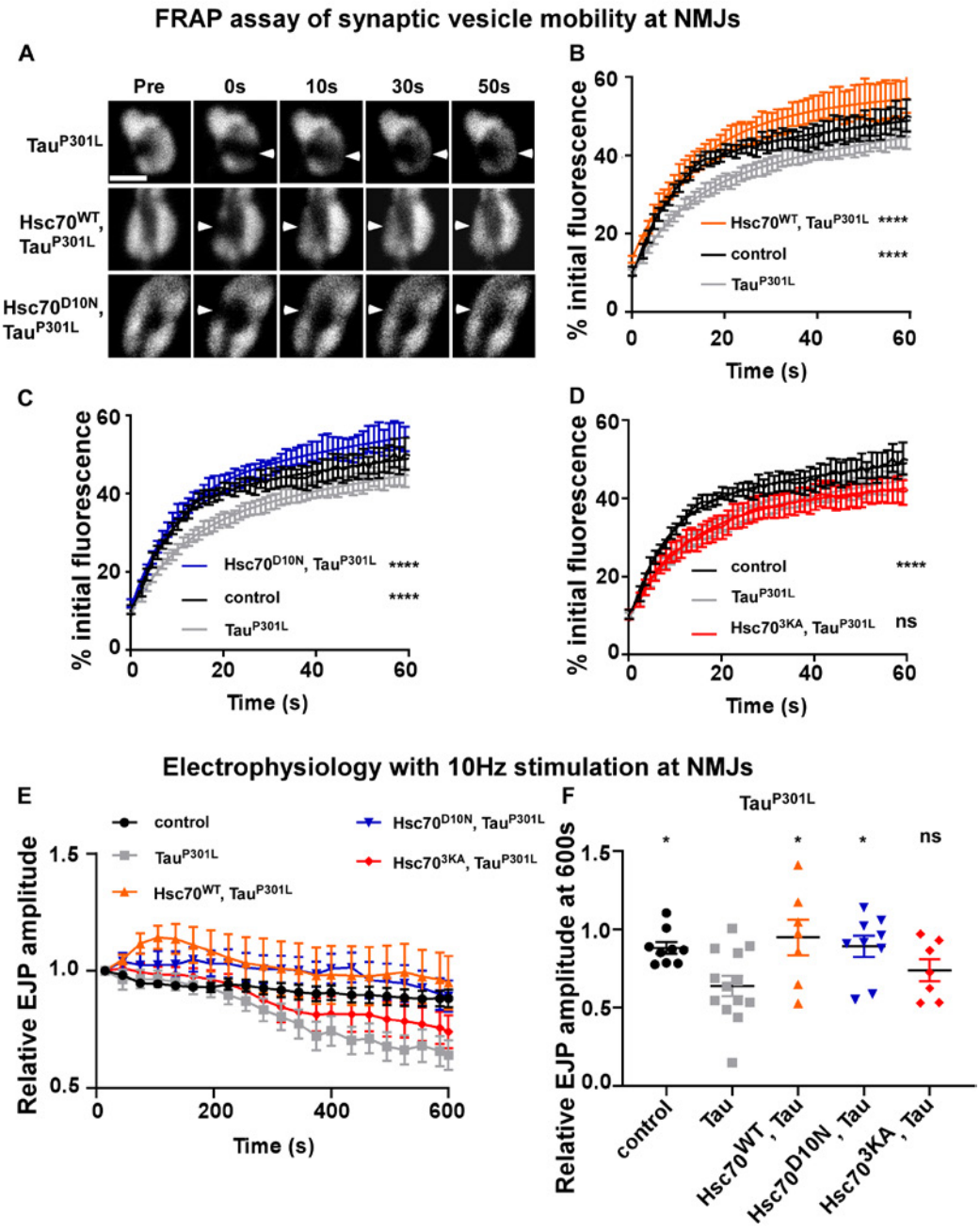

Figure 2. Increased Hsc70-4 mediated endosomal microautophagy rescues TauP301L-induced synaptic vesicle mobility and neurotransmission defects at NMJs

A–D) FRAP assay of synaptic vesicle mobility within presynaptic boutons. *Drosophila* larvae express Synaptotagmin-GFP (Syt-GFP) and TauP301L with or without wild type (WT), chaperone dead (D10N) or endosomal microautophagy dead (3KA) Hsc70-4 under the control of the D42-Gal4 motor neuron driver. **A)** Representative images of Syt-GFP signal before and after photobleaching show fluorescence recovery of a small area (arrowhead) after photobleaching of Syt-GFP fluorescence in presynaptic boutons during a 60 second time frame. Scale bar, 5 µm. **B-D)** Plots of Syt-GFP fluorescence recovery over time fit to a double-exponential curve depicting relative vesicle mobility in control (black), TauP301L(grey), Hsc70WT, TauP301L (orange), Hsc70D10N, TauP301L (blue), and Hsc703KA, TauP301L (red) larvae. Plots depict mean ± SEM (n is 8-23 boutons from ≥8 animals; A two-way ANOVA with Dunnett's correction for multiple comparisons was performed to determine significance levels between all four genotypes; ns is not significant, **** $p<0.0001$

E–F) Electrophysiological recordings of neurotransmitter release at NMJs. **E)** Plot of evoked junction potential (EJP) amplitudes in response to 10-Hz stimulation with 2 mM Ca^{2+} for 10 min in control (D42-GAL4>); TauP301L (D42-GAL4> TauP301L); Hsc70WT, TauP301L (D42-GAL4> Hsc70WT, TauP301L); Hsc70D10N, TauP301L (D42-GAL4> Hsc70D10N, TauP301L) and Hsc703KA, TauP301L (D42-GAL4> Hsc703KA, TauP301L) larvae. Amplitudes are binned at 30 s intervals and normalized to the average of the first 15 s. Graph depicts mean ± SEM. **F)** Relative EJP amplitude at 600 s plotted as individual data points. Graph depicts mean ± SEM. (number of dots is number of NMJ recordings from ≥6 animals) An ordinary one-way ANOVA with Dunnett's correction for multiple comparison was performed to determine significance levels between all five genotypes; ns, not significant, *$p < 0.05$.

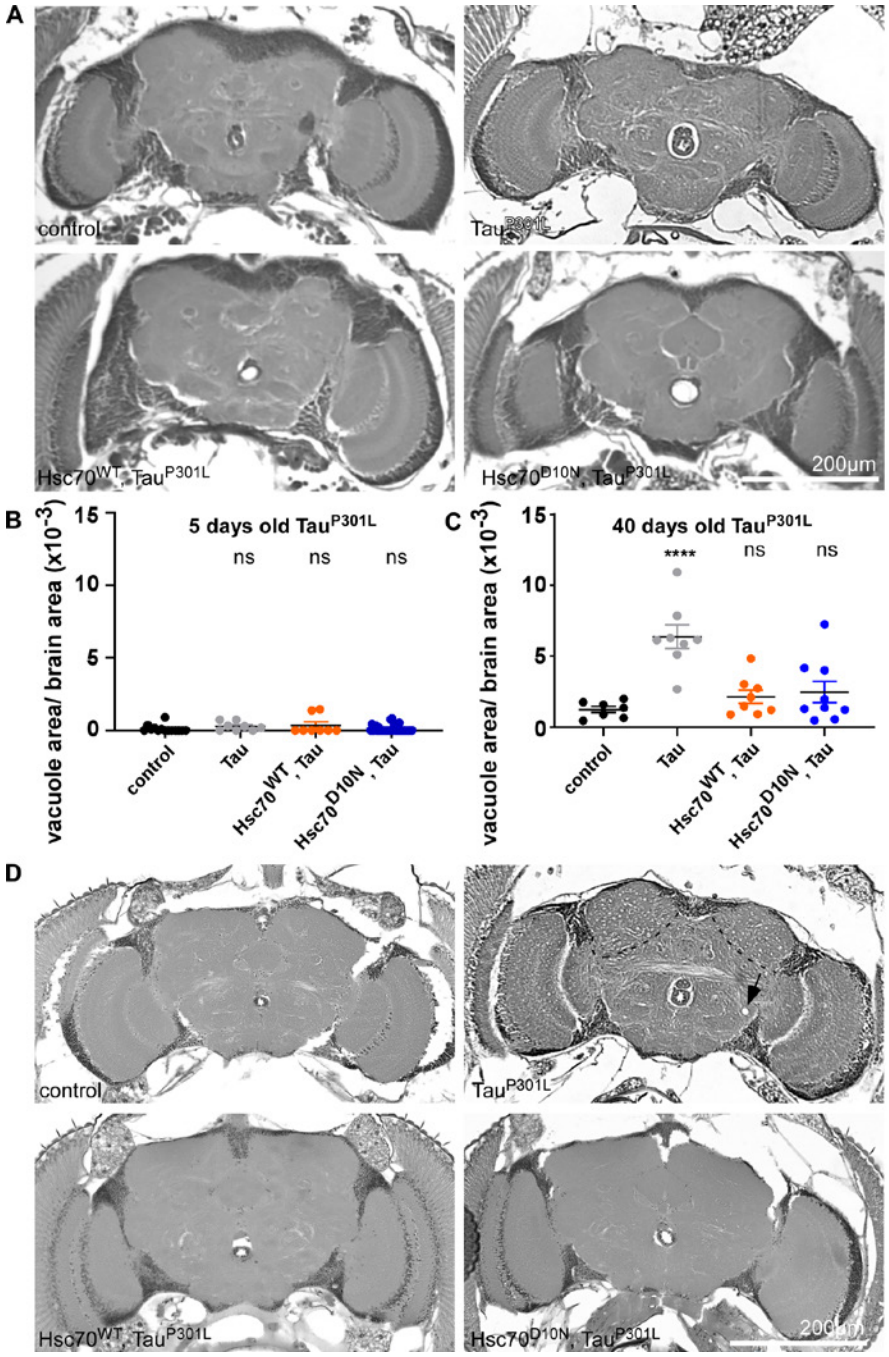

Figure 3. TauP301L induced neurodegeneration is rescued with increased endosomal microautophagy
A and D) Brain sections of 5-day-old **(A)** and 40-day old **(D)** control (nSyb-GAL4>); and transgenic TauP301L (nSyb-GAL4> TauP301L); Hsc70WT, TauP301L (nSyb-GAL4> Hsc70WT, TauP301L) and Hsc70D10N, TauP301L (nSyb-GAL4> Hsc70D10N, TauP301L) adult flies were stained with H&E. **B and C)** Neurodegeneration was assessed by quantification of vacuole area normalized over brain area. **B)** Neurodegeneration was not detected in 5-day old control flies and transgenic flies expressing TauP301L with or without Hsc70-4. **C)** Tau-induced neurodegeneration was significantly reduced comparable to control levels by the expression of Hsc70WT and Hsc70D10N in the brains of 40-day-old TauP301L flies. Arrow and encircled area indicate vacuolar degeneration. Data points represent the mean ± SEM. (number of dots indicate the number of animals (≥7)). An ordinary one-way ANOVA with Dunnett's correction for multiple comparison was performed to determine significance levels between all four genotypes; ns, not significant, **** p<0.0001.

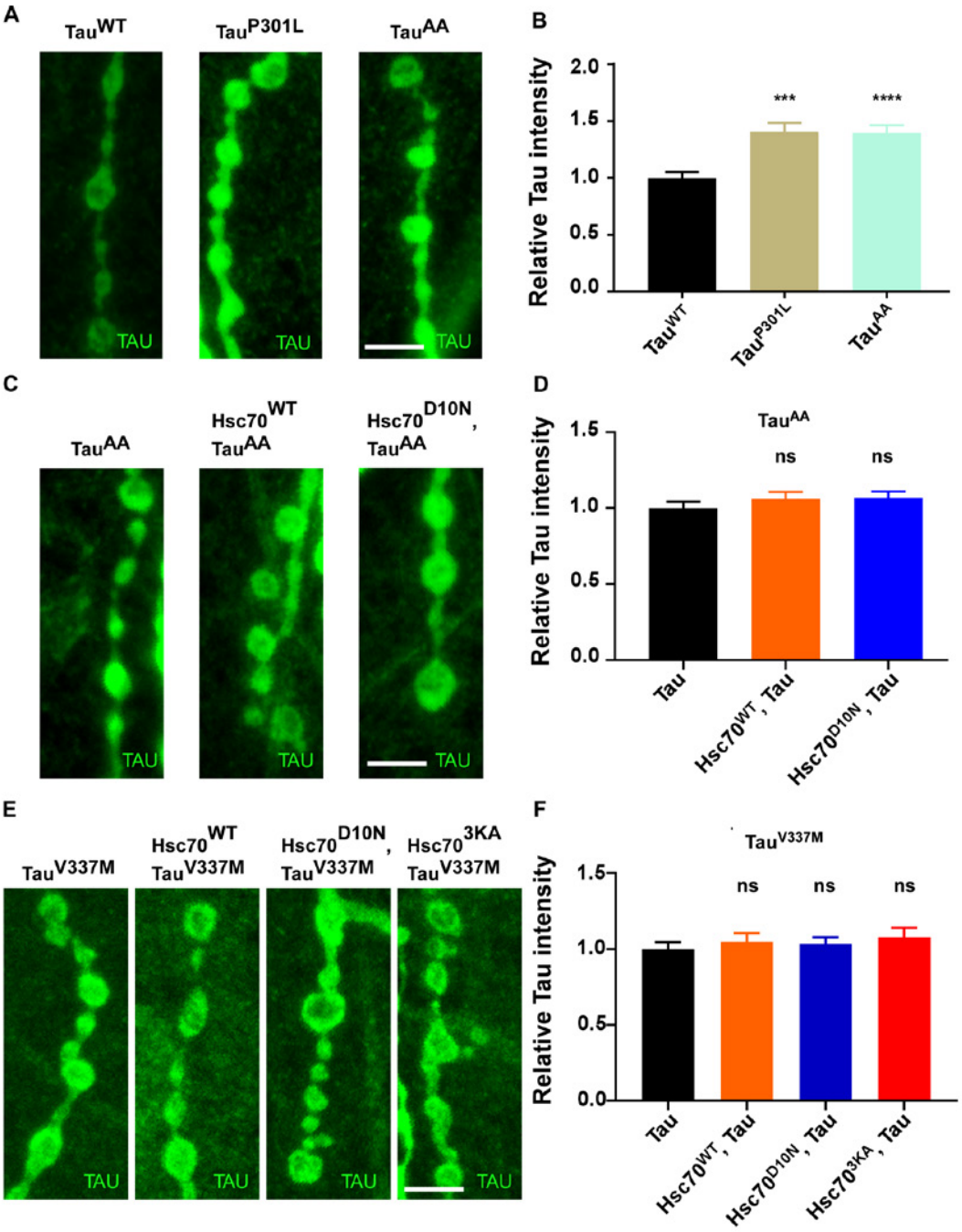

Figure 4. KFERQ-motif mutant Tau is not reduced with increased endosomal microautophagy at presynapses
A) Representative images of Tau intensities in boutons at neuromuscular junctions expressing wild type Tau (D42-GAL4> TauWT), mutant TauP301L (D42-GAL4> TauP301L) or mutant TauAA (D42-GAL4> TauAA). **B)** Quantification of Tau intensities in boutons at neuromuscular junctions expressing wild type Tau, mutant TauP301L or mutant TauAA. **C)** Representative images of Tau intensities at neuromuscular junction of TauAA mutant neurons (D42-GAL4> TauAA) or TauAA mutant neurons that express wild type (D42-GAL4> Hsc70WT, TauAA) or chaperone dead (D42-GAL4> Hsc70D10N, TauAA) Hsc70-4. **D)** Quantification of Tau intensities in boutons at neuromuscular junctions of TauAA mutant neurons or TauAA mutant neurons expressing wild type (WT) or chaperone dead (D10N) Hsc70-4. **E)** Representative images of Tau intensities in boutons at neuromuscular junctions of TauV337M mutant neurons (D42-GAL4> TauV337M) or TauV337M mutant neurons that express wild type (D42-GAL4> Hsc70WT, TauV337M), chaperone dead (D42-GAL4> Hsc70D10N, TauV337M) or endosomal microautophagy dead (D42-GAL4> Hsc703KA, TauV337M) Hsc70-4. **F)** Quantification of Tau intensities in boutons at neuromuscular junctions of TauV337M mutant neurons or TauV337M mutant neurons that express wild type (WT), chaperone dead (D10N) or endosomal microautophagy dead (3KA) Hsc70-4. Scale bar is 5µm. Bar graphs depict mean ± SEM. Number of larvae is 4-8 per genotype for (A-B) and 8 per genotype for (C-F). An ordinary one-way ANOVA with Dunnett's correction for multiple comparisons was performed to determine significance levels between multiple genotypes; ns is not significant, *** p<0.001, **** p<0.0001.

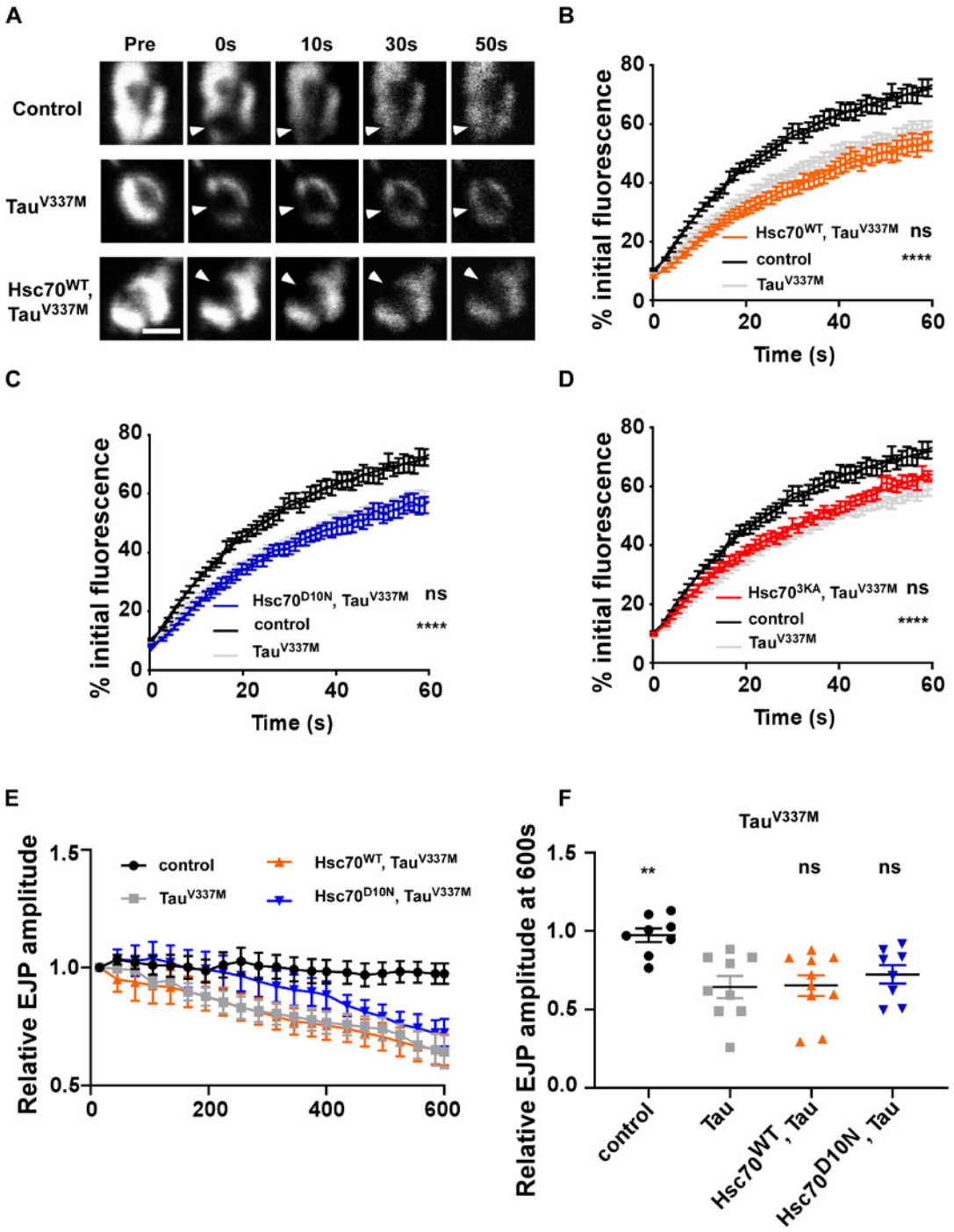

Figure 5. Presynaptic dysfunction in KFERQ-motif mutant Tau is not rescued with increased endosomal microautophagy
A) Representative images of Syt-GFP fluorescence recovery at time points right before (pre) and after photobleaching of small area (arrowhead) (0, 10, 30 and 50 seconds) in control (D42-GAL4> Syt-GFP), Tau^{V337M} (D42-GAL4> Syt-GFP; Tau^{V337M}) and Tau^{V337M} mutant presynaptic boutons expressing Hsc70^{WT} (D42-GAL4> Syt-GFP; Hsc70^{WT}, Tau^{V337M}). Scale bar, 5 µm. **B-D)** Plots of Syt-GFP fluorescence recovery over time fit to a double-exponential curve depicting relative vesicle mobility in control (black), TauV337M (grey), Hsc70WT, TauV337M (orange), Hsc70D10N, TauV337M (blue), and Hsc703KA, TauV337M (red) larvae. Plots depict mean ± SEM (n is 8-23 boutons from ≥8 animals; A two-way ANOVA with Dunnett's correction for multiple comparisons was performed to determine significance levels between all five genotypes; ns is not significant, **** p<0.0001
E–F) Electrophysiological recordings of neurotransmitter release at NMJs. **E)** Plot of evoked junction potential (EJP) amplitudes in response to 10-Hz stimulation with 2 mM Ca^{2+} for 10 min in control (D42-GAL4>); TauP301L (D42-GAL4> TauP301L); Hsc70WT, TauP301L (D42-GAL4> Hsc70WT, TauP301L); Hsc70D10N, TauP301L (D42-GAL4> Hsc70D10N, TauP301L); Hsc703KA, TauP301L (D42-GAL4> Hsc703KA, TauP301L). Amplitudes are binned at 30-s intervals and normalized to the average of the first 15 s. Graph depicts mean ± SEM. **F**) Relative EJP amplitude at 600 s plotted as individual data points. Graph depicts mean ± SEM. (number of dots is number of NMJ recordings from ≥6 animals) An ordinary one-way ANOVA with Dunnett's correction for multiple comparison was performed to determine significance levels between all five genotypes; ns, not significant, **p < 0.01.

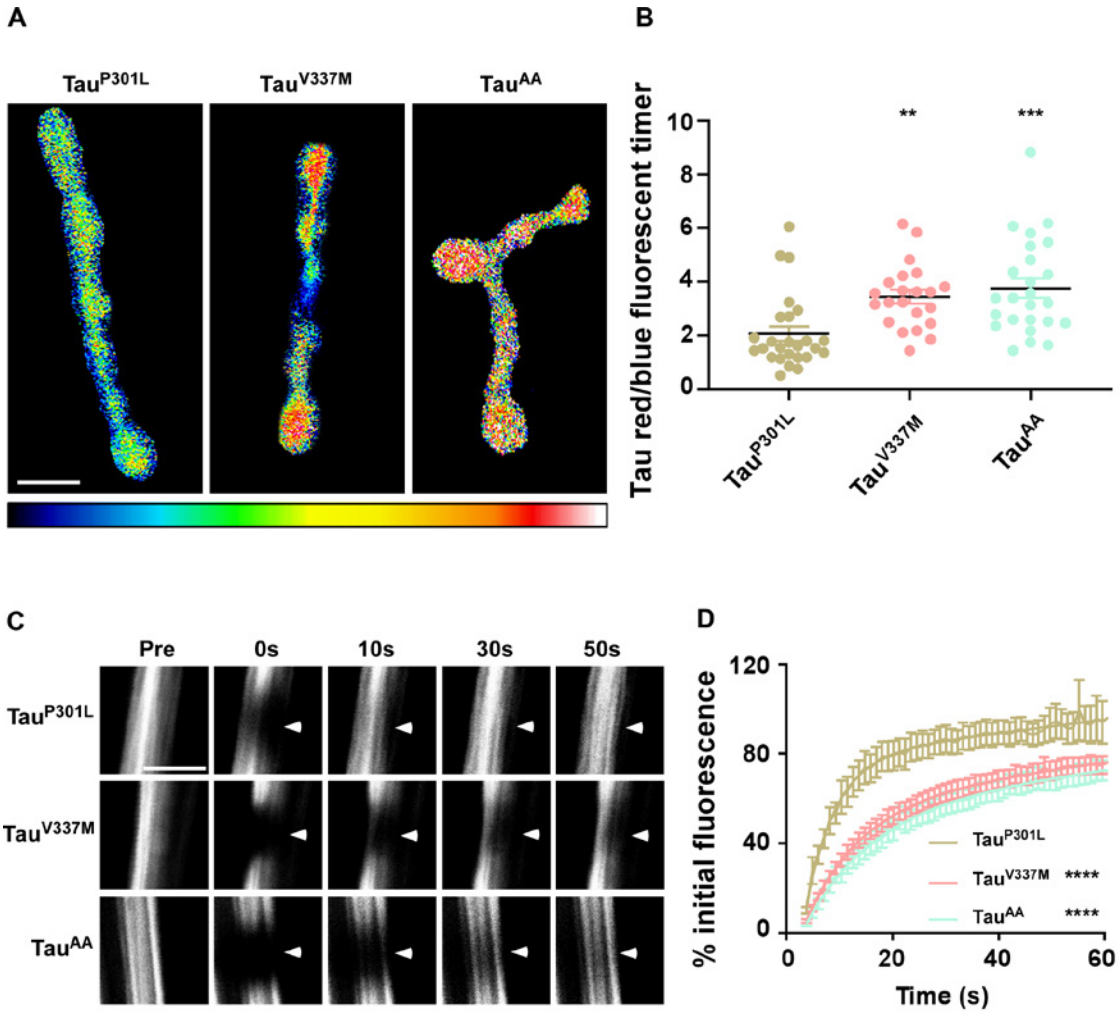

Figure 6. Tau mutations diversely affect turnover of Tau at presynapses and axonal Tau mobility.
A and B) images A) and quantification B) of the ratio of red over blue fluorescence intensities of synaptic boutons shown using the indicated lookup table. The Tau-fluorescent timer was expressed using D42-GAL4 in Tau^{P301L}, Tau^{V337M} and Tau^{AA} mutants. Scale bar 5µm. plotted as individual data points. Graph depicts individual data points and mean ± SEM. (number of dots is number of synapses imaged from ≥8 animals. C) Representative images of Tau-GFP fluorescence recovery at time points right before (pre) and after photobleaching of a defined area (arrowhead) (0, 10, 30 and 50 seconds) in Tau^{P301L} (D42-GAL4> Tau^{P301L}-GFP), Tau^{V337M} (D42-GAL4> Tau^{V337M}-GFP) and Tau^{AA} (D42-GAL4> Tau^{AA}-GFP) mutant presynaptic boutons. Scale bar, 5 µm. D) Plots of Tau-GFP fluorescence recovery over time fit to a double-exponential curve depicting Tau mobility in Tau^{P301L} (brown), Tau^{V337M} (pink) and TauAA mutants (green). Plots depict mean ± SEM (n is 10-23 boutons from ≥8 animals; A two-way ANOVA with Dunnett's correction for multiple comparisons was performed to determine significance levels between all genotypes; ** p< 0.01, *** p<0.001, **** p<0.0001

4. Publications

- Uytterhoeven, V. *et al.* (2020) Increased HSC704/HSPA8 regulated autophagy reduces taumediated synaptic dysfunction. *Alzheimer's Dement.* 16 (suppl 3). Doi: 10.1002/alz.037892

5. References

1. Zhou, L. *et al.* (2017) Tau association with synaptic vesicles causes presynaptic dysfunction. *Nat. Commun.* 8, 1–29
2. McInnes, J. *et al.* (2018) Synaptogyrin-3 Mediates Presynaptic Dysfunction Induced by Tau. *Neuron* 97, 823–835.e8
3. LargoBarrientos, P. *et al.* (2020) Loss of synaptogyrin3 rescues tauinduced memory defects and synaptic loss in the presence of microglial activation. *Alzheimer's Dement.* 16, 1–11
4. Uytterhoeven, V. *et al.* (2015) Hsc70-4 Deforms Membranes to Promote Synaptic Protein Turnover by Endosomal Microautophagy. *Neuron* 88, 735–748
5. Uytterhoeven, V. *et al.* (2015) Hsc70-4 Deforms Membranes to Promote Synaptic Protein Turnover by Endosomal Microautophagy. *Neuron* 88, 735–748
6. Caballero, B. *et al.* (2018) Interplay of pathogenic forms of human tau with different autophagic pathways. *Aging Cell* 17,
7. Uytterhoeven, V. *et al.* (2015) Hsc70-4 Deforms Membranes to Promote Synaptic Protein Turnover by Endosomal Microautophagy. *Neuron* 88, 735–748
8. Shupliakov, O. *et al.* (2011) How synapsin I may cluster synaptic vesicles. *Semin. Cell Dev. Biol.* 22, 393–399
9. Selkoe, D.J. (2002) Alzheimer's disease is a synaptic failure. *Science* 298, 789–91
10. Jackson, J. *et al.* (2019) Targeting the synapse in Alzheimer's disease. *Front. Neurosci.* 13, 1–8
11. Wittmann, C.W. *et al.* (2001) Tauopathy in Drosophila: neurodegeneration without neurofibrillary tangles. *Science* 293, 711–4
12. Devos, S.L. *et al.* (2018) HHS Public Access. 9, 1–30
13. Yoshiyama, Y. *et al.* (2007) Synapse Loss and Microglial Activation Precede Tangles in a P301S Tauopathy Mouse Model. *Neuron* 53, 337–351
14. Hardy, J. *et al.* Pathways to Alzheimer's disease. DOI: 10.1111/joim.12192
15. Passarella, D. and Goedert, M. (2018) Beta-sheet assembly of Tau and neurodegeneration in Drosophila melanogaster. *Neurobiol. Aging* 72, 98–105
16. Barghorn, S. *et al.* (2000) Structure, microtubule interactions, and paired helical filament aggregation by tau mutants of frontotemporal dementias. *Biochemistry* 39, 11714–11721
17. Deture, M. *et al.* (2000) Missense tau mutations identified in FTDP-17 have a small effect on tau-microtubule interactions. *Brain Res.* 853, 5–14
18. Xia, Y. *et al.* (2019) Impaired tau-microtubule interactions are prevalent among pathogenic tau variants arising from missense mutations. *J. Biol. Chem.* 294, 18488–18503
19. Di Primio, C. *et al.* (2017) The distance between N and C termini of tau and of FTDP-17 mutants is modulated by microtubule interactions in living cells. *Front. Mol. Neurosci.* 10,
20. Konzack, S. *et al.* (2007) Swimming against the tide: Mobility of the microtubule-associated protein tau in neurons. *J. Neurosci.* 27, 9916–9927
21. Karch, C.M. *et al.* Human fibroblast and stem cell resource from the Dominantly Inherited Alzheimer Network. DOI: 10.1186/s13195-018-0400-0

Geneeskundige Stichting Koningin Elisabeth
Fondation Médicale Reine Elisabeth
Königin-Elisabeth-Stiftung für Medizin
Queen Elisabeth Medical Foundation

Progress report of the research project of the young researcher

Dr. Emanuel van den Broeke
Université Catholique de Louvain (UCLouvain)

Dr. Emanuel van den Broeke
Postdoctoral researcher, laboratory Algology (prof. André Mouraux),
Institute of Neuroscience (IONS),
division Systems and Cognition (COSY),
UCLouvain, Brussels
www.nocions.org/emanuel-vandenbroeke

The involvement of top-down facilitatory serotonergic pathways in nocebo-induced pain hypersensitivity.

1. Summary of the project

The aim of the project is to assess if serotonergic pathways play a role in the facilitatory effect that negative expectations have on hyperalgesia (increased pain sensitivity). High frequency electrical stimulation will be used to induce hyperalgesia. Before the induction of hyperalgesia, negative expectations about the outcome of HFS (hyperalgesia) will be induced. To investigate the contribution of serotonergic pathways to this expectation-induced hyperalgesia, Odansetron, a 5HT3 antagonist, will be given to participants before the induction of negative expectations.

2. Status project

Due to the COVID pandemic and lockdown we were not able to progress as much as we wanted. At the start of the project we reconsidered the idea of inducing negative expectations about hyperalgesia. This because we think patients are more likely to have negative expectations about their pain than about evoked hyperalgesia. Therefore, inducing negative expectations about HFS, and assessing its effect on the subsequent development of hyperalgesia, would be most likely more clinically relevant. We thus redesigned the experiment and conducted a pilot study to test if inducing negative expectations about HFS is feasible and sufficiently powerful (in terms of effect size). Based on the results of this pilot study we have further improved the new protocol and is now ready to be tested. When the measures related to the pandemic are reduced we are able to continue.

3. Publications acknowledging the financial support of the FMRE

- van den Broeke EN, Vanmaele T, Mouraux A, Stouffs A, Biurrun-Manresa J. and Torta DM. Perceptual correlates of homosynaptic long-term potentiation in human nociceptive pathways: a replication study R. Soc. Open. Sci. 2021; 8200830. http://doi.org/10.1098/rsos.200830.

Geneeskundige Stichting Koningin Elisabeth
Fondation Médicale Reine Elisabeth
Königin-Elisabeth-Stiftung für Medizin
Queen Elisabeth Medical Foundation

Progress report of the research project of the young researcher

Eline Wauters, PhD (VIB)
Universiteit Antwerpen (UAntwerpen)

Eline Wauters, PhD (VIB)
Neurodegenerative Brain Diseases,
VIB Center for Molecular Neurology,
Laboratory of Neurogenetics, I
nstitute Born-Bunge,
University of Antwerp,
Antwerp, Belgium

Onset age variability in *GRN*-associated frontotemporal lobar degeneration: identification of a functional onset age modifier

1. Research Summary

Frontotemporal lobar degeneration (FTLD) is the most common cause of neurodegenerative dementia at young age after Alzheimer's disease (AD). Mutations in the progranulin gene (*GRN*) are a major cause of FTLD, accounting for up to 11.2% of patients. The onset age of *GRN* mutation carriers ranges from 35 to 89 years. This broad onset age range points to the existence of modifiers that affect the onset age of *GRN*-associated neurodegeneration. Identifying these factors is of importance as they might represent targets for disease-delaying therapies.

In an extended Belgian founder family, segregating the *GRN* IVS1+5 G>C null mutation, patients present with disease at onset ages ranging from 45 to 80 years. In this family, we have previously identified a quantitative trait locus (QTL) for onset age. The aim of the project is to identify the functional gene and variant underlying the onset age variability, to study the modifier effect in induced pluripotent stem cell (iPSC) derived neurons and microglia, and to extend the findings to international patient cohorts.

2. Progress Report

2.1. Identification of functional QTL SNPs with a significant effect on onset age

From whole genome (n=23) and exome sequencing data (n=41) of *GRN* founder mutation carriers, I have selected variants located within the onset age QTL (n=635 variants, 620 of which are located in intronic and intergenic regions). To bridge the gap between a genomic locus and mechanisms, I am performing an unbiased high-throughput screen to prioritize functional variants. This technology, REEL-Seq (Regulatory Element Sequencing, (1)), progressed from the SNP-seq technology which I originally envisaged to use (2). I have performed a research stay in the lab of Dr. Li, who introduced both these innovative technologies (University of Pittsburgh (USA), August 2019). REEL-Seq is based on the design of two oligonucleotides for each studied variant – one with the wild-type and one with the alternative allele. This library of oligonucleotides will be incubated with nuclear extract. By performing consecutive cycles of incubation with nuclear extract, gel electrophoresis and PCR amplification, the sequences containing a functional SNP will be enriched in the sequence pool. Massive parallel sequencing (MiSeq, Illumina) will be performed in house (Neuromics Support Facility) to quantify the sequences.

I am currently performing the REEL-seq technology in house, using an oligonucleotide library containing QTL variants (Twist Bioscience). Afterwards, I will genotype the identified functional variants in the complete founder family and perform reporter gene assays to determine the effect of the variants on expression.

Fifteen of the 635 variants are located in exons (coding and non-coding). While these are also included in the REEL-seq library, I have moved forward with these variants in a parallel trajectory given the known relevance of variants in this region for protein function or expression.

I have genotyped the 15 exonic variants in members of the *GRN* founder family (n=170 individuals, including 79 *GRN* founder mutation carriers). Genotyping was performed via multiplex PCRs

for target enrichment of the regions encompassing the exonic variants (www.agilent.com, (3)). The amplicon libraries were sequenced (MiSeq, Illumina). Adapters were trimmed using Fastq-mcf. Reads were aligned to the reference genome hg19 with the Burrows-Wheeler Aligner (4). Variant calling and annotation were performed using GATK (5) and the GenomeComb package (6). For each variant I have estimated the effect on onset age in the *GRN* founder family using Loki (7). This analysis indicated that seven exonic variants have a significant effect on onset age ($p<0.05$). Six variants are located in 5' or 3' untranslated regions (UTR). One variant is located in a coding exon, leading to a missense mutation. We will evaluate the functional effect of the UTR variants using luciferase reporter assays. To assess the functionality of the missense mutation, we will overexpress the wild-type and mutant protein in a cell model and evaluate effects of the mutation on the known protein function.

2.2. Compare gene expression in biomaterials of patients with early and late onset of disease

We have performed transcriptome sequencing on lymphoblast-derived RNA of eight *GRN* founder mutation carriers. To study differential gene expression between early- and late-onset disease, we have compared expression levels between individuals with different genotypes at a QTL variant which has a significant effect on onset age. For this variant, heterozygous (AB) and homozygous (BB) variation carriers developed disease on average 9.0 and 7.9 years later in comparison to homozygous carriers of the wild-type allele ($p<0.00001$ and $p=0.0002$, respectively) (**Figure 1**).

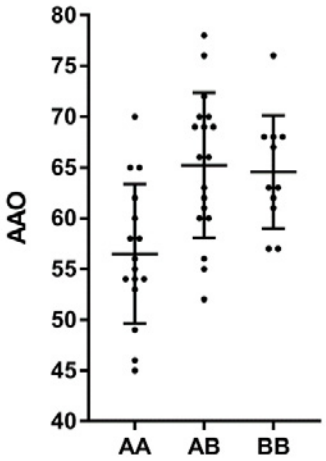

Figure 1: Onset age distributions in the *GRN* founder family for one of the QTL variants with a significant effect on onset age. Patients with known onset age and genotype were included. The mean onset age for each genotype and the standard deviations are visualized. AAO: age at onset. AA/AB/BB: genotypes.

RNA was isolated from lymphoblast cell lines of eight *GRN* founder mutation carriers with different genotypes for the QTL variant. The onset age ranged from 56 to 68 years in six patients. Two additional mutation carriers were selected with current ages of 72 years and 75 years. The coding transcriptome was captured (TruSeq Stranded mRNA Library Prep kit, Illumina) and resulting libraries were sequenced (NextSeq, Illumina). We performed quality control (FastQC, http://www.bioinformatics.babraham.ac.uk/projects/fastqc/), adapter removal and low quality read trimming (Trimmomatic, (8)). Reads were mapped to hg38 with Hisat2, using Ensembl v84 gene annotation (9). FeatureCounts was used for transcript quantification (10).

Expression levels were compared between four homozygous carriers of the wild-type allele and four homozygous variation carriers of the QTL variant. Differentially expressed genes were identified with DESeq2 (11). Sequencing batch and gender were included as covariates in the analysis. In total, we found 475 genes that were differentially expressed (Padj < 0.1). Enrichment

analysis of these genes using GOrilla (12) indicated an important role for endoplasmic reticulum (ER) unfolded protein response and ER stress.
We will expand our transciptomics studies and look for converging evidence in transcriptomics data for lymphoblast (n=58) and brain material (n=9) of *GRN* founder mutation carriers and non-carriers (n=14 lymphoblasts, n=6 brain) (QuantSeq 3' mRNA sequencing, Lexogen).

2.3. Investigation of the role of the QTL in onset age modification in international patient cohorts

We have evaluated the onset age modifying effect of the QTL in unrelated Belgian frontotemporal dementia (FTD) patients without *GRN* mutations (n=293; mean onset age 62.9 ± 10.5 y) by genotyping QTL tagging variants (n=21). Homozygous carriers of the top associated SNP developed disease on average 3.7 years later in comparison to patients homozygous for the wild-type allele (p=0.010, Mann-Whitney U), indicating that the modifier locus also has an effect in *GRN*-unrelated FTD. To replicate the findings obtained in the Belgian FTD cohort, we will screen international patient cohorts.

A genetic, clinical, and pathological overlap exists between neurodegenerative disorders such as FTD and AD. It is thus conceivable that QTL variants would affect the onset age of AD patients. To test this hypothesis, we have genotyped the QTL tagging variants in a cohort of unrelated Belgian AD patients (n=559; mean onset age 73.0 ± 9.3 y) and calculated association with onset age (univariate tests, covariates: APOE, gender). This indicated no significant effect (p>0.05).

3. References

1. Zhao et al, Nat Commun, 2020
2. Li et al, Nat Genet, 2018
3. Goossens et al, Hum Mutat, 2009
4. Li and Durbin, Bioinformatics, 2009
5. McKenna et al, Genome Res, 2010
6. Reumers et al, Nat Biotechnol, 2012
7. Heath, Am J Hum Genet, 1997
8. Bolger et al, Bioinformatics, 2014
9. Kim et al, Nat Methods, 2015
10. Liao et al, Bioinformatics, 2014
11. Love et al, Genome Biol, 2014
12. Eden et al, Bioinformatics, 2009

4. Relevant Information

I have obtained a Postdoctoral Fellowship of the Research Foundation - Flanders (FWO) (01-10-2019 – 30-09-2022), as well as a small research grant from the Research Council of the University of Antwerp (01-04-2020 – 31-03-2021, €10.000). This will support the extension of the REEL-seq screen towards using also nuclear extract from iPSC-derived neurons and microglia.

Geneeskundige Stichting Koningin Elisabeth
Fondation Médicale Reine Elisabeth
Königin-Elisabeth-Stiftung für Medizin
Queen Elisabeth Medical Foundation

Geneeskundige Stichting Koningin Elisabeth – G.S.K.E.
Fondation Médicale Reine Elisabeth – F.M.R.E.
Queen Elisabeth Medical Foundation – Q.E.M.F.

Mailing address:

The scientifique director:
Prof. dr. Jean-Marie Maloteaux
3, avenue J.J. Crocq laan
1020 Bruxelles - Brussel
Belgium
Tel.: +32 2 478 35 56
E-mail: jean-marie.maloteaux@uclouvain.be

Secretary:
Mr. Erik Dhondt
3, avenue J.J. Crocq laan
1020 Bruxelles - Brussel
Belgium
Tel.: +32 2 478 35 56
E-mail: fmre.gske@skynet.be
erik.dhondt@skynet.be
e.l.dhondt@skynet.be

www.fmre-gske.be
www.fmre-gske.eu
www.fmre-gske.com